Norwegian University
of Life Sciences

Master's Thesis 2021 60 ECTS
Faculty of Chemistry, Biotechnology and Food Science

Production and surface anchoring of *Mycobacterium tuberculosis* and SARS-CoV-2 antigens in *Lactobacillus plantarum*

Lene Trondsen
Master of Technology, Chemistry and Biotechnology

Acknowledgments

The work presented in this thesis was carried out at the Faculty of Chemistry, Biotechnology and Food Science of the Norwegian University of Life Sciences with Dr. Geir Mathiesen, Ph.D. Candidate Kamilla Wiull and Professor Vincent Eijsink as supervisors.

First, I want to thank my main supervisor Geir Mathiesen for being such a motivating, supportive and excellent supervisor. I have learned so much from working with you and could not have asked for a better supervisor! I would also like to especially thank Kamilla Wiull for always being available and for all her help with answering questions, guidance in the laboratory and motivating me through this period. In addition, I would also like to thank Sofie Kristensen for helping me in the laboratory and answering all my questions. Further, I would also like to thank the rest of the PEP-group. It has been a privilege to work in the PEP-group with so many knowledgeable and inspiring people.

At last, I would like to thank my family for their support during this time. A special thanks to Jo Fredrik for his encouragement, support and for always believing in me, I am so grateful.

Ås, February 2021

Lene Trondsen

Abstract

Lactic acid bacteria (LAB) are considered good candidates for delivery of antigens because they are regarded as safe to consume by humans and can survive the rough conditions in the gastrointestinal tract, to mention some desirable traits. *Lactobacillus plantarum* has shown to be one of the most promising LAB as a vaccine deliverer. The inducible expression system pSIP has in this study been used to express the *Mycobacterium tuberculosis* antigens Ag85B, ESAT6 and Rv2660c (named H56) and the severe acute respiratory syndrome coronavirus 2 (SARS-CoV-2) antigens NTD and RBD in *L. plantarum*. In addition, the antigens were displayed at the surface of *L. plantarum* with different cell membrane and cell wall anchors. H56 antigens were displayed at the surface with a lipoprotein anchor (cell membrane anchor), LysM anchor and LPXTG anchor (cell wall anchors), while the SARS-CoV-2 antigens were displayed at the surface with a lipoprotein anchor and LPXTG anchor.

The vaccine candidates in this study were constructed because the world is in need of a new and improved vaccine against tuberculosis and due to the recently emerged worldwide pandemic COVID-19. Tuberculosis (TB) is a disease causing over one million deaths every year despite there already exists a vaccine against the disease, the BCG vaccine. The COVID-19 pandemic has taken over 2 million lives in less than a year and the world has been in desperate need of a vaccine. Fortunately, several successful vaccines have recently been approved against the disease.

In this study, three vaccine candidates against tuberculosis, and four vaccine candidates against COVID-19 were constructed. *L. plantarum* successfully produced both the TB antigens and the SARS-CoV-2 antigens and displayed them at the surface of the bacteria. Growth analyses showed that bacteria with cell membrane anchored antigens generally had a higher growth rate than bacteria with antigens anchored to the cell wall. However, bacteria harbouring the cell wall anchored antigens showed stronger fluorescent signal in flow cytometry assays, indicating more antigens were exposed at the surface. For the purpose of using these recombinant bacteria as vaccines, it is an advantage that the growth is as high as possible, and the antigens have to be exposed at the surface of the bacteria. Based on the characterization done in the present study, the most promising vaccine candidates against tuberculosis were *L. plantarum* harbouring the lipoprotein and LysM anchored H56, and against COVID-19, *L. plantarum* harbouring the lipoprotein anchored SARS-CoV-2 antigens.

Sammendrag

Melkesyrebakterier anses som gode kandidater for levering av antigener fordi de blant annet er betraktet som trygge å konsumere av mennesker og kan overleve de tøffe forholdene i mage-tarmkanalen. *Lactobacillus plantarum* har vist seg å være en av de mest lovende melkesyrebakteriene for levering av vaksiner. I dette studiet har det induserbare utrykkingssystemet pSIP blitt brukt til å utrykke *Mycobacterium tuberculosis* antigenene Ag85B, ESAT6 og Rv2660c (kalt H56) og SARS-CoV-2 antigenene NTD og RBD i *L. plantarum*. I tillegg ble antigenene eksponert på overflaten av *L. plantarum* ved hjelp av ulike cellemembran og cellevegg ankere. H56 antigenet ble ankret til overflaten med et lipoproteinanker (cellemembran anker), LysM anker og LPXTG anker (cellevegg ankre), mens SARS-CoV-2 antigenene ble ankret til overflaten med et lipoprotein anker og LPXTG anker.

Vaksinekandidatene i dette studiet ble laget fordi verden har behov for en ny og forbedret vaksine mot tuberkulose og grunnet den nylige verdensomspennende pandemien COVID-19. Tuberkulose (TB) er en sykdom som forårsaker over en million dødsfall hvert år på tross av at det allerede eksisterer en vaksine mot sykdommen, BCG vaksinen. På under et år har COVID-19 pandemien krevd over 2 millioner liv og verden har hatt et desperat behov for en vaksine. Heldigvis har flere vellykkede vaksiner nylig blitt godkjent mot denne sykdommen.

I dette studiet har tre vaksiner mot tuberkulose og fire vaksiner mot COVID-19 blitt laget. *L. plantarum* produserte både TB antigen og SARS-CoV-2 antigen vellykket og eksponerte antigenene på overflaten av bakterien. Vekstanalysene viste at bakterier med cellemembranankrede antigen generelt hadde høyere vekstrate enn bakterier med antigen ankret til celleveggen. I motsetning viste bakterier med celleveggankrede antigen sterkere fluorescenssignal i flowcytometri-analysene, som indikerte at flere antigen var eksponert på overflaten. Med formål om å bruke disse rekombinante bakteriene som vaksiner, er det en fordel at veksten er så høy som mulig og at antigenene er eksponert på overflaten av bakteriene. Basert på karakteriseringen gjort i dette studiet var de mest lovende vaksinekandidatene mot tuberkulose *L. plantarum* med lipoproteinankret og LysM ankret H56, og mot COVID-19, *L. plantarum* med lipoproteinankrede SARS-CoV-2 antigen.

Abbreviations

BCG	Bacillus Calmette-Guérin
BSA	Bovine Serum Albumin
BHI	Brain-heart-infusion
DC	Dendritic cell
DTT	Dithiothreitol
FITC	Fluorescein isothiocyanate
GIT	Gastrointestinal tract
GRAS	Generally Regarded As Safe
HK	Histidine protein kinase
LAB	Lactic acid bacteria
LDS	Lithium dodecyl sulfate
MDR-TB	Multidrug-resistant tuberculosis
MRS	De Man, Rogosa and Sharpe
NICE	Nisin-controlled expression
OFA	Oncofetal antigen
PCR	Polymerase Chain Reaction
RR	Response regulator
rpm	Revolution per minute
SARS-CoV-2	Severe acute respiratory syndrome coronavirus 2
SDS-PAGE	Sodium dodecyl sulfate polyacrylamide gel
TB	Tuberculosis

Contents

1 Introduction

Lactic acid bacteria (LAB) are a group of bacteria naturally found in humans, and for hundreds of years LAB have been added in food products due to their fermentation ability. In addition, LAB have been found to survive the passage through the gastrointestinal tract (GIT). Thus, the bacteria are safe for humans and can survive long enough to be able to deliver antigens to the immune cells. These are some properties that makes LAB good vaccine delivery candidates.

In this study, the LAB *Lactobacillus plantarum* is modified to produce *Mycobacterium tuberculosis* antigens and severe acute respiratory syndrome coronavirus 2 (SARS-CoV-2) antigens as vaccine candidates against the diseases tuberculosis (TB) and COVID-19, respectively. The work with the TB antigens is an extension of the previous work done by others, while the work with the SARS-CoV-2 antigens is new.

TB is a disease causing over a million deaths every year, while the newly emerged COVID-19 pandemic has in under a year caused over 2 million deaths worldwide. In the last 100 years, the BCG vaccine has provided protection against tuberculosis, but a disadvantage with this vaccine is that it only offers protection for children and young adults. Currently, three vaccines against COVID-19 have been approved by the EU. However, since these vaccines are brand new, all the effects and side-effects of the vaccine are not fully known. Therefore, it is important to continue the research on possible vaccine candidates.

1.1 Lactic acid bacteria

LAB are gram-positive bacteria with the shape of cocci or rods. Gram-positive bacteria have a thick peptidoglycan cell wall outside their cell membrane, in contrast to gram-negative bacteria such as *Escherichia coli,* which have a thin peptidoglycan cell wall between their two cell membranes. LAB produces energy by breaking down carbohydrates through fermentation, with lactic acid as the main product.

Traditionally LAB have been used to produce and preserve food, and still today, they play a significant role in the food industry. LAB have the status "Generally Recognized As Safe" (GRAS) given by the American Food and Drug Administration (FDA), meaning they are safe to consume by humans. LAB are found in food products such as milk and dairy products,

meats, vegetables, and bread (Aguirre & Collins, 1993), and they are natural inhabitants of the GIT and on mucosal surfaces (Aguirre & Collins, 1993).

Some LAB are probiotic, which means they are live bacteria with health-promoting effects (Holzapfel et al., 1998; Marteau & Rambaud, 1993). It has also been shown that LAB may have adjuvant properties, meaning they enhance the immune response when delivering antigens (Wyszyńska et al., 2015).

1.2 *Lactobacillus plantarum*

A large group of the LAB is the genus *Lactobacillus*, which contains more than 150 species (Salvetti et al., 2012). One of the species belonging to *Lactobacillus* is *L. plantarum*. *L. plantarum* is found in several food products such as dairy and meat, as well as in the GIT of humans (Kleerebezem et al., 2003).

In 2003, the complete genome of *L. plantarum* WCFS1 was sequenced by Kleerebezem et al. (2003) which is one of the largest known genomes among the LAB. The strain inhabits many regulatory and transport functions, which explains the flexibility and adaptivity of *L. plantarum* and why it can be found in many different environments (Kleerebezem et al., 2003). A study by Kuczkowska et al. (2019) compared 8 different *Lactobacillus* species as immunogenic carriers of *M. tuberculosis* antigens. The study showed that *L. plantarum* was one of two species which showed most promise as a vaccine carrier of the TB antigens.

1.3 Bacteria as live vectors for antigen delivery

Most pathogens enter the human body through mucosal surfaces. Therefore, this would be an interesting site to introduce a vaccine. Today, however, most vaccines are administered through injections. An advantage of administering the vaccines through injection is that the quantity of antigens is known and specific antibodies formed can be measured in a blood sample. However, administering vaccines through nasal, oral, vaginal, or rectal routes are the most effective ways of inducing a mucosal immune response (Neutra & Kozlowski, 2006). A challenge with mucosal administration is that the vaccines encounter the same rough challenges as the pathogens entering the mucosal sites do. The vaccines can, for example, be degraded or diluted, which means large doses of vaccines may be required, and it can also be challenging to estimate the correct dose (Neutra & Kozlowski, 2006). An advantage with

mucosal administration over injections is that the vaccine is easier to administer, requiring fewer trained personnel, which would make it available to more people. Also, mucosal vaccines have the ability to induce both a systemic and mucosal immune response (Bermúdez-Humarán et al., 2011).

Using food-grade bacteria as live vectors for delivering antigens is a newer vaccination strategy. This strategy is safer compared to a more classical vaccine strategy using live attenuated bacteria, which includes the risk of causing a disease rather than preventing it. LAB are attractive candidates as vectors for antigen delivery as they are considered safe, some have probiotic and adjuvant properties, and most strains, such as *L. plantarum,* can survive the rough conditions through the GIT. The LAB can either produce the antigens and keep them intracellularly, deliver the antigens to the extracellular environment, or anchor them to the cell surface. Surface displayed antigens may be the best way for delivery, as the cell surface can provide protection against degradation of the target protein. In addition, the surface localization more easily allows the antigens to interact with the immune system, while intracellular proteins are hidden without lysis of the cell.

1.4 Inducible gene expression systems

Inducible gene expression systems make it possible to control the expression of interesting genes by adding external stimuli that induce the gene expression. Inducible systems can ensure high and controlled expression of genes (Sørvig et al., 2005). The inducible gene expression system, the so-called pSIP expression system (Sørvig et al., 2003; Sørvig et al., 2005), used in this study, is reviewed closer in this section.

Inducible gene expression systems allow the expression of the genes to be controlled by factors such as temperature, pH or addition of additives (Diep et al., 2009). One of the first and a still widely used inducible expression system in LAB are the NIsin-Controlled gene Expression system (NICE-system) (de Ruyter et al., 1996; Kuipers et al., 1997). The NICE-system was originally developed in *Lactococcus lactis* as a two-plasmid system induced by the bacteriocin nisin. Later, the system was further developed in *Lactobacillus*, but results have shown that the NICE-system is not suitable for *L. plantarum* due to large basal gene expression activity without induction of nisin (Pavan et al., 2000; Sørvig et al., 2003).

Another inducible expression system developed is the so-called pSIP system (Sørvig et al., 2003; Sørvig et al., 2005). The inducible pSIP-expression vectors were developed by Sørvig et al. mainly for use in *Lactobacillus sakei* and *L. plantarum.* The expression system is based on genes naturally used to produce the bacteriocins sakacin A and sakacin P. The pSIP vectors are comprised of cassettes with restriction sites, making it easy to exchange the vector components through restriction enzyme digestion and ligation (Sørvig et al., 2003; Sørvig et al., 2005) (Figure 1.1). The main components of the vectors are the genes encoding a histidine protein kinase (HK protein) and a response regulator protein (RR protein), and the promoter which controls these genes (Figure 1.1). The promotor is induced by a peptide pheromone, which activates the HK and RR protein production. This gene operon originally consists of a third gene (*sppIP*), encoding the inducer peptide (SppIP). This gene is deleted from the system to be able to strictly control the expression of the target proteins. For activation of the system, the addition of the extracellular inducer peptide (SppIP) is required. When adding the inducer peptide, the HK protein will be phosphorylated. The phosphate group is then transferred to the RR protein by the HK protein. Phosphorylated RR protein binds to the

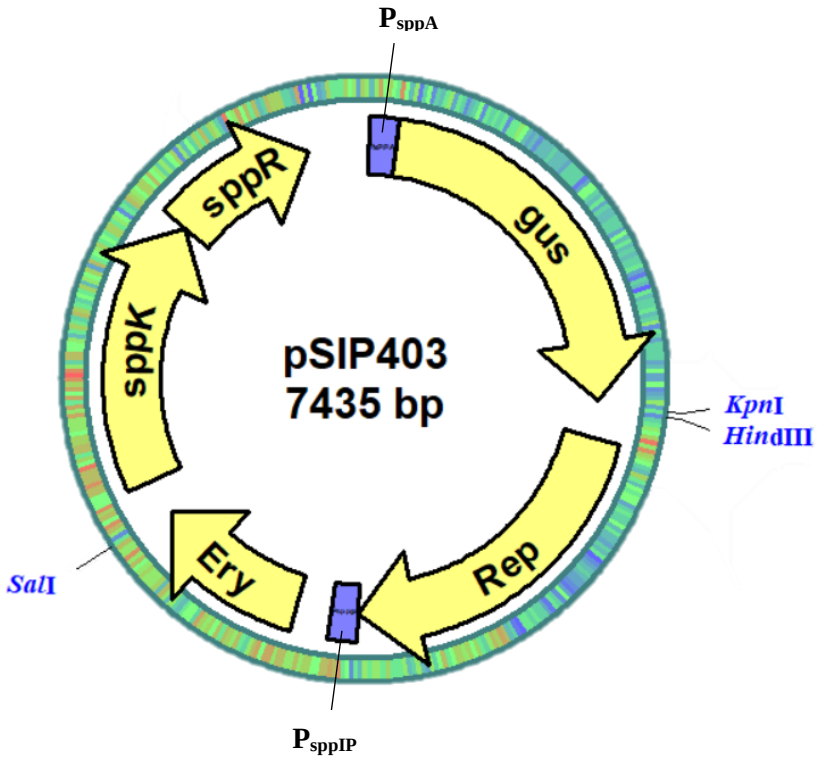

Figure 1.1. Representation of the expression vector pSIP403. P_{sppA}: inducible promoter; *gus*: β-glucuronidase; Rep: replicons pUC(pGEM)ori from *E. coli* and 256rep from *L. plantarum*; P_{sppIP}: inducible promoter; *ery*: Erythromycin resistance marker; *sppK*: Histidine protein kinase; *sppR*: response regulator. Downstream of P_{sppA} is the cloning site for insertion of target genes. *Kpn*I, *Hind*III and *Sal*I are some of the restriction sites used in this study.

inducible promotors located upstream of the genes encoding the RR and HK protein and downstream of these genes (the inducible promotors for the pSIP403 vector, P_{sppA} and P_{sppIP}, are shown in Figure 1.1). Binding to the promotors results in massive expression of the target genes and production of more HK- and RR-proteins. The HK and RR proteins will continuously be expressed, which will lead to an explosive production of the target protein.

Modifications of the pSIP-system have later been done for the secretion of heterologous proteins (Mathiesen et al., 2008) and for cell surface anchoring of heterologous proteins (Fredriksen et al., 2010; Fredriksen et al., 2012; Kuczkowska et al., 2016). The pSIP-system can be applied to a wide variety of proteins. Fredriksen et al. (2010) cloned the tumor immunogen oncofetal antigen (OFA) which is expressed on mammalian cancers into a pSIP-vector, and OFA was displayed at the surface of *L. plantarum*. The recombinant bacteria were then orally administered in mice, which induced an immune response against OFA. A *Chlamydia trachomatis* antigen was cloned into a pSIP-vector and displayed on the surface of *L. plantarum* (Kuczkowska et al., 2017). Kuczkowska et al. (2017) showed that the recombinant bacteria induced antigen-specific IgA response in the vaginal cavity after mucosal booster immunization. *Mycobacterium tuberculosis* antigens have also been cloned into the pSIP-vectors in *L. plantarum* (described in more detail in section 1.6.1). In this study, both antigens from *M. tuberculosis* and from severe acute respiratory syndrome coronavirus 2 (SARS-CoV-2) was cloned into pSIP-vectors. All these different uses of the pSIP-vectors demonstrate the large variety of what the system can be used for.

1.5 Secretion and anchoring of proteins in lactic acid bacteria

Expression and secretion of heterologous proteins is executed by the recombinant *L. plantarum WCSF1* bacteria before displaying the proteins at the surface by an anchoring. This is done for the purpose of developing a live vaccine using lactic acid bacteria as a delivery vector. To secrete the proteins to the desired location, i.e., the place they are to be anchored, signal peptides are fused to the proteins. The anchor and heterologous proteins are expressed and secreted as one unit, translationally fused together. Depending on the type of anchor, the heterologous proteins are anchored to the cell membrane or the cell wall, thus displayed at the surface of the bacteria.

The envelope of Gram-positive bacteria consists of a cell membrane and a thick peptidoglycan cell wall. Proteins synthesized in the cytosol by ribosomes have to pass this

envelope to be anchored to the cell surface. To secure that the proteins are transported to the right location, signal peptides are added to the proteins (Kleerebezem et al., 2010). The signal peptides may be cleaved off by signal peptidases once they are translocated over the cell membrane. The signal peptidase can cleave the protein at different sites to remove the signal peptide. Whether the protein is anchored to the cell wall or to the cell membrane depends on the cleavage site of the signal peptide. The proteins anchored to the cell wall contain signal peptides with the cleavage site A-X-A, which is cut by signal peptidase I (van Roosmalen et al., 2004). The proteins that are anchored to the membrane after translocation contain signal peptides with the cleavage site L-X-X-C, which is cleaved by signal peptidase II (Sutcliffe & Harrington, 2002).

There are multiple strategies for anchoring heterologous proteins to the cell surface. The four main strategies are by fusing the proteins to either an N-terminal transmembrane anchor, lipoprotein anchor, LPXTG peptidoglycan anchor or a LysM anchor (Figure 1.2) (Michon et al., 2016). The N-terminal transmembrane anchor and lipoprotein anchor are anchored to the cell membrane, while the LPXTG peptidoglycan anchor and LysM anchor are anchored to the cell wall (Figure 1.2). It is used three anchors in this study, the lipoprotein anchor, the LPXTG anchor and the LysM anchor, which are described in more detail below.

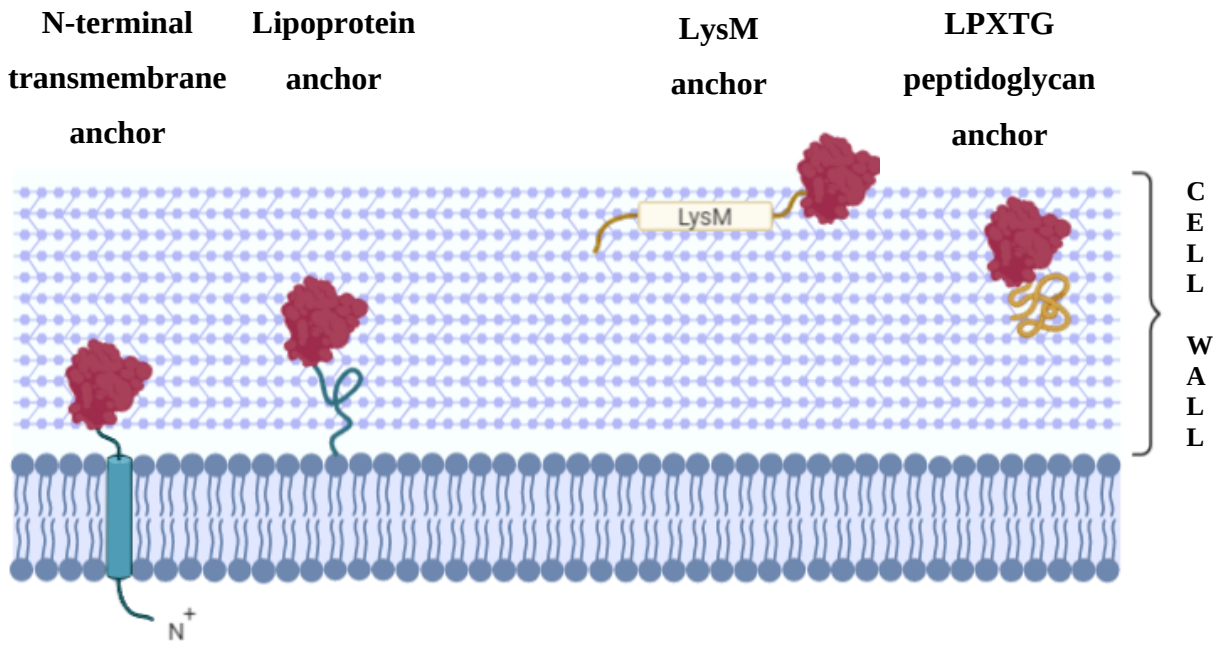

Figure 1.2. Anchoring strategies of proteins in lactobacilli. The most exploited anchoring strategies used to anchor proteins to the cell membrane and the cell wall in *Lactobacillus*. The sequence that anchor the protein to the cell membrane are shown in blue and the sequence that anchor the protein to the cell wall are shown in orange. The antigens attached to the anchors are shown in red.

1.5.1 Lipoprotein anchor

The lipoprotein anchors with the attached protein are anchored to the cell membrane by its N-terminal end through a lipobox, which is part of the signal peptide (Michon et al., 2016). After secretion, the lipoprotein anchor undergoes an enzymatic reaction. A cysteine in the lipoprotein's cleavage site called lipobox will be coupled with a phospholipid in the cell membrane catalyzed by the enzyme diacylglycerol transferase. After, the enzyme SPaseII will cleave off the signal peptide resulting in covalent binding of the cysteine to one of the cell walls phospholipids.

Multiple studies have successfully used lipoprotein anchors in their work (Fredriksen et al., 2012; Kuczkowska et al., 2016; Wiull, 2018; Øverland, 2013). In a study by Øverland (2013), a lipoprotein anchor derived from *L. plantarum* named pLp1261, were fused to the *M. tuberculosis* antigens Ag85B and ESAT6 (called H1). Further testing of the lipoprotein anchor fused with H1 was done by Kuczkowska et al. (2016), which managed to successfully express and anchor the H1 antigen to the cell membrane in *L. plantarum*. Kuczkowska et al. (2016) also showed that the lipoprotein anchor fused with H1 induced immune response in mice after immunization through nasal and oral administration.

1.5.2 LysM anchor

Proteins harbouring a lysine motif domain (LysM domain) can be used for binding heterologous proteins non-covalently to the cell wall, specifically to peptidoglycan (Michon et al., 2016). The length of the LysM domain is 44-65 amino acids, and it usually appears in the C- or N-terminal end of proteins. LysM domains are often found in peptidoglycan hydrolase proteins (Buist et al., 2008). Specifically, the domain most likely interacts non-covalently with the N-acetylglucosamine (NAG) monomers in the peptidoglycan layer (Buist et al., 2008).

The LysM anchor derived from *L. plantarum* named pLp3014, containing a single LysM domain, has previously been used to anchor the fusion antigen H1 to the cell wall of *L. plantarum* (Målbakken, 2014). It was constructed a fusion between the LysM part in the pLp3014 protein and the H1 antigen.

1.5.3 LPXTG peptidoglycan anchor

The LPXTG peptidoglycan anchor can fuse heterologous proteins covalently to the cell wall via an LPXTG motif (Michon et al., 2016). The protein is fused in N-terminus to the anchor containing the LPXTG motif (Figure 1.3). Located downstream of the motif are several hydrophobic amino acids followed by a few positively charged amino acids (Figure 1.3). In front of the inserted protein, a signal peptide is needed, responsible for transporting the anchor with attached protein out of the cell (Figure 1.3). After secretion, the LPXTG motif is cleaved between the amino acids threonine and glycine by the enzyme sortase. The anchor is subsequently bound to the cell wall through the threonine residue with its C-terminal end.

Figure 1.3. Illustration of the main components of a LPXTG peptidoglycan anchor. SP: signal peptide; LPXTG: motif; +aa: positively charged amino acid residues.

LPxTG peptidoglycan anchors have been successfully used in several studies (Berggreen, 2020; Fredriksen et al., 2010; Kuczkowska et al., 2016; Øverland, 2013). The H1 antigen was fused with the cell wall anchor derived from *L. plantarum*, named cwa2, by Øverland (2013), and further testing by Kuczkowska et al. (2016) showed successful expression and display of the antigens on the cell surface using this anchor (cwa2). In addition to the lipoprotein anchor, the cwa2 anchor fused with H1 also showed induced immune response in mice (further described in section 1.5.1) (Kuczkowska et al., 2016). However, a drawback of using the cwa2 anchor sequence is that it often has resulted in reduced viability and growth rate of the producer. Recently, Berggreen (2020) tested several cell wall anchors derived from *L. plantarum* to analyse if any other cell wall anchors would be a better candidate for delivering the fusion antigen H1 than the frequently used cwa2. The results showed that the LPXTG anchor named pLp3001 was more promising than the cwa2 anchor regarding growth when the recombinant bacteria are harvested for flow cytometry and western blot analysis.

1.6 Tuberculosis

Tuberculosis (TB) is one of the deadliest diseases worldwide caused by a single infectious agent. The infectious agent causing TB is *Mycobacterium tuberculosis*. The disease is airborne and usually affects the lungs, which may cause fever, coughing and chest pain (Fogel, 2015). According to the World Health Organization (WHO), 10 million people fell ill and 1.4 million people died from the disease in 2019. As much as 1/3 of the world's population is infected by latent TB, and about 5-10 % risk going from the latent state to active TB (which causes disease) (Fogel, 2015). People worldwide are at risk of contracting this disease; however, most people infected with *M. tuberculosis* live in poverty and economic distress (World Health Organization, 2020b). Also, most people that develop TB are adults. Today TB is both treatable and curable, and there is also a vaccine available for TB, the live attenuated *Mycobacterium bovis* Bacillus Calmette-Guérin (BCG) vaccine (Andersen & Doherty, 2005). The WHO End TB strategy is reducing the cases of TB by 90 % compared to 2015. The BCG vaccine was first used as a vaccine 100 years ago (in 1921) (Luca & Mihaescu, 2013) and is still the only licensed vaccine against TB. The vaccine prevents severe TB in children (World Health Organization, 2020b), such as TB meningitis (Andersen & Doherty, 2005). The protection of the vaccine, however, does not last more than 10-20 years (Comstock et al., 1976; Hart & Sutherland, 1977; Sterne et al., 1998). Thus, the most prominent vaccine strategy might be to develop a booster vaccine to maintain the immunity received by the BCG vaccine (Andersen & Doherty, 2005).

A major concern is the development of drug-resistant, and especially multidrug-resistant (MDR) TB. In 2019, over 200 000 people were diagnosed with rifampicin-resistant TB or MDR, an increase of 10% from 2018 (World Health Organization, 2020b). When people infected with TB does not respond to either of the two most effective first-line drugs against TB, isoniazid and rifampicin, they have developed MDR-TB (World Health Organization, 2020b). Most MDR-TB are curable with second-line drugs, but these require extensive treatment.

1.6.1 *Mycobacterium tuberculosis* antigens

M. tuberculosis antigens used in this study are Ag85B, ESAT-6 and Rv2660c. The antigens are translationally fused together, named H56 (Aagaard et al., 2011). Ag85B is considered to have high immunogenicity (Kuczkowska et al., 2016), and ESAT6 is the main target for T-

cells in the early infection phase, in addition, to possess strong antigenic properties (Kuczkowska et al., 2016). Rv2660c is a latency-associated antigen able to induce prominent immune responses (He et al., 2015). The antigen is expressed late in infection at stable levels when the expression of other genes declines (Aagaard et al., 2011).

Previous studies have used the combination of the two antigens Ag85B and ESAT-6, called the H1 vaccine (Dietrich et al., 2007; Kuczkowska et al., 2016; Kuczkowska et al., 2019; Langermans et al., 2005). Kuczkowska et al. (2016) produced and anchored the H1 antigen at the surface of *L. plantarum* successfully. The anchors used were the lipoprotein anchor 1261 and cell wall anchor, cwa2. The vaccine candidates induced antigen-specific proliferative responses in blood cells from patients with TB. Also, in mice, the vaccine candidates induced immune responses after nasal and oral administration. To improve the prominent vaccine candidate H1, the antigen Rv2660c has been added to induce even greater immune responses (Aagaard et al., 2011). Aagaard et al. (2011) showed that Rv2660c alone did not give protective immune responses; however, when included in the H56 vaccine, the immune response in mice was amplified five-to tenfold. Also, H56 was almost ten times more efficient at reducing the number of *M. tuberculosis* than H1. Mice administered with H56 vaccine were protected from tuberculosis up to at least 24 weeks after infection. The H56 vaccine in this study was comprised of purified H56 antigen from *E. coli* and a cationic adjuvant.

1.7 COVID-19

COVID-19 is an ongoing pandemic in the world, which has caused 2 227 420 deaths worldwide as of 2 February 2021, according to WHO. COVID-19 is a respiratory disease caused by the severe acute respiratory syndrome coronavirus 2 (SARS-CoV-2). The most common symptoms of the disease are fever, dry cough and fatigue and more severe symptoms are shortness of breath, loss of appetite and chest pains (World Health Organization, 2020a). The incubation period is usually 5-6 days but can range between 1-14 days. All people are at risk of being severely ill or die from this disease, but people with underlying medical problems and people over the age of 60 have a higher risk. The main transmission route of SARS-CoV-2 between individuals is through respiratory droplets by coughing or sneezing of an infected person (Estrada, 2020).

SARS-CoV-2 belongs to the genus *Betacoronavirus*, along with SARS-CoV, MERS-CoV and Bat SARS-like coronaviruses (Chen et al., 2020). The genome of coronaviruses are single-

stranded positive-sense RNA (+ssRNA), approximately 30 kb large (Chen et al., 2020; Khailany et al., 2020). Approximately two-thirds of the SARS-CoV-2 genome consists of the polypeptides 1a and 1b, which are later processed into 16 non-structural proteins, while approximately one-third of the genome consists of at least four structural proteins, the spike protein (S), the envelope (E), the membrane (M) and the nucleocapsid (N) (Figure 1.4) (Chen et al., 2020; Khailany et al., 2020). In addition, SARS-CoV-2 contains six accessory proteins (not included in the figure) (Khailany et al., 2020).

Figure 1.4. Genomic structure of SARS-CoV-2. pp1a and pp1b: polyprotein 1a and 1b; S: spike proteins; E: envelope proteins; M: membrane proteins; N: nucleocapsid proteins.

The genome sequence similarity between two Bat SARS-like coronaviruses (bat-SL-CoVZC45 and bat-SL-CoVZXC21) and SARS-CoV-2 is 88 %, while the similarity is lower for SARS-CoV and MERS-CoV, approximately 79 % and 50 %, respectively (Lu et al., 2020). COVID-19 is caused by zoonosis, which is the transmission of a disease directly from animals to humans or indirectly through an intermediate species (Ye et al., 2020). The origin reservoir of the virus causing the disease is the bat, but the intermediate species is still unknown (Petrosillo et al., 2020). However, there have been studies suggesting that the intermediate species of COVID-19 might be the Malayan pangolins (*Manis javanica*) (Lam et al., 2020; Zhang et al., 2020). Lam et al. (2020) report strong similarities between the receptor-binding domain (RBD) of pangolin-associated viruses and SARS-CoV-2.

According to WHO, there are 63 vaccines against COVID-19 in clinical development and 174 vaccines in pre-clinical development as of 02.02.2021 (World Health Organization, 2021). The following three vaccines have been approved in the EU as of 02.02.2021: Comirnaty (also called BNT162b2, produced by Pfizer and BioNTech), COVID-19 Vaccine AstraZeneca and COVID-19 Vaccine Moderna (European Medicines Agency, 2021). The Pfizer and BioNTech vaccine and Moderna vaccine are mRNA vaccines, meaning they act as the recipe of a protein, in this case, the spike protein. The spike protein is a protein on the surface of SARS-CoV-2 responsible for binding to and entering host cells (Wrapp et al., 2020). However, in this study, *L. plantarum* is modified to produce pieces of the spike protein and deliver them directly to the immune system. This is a similar strategy that the AstraZeneca

vaccine uses, but this vaccine consists of an adenovirus instead of the LAB *L. plantarum*, which is modified to produce the entire spike protein (European Medicines Agency, 2021). All the effects and side-effects of these newly produced vaccines are not fully known, which is why it is important to continue the research on possible vaccine candidates until all the effects of this vaccine are fully known or to find other vaccines that work even better.

1.7.1 SARS-CoV-2 antigens

SARS-CoV-2 antigens selected for expression in this study are the N-terminal domain (NTD) and the receptor-binding domain (RBD).

NTD and RBD are part of subdomain 1 (SD1) of the spike protein (Figure 1.5). The spike protein, responsible for binding to and entering host cells, is divided into two subunits SD1 and SD2 (Figure 1.5) (Wrapp et al., 2020). SD1 is responsible for recognizing the host receptor, while SD2 for membrane fusion (Wang et al., 2020). The spike protein is located at the surface of SARS-CoV-2 (Naqvi et al., 2020).

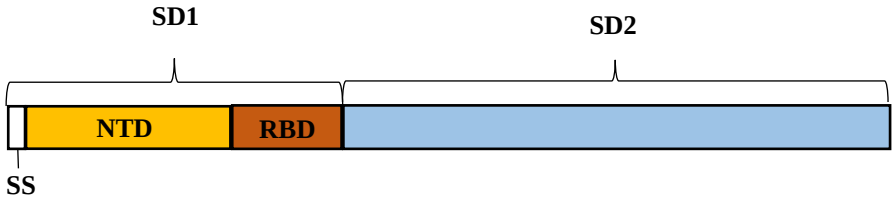

Figure 1.5. Structure of the spike protein. SD1: subdomain 1; SD2: subdomain 2; SS: signal sequence; NTD: N-terminal domain; RBD: receptor binding domain.

More specifically, RBD is responsible for binding to the receptor angiotensin-converting enzyme 2 (ACE2) found on the surface of human host cells, enabling the virus to enter the cells (Wang et al., 2020; Zhou et al., 2020). Expression of ACE2 is found in enterocytes (cells of the inner surface of the intestines), renal tubules (tube in the kidney), gallbladder, cardiomyocytes (cells that makes up the heart muscle), male reproductive cells, placental trophoblasts (specialized cells of the placenta), ductal cells (cells found in the pancreas), eye, and vasculature (the arrangement of blood vessels) (Hikmet et al., 2020). However, in the respiratory system, Hikmet et al. (2020) found limited expression of the receptor, which is interesting since SARS-CoV-2 causes a respiratory disease (COVID-19).

The other domain included as a SARS-CoV-2 antigen in this study, NTD, has a less understood function (Chi et al., 2020). It is still included since it is a part of the spike protein which play a vital role for the virus.

The hypothesis is that the NTD and RBD domains will induce an immune response by the immune cells. Then, hopefully, when SARS-CoV-2 later enters the body, the immune cells will produce neutralizing antibodies which will bind to the spike protein and prevent the virus from binding to and enter the target cells.

1.8 The aim of this study

The aim of this study has been to use the pSIP expression system in *L. plantarum* WCFS1 to produce *M. tuberculosis* and SARS-CoV-2 antigens and display the antigens at the surface of the bacteria. The purpose of this has been to do initial characterization of the vaccine candidates against TB and COVID-19 as the first steps of developing vaccines against the respective diseases. The work on the TB antigens is part of a larger project, where the goal is to make a LAB-based vaccine against *M. tuberculosis*. The vaccine is to be administered through the mucosal sites, mainly nasally and orally. The work on the SARS-CoV-2 is brand-new and was included in this study because of the ongoing worldwide pandemic, COVID-19.

Previously, the *M. tuberculosis antigens* Ag85B and ESAT6 (named H1) has been cloned into the pSIP system in *L. plantarum* WCFS1 successfully. However, studies have reported another *M. tuberculosis* antigen, Rv2660c, to induce promising immune responses. Rv2660c has been implemented in a fusion antigen with Ag85B and ESAT6 (named H56), were administered nasally and orally in mice it induced an even better immune response against TB than the H1 vaccine candidate. Because of these promising studies, it was desired to clone this fusion antigen (H56) into the pSIP system in *L. plantarum* WCFS1. Different anchoring strategies were used to display H56 on the surface of *L. plantarum*, anchoring the fusion antigen to the cell membrane with a lipoprotein anchor or to the cell wall with an LPXTG peptidoglycan anchor or a LysM anchor. This was to test if one anchoring method would provide better results than the others.

There was also curiosity around the recently emerged SARS-CoV-2 and whether antigens from this virus could be cloned into the pSIP system in *L. plantarum*. The spike protein of SARS-CoV-2 is responsible for, among other things, binding to and entering host cells, which are the first steps a virus takes in order to replicate itself. Thus, the spike protein is essential

for SARS-CoV-2. Specifically, it is the NTD and RBD domains of the spike protein which are responsible for binding to and entering host cells and is why these two antigens were chosen. The goal is that these antigens will make the immune cells produce neutralizing antibodies against SARS-CoV-2. Also, different anchors were fused to the SARS-CoV-2 antigens, the lipoprotein anchor, which is anchored to the cell membrane, and the LPXTG peptidoglycan anchor, which is anchored to the cell wall.

2 Materials

2.1 Laboratory equipment

Laboratory equipment	Supplier
Adhesive Film for Microplates, Color-Coded	VWR
Cryovials, 1.5 mL	Sarstedt
Disposable cuvette, 1.5 mL	Brand
Electroporation cuvette, Gene Pulser®, 0.2 cm	Bio-Rad
Eppendorf tubes, 1.5 and 2.0 mL	Axygen
Falcon 2059 Polypropylene Round Bottom tube, 14 mL	Becton Dickinson
FastPrep® tube	Fisher Scientific
Glass beads	Sigma
Microwell plate, 96 wells	Thermo Scientific
Nunc tube, 15 and 50 mL	Nunc
PCR tube, 0.2 mL	Axygen
Pipetboy comfort	Integra
Pure Nitrocellulose Membrane (0.45 µm)	Bio-Rad
Serological pipette, 5, 10 and 25 mL	Sarstedt
Slides and cover slip, Menzel-gläser	Thermo Scientific
Sterile filter, 0.2 µM pore size	Sarstedt
Syringe, 50 mL	Plastipak
Various glass equipment	
Waterbath	Julaba

Instruments	Supplier
Azure c400	Azure biosystems
Centrifuge	
Allegra X-30R Centrifuge	Beckman Coulter
Eppendorf centrifuge 5418R	Eppendorf
Heraeus Pico 21 centrifuge	Thermo Scientific
Heraeus Multifuge X1R	Thermo Scientific
Micro centrifuge MiniStar silverline	VWR

CertoClav	OneMed
Electrophoresis electricity supplier	Bio-Rad
FastPrep® - 24 Tissues and Cell homogenizer	MP Biomedicals
GelDoc EZ imager	Bio-Rad
Gene Pulser II	Bio-Rad
Incubator	Termaks
Inverted Light Microscope, Leica DM IL	Leica Microsystems
Leica TCS SP5 Confocal laser scanning microscope	Leica Microsystems
MacsQuant®Analyser	Miltenyi Biotec
Multiscan FC	Thermo Scientific
PCR-machine	
Mastercycler gradient	Eppendorf
SimpliAmp Thermal Cycler	Applied Biosystems
Labcycler	SensoQuest
pH-meter	Metrohm
Pulse Controller Plus	Bio-Rad
Qubit® Fluorometer	Invitrogen
SNAP i.d. Protein Detection System	Millipore
Ultrospec 10 Cell Density Meter	Amersham Biosciences

Software	Supplier
AzureSpot Analysis Software	Azure Biosystems
CLC DNA Main Workbench 7	Qiagen
MacsQuantify™ Software	Miltenyi Biotec
pDRAW32	AcaClone Software
SkanIt Software 2.5.1	Thermo Scientific

2.2 Chemicals

Chemicals	Supplier
Ampicillin, $C_{16}H_{19}N_3O_4S$	Sigma-Aldrich
Brain-Heart Infusion (BHI)	Oxoid
De Man, Rogosa, Sharpe (MRS)	Oxoid

Disodium phosphate, Na_2HPO_4	Merck
Dithiothreitol (DTT), $C_4H_{10}O_2S_2$	Sigma-Aldrich
Erytromycin, $C_{37}H_{67}NO_{13}$	Merck
Ethanol, C_2H_5OH	Sigma-Aldrich
Glycerol, $C_3H_8O_3$	Merck
Glycine, $C_2H_5NO_2$	Duchefa Biochemie
Magnesium Chloride, $MgCl_2$	Merck
PeqGreen	Peqlab
Polyethylene glycol, PEG_{1450}	Aldrich
Potassium Chloride, KCl	Merck
Potassium dihydrogen phosphate, KH_2PO_4	Merck
SeaKem® LE Agarose	Lonza
Sodium Chloride, NaCl	Merck
Sucrose, $C_{12}H_{22}O_{11}$	VWR Chemicals
Super Optimal broth with Catabolite repression (S. O. C.)	Invitrogen
Tris-HCl, $C_4H_{11}NO_3HCl$	Amresco
Tween-20	Sigma-Aldrich

2.3 Proteins and enzymes

Protein/enzyme	Supplier
Antibodies	
Anti-Mouse IgG-FITC	Sigma
Anti-Rabbit IgG-FITC	Sigma
HRP-Rabbit Anti-Mouse IgG	Invitrogen
HRP-Goat Anti-Rabbit IgG	Invitrogen
ESAT6 Mouse mcAb (ab26246)	Abcam
SARS-CoV/SARS-CoV-2 Spike RBD Polyclonal Antibody	MyBioSource
Bovine Serum Albumin (BSA)	Sigma

Restriction enzymes and buffers	
HindIII	NEB
KpnI	NEB
MluI-HF®	NEB
SalI- HF®	NEB
MluI	Thermo Scientific
KpnI	Thermo Scientific
Buffer 2.1	NEB
10X FastDigest Green Buffer	Thermo Scientific
Inducer peptide, SppIP	CASLO
MagicMark® XP Western Protein Standard	Invitrogen
RED Taq DNA Polymerase Master Mix	VWR

2.4 DNA

DNA	Supplier
DNA-standards	
GeneRuler™ 1 kb DNA ladder	Fermentas
Quick-Load® Purple 1 kb DNA Ladder	NEB

2.5 Bacterial strains and plasmids

Bacterial strains and plasmids used in this study are described in Table 2.1 and Table 2.2, respectively.

Table 2.1. Bacterial strains used in this study.

Bacterial strain	**Source**
***Escherichia coli* TOP10**	Invitrogen
***Lactobacillus plantarum* WCFS1**	(Kleerebezem et al., 2003)
Stellar™ Competent Cells	Takara

Table 2.2. Plasmids used in this study.

Plasmid	Description	Source
pEV	Empty vector. pSIP401 derivative lacking any target genes.	(Fredriksen et al., 2012)
pLp_1261_Ag85B_ESAT6_DC (pLp1261_H1)	pSIP401 derivative for production of Ag85B-ESAT6 with the Lp_1261 lipoprotein-anchor signal sequence.	(Kuczkowska et al., 2016; Øverland, 2013)
pLp_1261_ Ag85B_ESAT6_Rv2660c_DC (pLp1261_H56)	A derivative of pLp1261_H1 where the antigen Rv2660c has been added.	This work
pLp_1261_RBD_DC (pLp1261_RBD)	A derivative of pLp1261_H1 where the antigen RBD has replaced H1.	This work
pLp_1261_NTD_RBD_DC (pLp1261_NTD_RBD)	A derivative of pLp1261_H1 where the antigens NTD and RBD has replaced H1.	This work
pLp_3050_DC_Ag85B_ESAT6_cwa3001 (pLp3001_H1)	A derivative of pLp3050_DC_H1_cwa2 where cwa3001 has replaced cwa2.	(Berggreen, 2020)
pLp_3050_DC_Ag85B_ESAT6_Rv2660c_cwa3001 (pLp3001_H56)	A derivative of pLp3001_H1 where the antigen Rv2660c has been added.	This work
pLp_3050_DC_RBD_cwa3001 (pLp3001_RBD)	A derivative of pLp3001_H1 where the antigen RBD has replaced H1.	This work

pLp_3050_DC_NTD_RBD_cwa3001 (pLp3001_NTD_RBD)	A derivative of pLp3001_H1 where the antigens NTD and RBD has replaced H1.	This work
pLp_3014_ Ag85B_ESAT6_DC (pLp3014_H1)	pSIP401 derivative for production of Ag85B-ESAT6 with the Lp_3014 LysM-anchor signal sequence.	(Målbakken, 2014)
pLp_3014_ Ag85B_ESAT6_Rv2660c_DC (pLp3014_H56)	A derivative of pLp3014_H1 where the antigen Rv2660c has been added.	This work
pJET1.2_ESAT6-Rv266v	The pJET1.2 plasmid that contains the antigens ESAT6 and Rv2660c.	GeneScript
pUC57_DC_NTD_RBD	The pUC57 plasmid that contains the antigens NTD and RBD, and a dendritic cell-binding peptide (DC).	GeneScript

2.6 Primers

Primers used in this study are shown in Table 2.3. The primers were used for PCR reactions (section 3.6) and sequencing (section 3.12). The In-Fusion primers were designed as described in the protocol In-Fusion® HD Cloning Kit User Manual.

Table 2.3. Primers used in this study.

Name	Sequence*	Restriction enzyme	Description
ESAT_SEK_F	GGAATTTTGCTGGTATTGAAGC		Forward primer for sequencing of the antigen ESAT6
NTD_sekF	GTTAGTGGTACGAATGGTAC		Forward primer for sequencing of the antigen NTD
RBD_sekR	GCACTGTTGTACAAGACAC		Reverse primer for sequencing of the antigen RBD
SeqAg85_R	CCCATTGATGGACTTGGAAC		Reverse primer for sequencing of the antigen Ag85B
SekF	GGCTTTTATAATATGAGATAATGCCGAC		Forward primer for sequencing of all pSIP derivatives
SekR	CCTTATGGGATTTATCTTCCTTATTCTC		Reverse primer for sequencing of all pSIP derivatives
1261_RBD_F	GATTGCGGCGGTCGACCCAAACATCACGAACTTGTG	SalI	In-fusion primer for insertion of the antigen RBD into pLp1261
1261_NTD_F	GATTGCGGCGGTCGACGTCAACTTAACAACCCGAAC	SalI	In-fusion primer for insertion of the antigen NTD_RBD into pLp1261
1261_RBD_R	CTGTAATTTGAAGCTTCTATGGACGCTGTGGGGTTGAATGGTATGATGGATAAAAGCCTGAACCGCAAACTGTGGCT	HindIII	In-fusion primer for insertion of the antigens RBD and NTD_RBD into pLp1261

1643_H56_F	CATTAGGTGCCGGTGGTACCGCGAT GACGGAAC	KpnI	In-fusion primer for insertion of the antigen Rv2660c into pLp1643_H1
1643_H56_R	GGTTTGCGTACGCGTGTGGAACTGA TTTAAGCCTAA	MluI	In-fusion primer for insertion of the antigen Rv2660c into pLp1643_H1
3001_RBD_F	GGCCTCCAAGGTCGACTTTTATCCA TCATACCATTCAACCCCACAGCGTC CATCAGGCCCAAACATCACGAACT TGTGT	SalI	In-fusion primer for insertion of the antigen RBD into pLp3001
3001_RBD_R	CGGCAGTGGCACGCGTACCGCAAA CTGTGGCT	MluI	In-fusion primer for insertion of the antigen RBD into pLp3001

*Underlining indicates restriction sites

2.7 Kits

Kit	Supplier
eBlot™ L1 Fast Wet Transfer System	GenScript
eBlot L1	
eBlot L1 NC Membrane	
eBlot L1 NC Membrane Transfer Buffer (5x)	
eBlot L1 NC Membrane Equilibration Buffer (10x)	
eBlot L1 NC Transfer Sponge	
In-Fusion® HD Cloning kit	Clontech
5X In-Fusion® HD Enzyme Premix	

Novex® NuPAGE® SDS-PAGE Gel system	Invitrogen
NuPAGE® Novex Bis-Tris gels 8 cm x 8 cm x 1 mm, 10 wells	
NuPAGE® LDS Sample Buffer (4X)	
NuPAGE® Reducing agent (10X)	
The NucleoSpin® Gel and PCR Clean-up	MACHEREY-NAGEL
The NucleoSpin® Gel and PCR Clean-up columns	
Collection Tubes, 2 mL	
Binding Buffer NTI	
Wash Buffer NT3	
Elution Buffer NE	
NucleoSpin® Plasmid	MACHEREY-NAGEL
Buffer A1	
Buffer A2	
Buffer A3	
Buffer A4	
Elution Buffer AE	
NucleoSpin® Plasmid/Plasmid (NoLid) column	
Collection Tubes, 2 mL	
Qubit® dsDNA BR Assay Kit	Invitrogen
Qubit® Assay Tubes	
Qubit® dsDNA BR Buffer	
Qubit® dsDNA Reagent	
Qubit® dsDNA Standard 1	
Qubit® dsDNA Standard 2	

Quick Ligation® kit	NEB
Quick Ligase Reaction Buffer (2X)	
Quick Ligase	
Q5® Hot Start High-Fidelity 2X Master Mix	NEB
SNAP i.d ® Protein Detection System	Millipore
SNAP i.d ® Single Well Blot Holder	
SNAP i.d ® Spacer	
SNAP i.d ® Blot roller	
Filter paper	
SuperSignal® West Pico Chemiluminescent Substrate	Thermo Scientific
Luminol/Enhancer	
Stable Peroxide Buffer	

2.8 Agars and media

The chemicals and suppliers used are listed in section 2.2.

Media

Brain-Heart-Infusion (BHI)

Media:

37 g BHI was dissolved in 1 L dH_2O, then sterilized in a CertoClav at 121 °C for 15 minutes.

Agar:

BHI-media was added 1.5 % (w/v) agar, then sterilization in a CertoClav at 121 °C for 15 minutes. The media was cooled to approximately 60°C before adding antibiotics. The agar-media was distributed in petri dishes. After solidification, the agar plates were stored at 4 °C.

De Man, Rogosa, Sharpe (MRS)

Media:

52 g MRS dissolved in 1 L dH_2O, then sterilized in a CertoClav at 115 °C for 15 minutes.

Agar:

MRS-media was added 1.5 % (w/v) agar, then sterilized in a CertoClav at 115 °C for 15 minutes. The media was cooled to approximately 60°C before adding antibiotics. The agar-media was distributed in petri dishes. After solidification, the agar plates were stored at 4 °C.

MRSSM-media

5.2 g MRS

17.1 g sucrose (0.5M)

2.0 g $MgCl_2$ x $6H_2O$ (0.1 M)

dH_2O up to 100 mL

The solution was sterile filtrated by using 0.2 µM pore size filter

Super Optimal broth with Catabolite repression (S.O.C)

Pre-made by manufacturer

2.9 Buffers and solutions

Buffer/solution	Supplier
Phosphate Buffered Saline (PBS) 10X 8 g/l NaCl 0.2 g/l KCl 1.44 g/l Na_2HPO_4 0.24 g/l KH_2PO_4	
TAE buffer (Tris-acetate-EDTA) (50X) Ready to use from supplier	Thermo Scientific

Tris Buffered Saline (TBS) 10X

150 mM NaCl

10 mM Tris-HCl, pH 8

Tris-Glycine-SDS (TGS) 10X Bio-Rad

Ready to use from supplier

TTBS

TBS

0.1 % (w/v) Tween-20

3 Methods

3.1 Cultivation of bacteria

Bacteria were cultivated in either liquid media or on solid agar with appropriate antibiotics.

Escherichia coli was cultivated in BHI media with erythromycin or ampicillin, and *Lactobacillus plantarum* in MRS media with erythromycin. *E. coli* in liquid media was incubated overnight in a shaking incubator at 37 °C and on solid media at 37 °C without shaking. *L. plantarum* was incubated at 37 °C without shaking for both liquid and solid media. The concentration of antibiotics used to cultivate the different bacteria are described in Table 3.1.

Table 3.1. Antibiotics used to cultivate *E. coli* and *L. plantarum*.

Antibiotics	**Liquid medium – *E. coli* (µg/mL)**	**Solid medium – *E. coli* (µg/mL)**	**Liquid medium – *L. plantarum* (µg/mL)**	**Solid medium – *L. plantarum* (µg/mL)**
Erythromycin	200	200	10	10
Ampicillin	200	100		

3.2 Storage of bacteria

For long-time storage of bacteria, 300 µL of sterile 87 % glycerol was added to 1000 µL overnight culture of bacteria in a cryovial. The glycerol stock was stored at –80 °C. The tube was inverted a few times for a homogeneous solution before it was placed in the freezer. The glycerol was added to protect the cells from damage at low temperatures.

For cultivation of bacteria from a glycerol stock, a toothpick was used under sterile conditions to pick a small amount of the glycerol stock and dropped into appropriate growth media supplemented with antibiotics.

3.3 Isolation of plasmids

Isolation of plasmids from bacteria was conducted with the NucleoSpin® Plasmid Kit. Protocol 5.1 or 5.2 provided by the manufacturer was followed, depending on whether the plasmid was high- or low-copy.

3.4 Determining the concentration of DNA

Materials

Qubit® dsDNA BR Assay Kit

Qubit® Fluorometer

DNA

Procedure

1. The Qubit Reagent was diluted 1:200 in Qubit BR Buffer in a working solution.
2. For calibration of the Qubit® Fluorometer, Standard 1 and Standard 2 was used. 10 µL of each standard was added to 190 µL of working solution in Assay Tubes, and the Fluorometer was calibrated following the instructions on the instrument.
3. 2 µL DNA was added to 198 µL working solution in an Assay Tube, and the DNA-concentration was determined by the Qubit Fluorometer.

3.5 Restriction enzyme digestion of DNA

Restriction enzymes were used for cutting the plasmids in different positions to remove or add a fragment of DNA. The restriction enzymes cut double-stranded DNA at specific sites. Two different restriction enzymes were applied to the DNA at the same time to reduce time consumption. The use of two restriction enzymes at the same time required compatible buffers and temperatures for digestion.

Materials

dH_2O

DNA

Compatible buffer

Restriction enzyme

Procedure

1. The components in Table 3.2 were mixed at room temperature in an eppendorf tube.
2. The mixture was incubated for 2 hours at 37 °C.
3. The mixture was then loaded onto an agarose gel.

Table 3.2. Components for restriction enzyme digestion of DNA.

Component	**Volume (µL)**
dH_2O up to	50
DNA	X
Buffer	5
Restriction enzyme	5*

*Maximum 10% of restriction enzymes were added in the reaction

3.6 Polymerase chain reaction (PCR)

PCR is a known method of DNA amplification. The method constitutes different steps where DNA is exposed to different temperatures, resulting in many identical copies of a DNA fragment. The different steps are denaturation, annealing and elongation. In the denaturation step, the DNA-reaction is heated to 94-98°C, causing the hydrogen bonds between the nucleotides to break and transforming the double-stranded DNA into single-stranded. The temperature is lowered to 50-72 °C in the annealing step, enabling primers to bind to the single-stranded DNA. The temperature is adapted to different primers used. Finally, the temperature is raised to 72 °C in the elongation step, where a complementary DNA strand of the template DNA is synthesized by DNA polymerase. The synthesis of DNA happens by the incorporation of deoxynucleotides (dNTPs) found in the solution. The length of this step is adapted to the length of the DNA template used. All these steps, denaturation, annealing, and elongation, are repeated for 25-35 cycles.

3.6.1 PCR using Q5® High-Fidelity DNA polymerase

Materials

Q5® Hot Start High-Fidelity 2X Master Mix

Primers

Template DNA

dH_2O

0.2 ml PCR tubes

PCR machine (the different PCR machines used are described in section 2.1)

Procedure

1. All the components in Table 3.3 were gently mixed in PCR tubes. The components were kept on ice in-between.
2. If necessary, the samples were spun to collect the liquid at the bottom of the tubes.
3. The tubes were transferred to a PCR machine.
4. The program described in Table 3.4 was followed.

Table 3.3. Components for PCR using Q5® High-Fidelity DNA polymerase.

Component	**Volume (µL)**	**Final concentration**
Q5® Hot Start High-Fidelity 2X Master Mix	25	1x
10 µM Forward Primer	2.5	0.5 µM
10 µM Reverse Primer	2.5	0.5 µM
Template DNA	Varying (normally 0.5-1)	
dH_2O	To 50	

Table 3.4. Thermocycling conditions for Q5 PCR.

Step	Temperature (°C)	Time	Cycles
Initial denaturation	98	30 seconds	1
Denaturation	98	10 seconds	25-35
Annealing	50-72*	30 seconds	
Elongation	72	20-30 seconds/kb**	
Final elongation	72	2 minutes	1
Hold	4-10	∞	

*The temperature varied depending on which primers being used.

**The length of the annealing step depends on the length of the DNA fragment being copied. The duration of the step is 20-30 seconds per 1000 bp DNA.

3.6.2 PCR using Taq DNA Polymerase

PCR with Red Taq DNA polymerase was essentially used to check if bacteria contained the desired plasmid after transformation. For this purpose, a toothpick was used to transfer bacteria from agar plates to PCR tubes. After the transformation of *L. plantarum*, the PCR tubes were microwaved for 1 minute with full effect to ensure lysis of the cells before adding the rest of the components in the PCR reaction.

Materials

RED Taq DNA Polymerase Master Mix

Primers

Template DNA

dH_2O

0.2 ml PCR tubes

PCR machine (the different PCR machines used are described in section 2.1)

Procedure

1. All the components in Table 3.5 were mixed gently in PCR tubes. The components were kept on ice in-between.
2. If necessary, the samples were spun to collect the liquid at the bottom of the tubes.
3. The tubes were transferred to a PCR machine.
4. The program described in Table 3.6 was followed.

Table 3.5. Components for PCR using Taq DNA polymerase.

Component	Volume (µL)	Final concentration
RED Taq DNA Polymerase Master Mix	25	1x
10 µM Forward Primer	1	0.2 µM
10 µM Reverse Primer	1	0.2 µM
Template DNA	Varying	
dH_2O	To 50	

Table 3.6. Thermocycling conditions for Taq PCR.

Step	Temperature (°C)	Time	Cycles
Initial denaturation	95	2 minutes	1
Denaturation	95	30 seconds	25-35
Annealing	50-65*	30 seconds	
Elongation	72	1 minute/kb**	
Final	72	5 minutes	1
Hold	4-10	∞	

*The temperature varied depending on which primers being used. The annealing temperature was 3-5 °C lower than T_m of the primers.

**The length of the annealing step depended on the length of the DNA fragment being copied. The duration of the step is 1 minute per 1000 bp DNA.

3.7 Agarose gel electrophoresis

Agarose gel electrophoresis is a method used to separate DNA fragments from each other. The fragments are separated by adding voltage, making the DNA fragments move towards a positive pole. The movement of the fragments occurs because of the negative charge of DNA. The DNA fragments are separated based on size, and smaller fragments will move faster on the gel than larger fragments because all DNA fragments have the same amount of charge per mass. peqGREEN is added to each sample applied to the gel to make the DNA fragments visible. By applying a ladder with known sizes along with the samples, the size of the DNA fragments on the gel can be determined.

Materials

1 x TAE Buffer

SeaKem® LE Agarose

peqGREEN

Loading dye

DNA ladder

GelDoc EZ imager

Procedure

1. 12 g SeaKem® LE Agarose was dissolved in 1 L 1 x TAE Buffer to make 1.2 % agarose. The 1.2 % agarose was then autoclaved at 121 °C for 15 minutes and kept at approximately 60 °C until use.
2. One agarose gel was made by mixing 60 ml of the 1.2 % agarose solution and 2.5 µL peqGREEN. The mixture was then poured into a moulding tray with combs.
3. After approximately 20 minutes, the gel was solid, and the combs were removed. The gel was then transferred to an electrophoresis chamber and covered with 1 x TAE Buffer.
4. Loading dye was added to the DNA-samples, and the samples were loaded into wells on the gel. A ladder was also loaded into one well.
5. The gel was run at 90 V for 25-60 minutes, depending on the expected fragment size.
6. GelDoc EZ was used to take pictures of the gel.
7. If DNA-fragments were to be used later, gel-slices with the DNA-fragments were excised using UV-light.

3.8 DNA extraction from agarose gels and DNA purification

The NucleoSpin® Gel and PCR Clean-up kit was used to extract DNA from agarose gels and purify PCR-amplified DNA. Protocol 5.1 or 5.2 provided by the manufacturer was followed, depending on whether PCR-product was purified or DNA was extracted.

3.9 Ligation

For cloning of recombinant DNA into different vectors, ligation is an essential process. Ligation is the covalent linking of two complementary DNA fragments catalyzed by a ligase enzyme. Ligase forms phosphodiester bonds between 3'- hydroxyl and 5' phosphate ends of the DNA fragments.

3.9.1 Quick ligation

Materials

Quick Ligase Reaction Buffer (2X)

Vector DNA

Insert DNA

Nuclease-free Water

Quick Ligase

Procedure

1. NEBioCalculator (https://nebiocalculator.neb.com/#!/ligation) was used to calculate the amount of insert to be added in the reaction. A molar ratio of 1:3 vector to insert was applied, where the amount of vector should be 50 ng.
2. The components in Table 3.7 were gently mixed in an eppendorf tube at room temperature. Quick Ligase was the last component to be added.
3. The mixture was incubated at room temperature (25 °C) for 5 minutes.
4. The mixture was kept on ice for further use or stored at -20 °C.

Table 3.7. Components for Quick ligation.

Component	Volume
Quick Ligase Reaction Buffer (2X)*	10 µL
Vector DNA	50 ng
Insert DNA	x ng**
Nuclease-free Water	Up to 20 µL
Quick Ligase	1 µL

*Quick Ligase Reaction Buffer was thawed and resuspended at room temperature

** The amount of vector and insert should be 50 ng or more.

3.9.2 In-Fusion Cloning

The In-Fusion® HD Cloning Kit is used for the cloning of DNA fragments into any desired vector. What distinguishes in-fusion cloning from other cloning techniques is using the in-fusion enzyme. The enzyme fuses a linearized vector and an insert-fragment by recognizing a 15 base pair overhang at each end of the insert-fragment. Primers are designed with this 15 base pair overhang and are bound to the insert-fragment in a PCR-reaction. The 15 base pairs are complementary to the ends of the linearized vector.

Materials

5X In-Fusion® HD Enzyme Premix

Linearized vector

Purified PCR fragment (insert)

dH_2O

Procedure

1. The In-Fusion molar ratio calculator (https://www.takarabio.com/learning-centers/cloning/primer-design-and-other-tools/in-fusion-molar-ratio-calculator) was used to calculate the amount of insert and vector to be added in the reaction. A molar ratio of 1:2 vector to insert was applied.
2. The components of Table 3.8 were mixed in an eppendorf tube.
3. The mixture was incubated for 15 minutes at 50 °C, then placed on ice.
4. The ligation mix was either transformed into competent cells or stored at -20 °C.

Table 3.8. Components for in-fusion cloning.

Components	**Volume (µL)**
5X In-Fusion® HD Enzyme Premix	2
Vector	x
Insert	x
dH2O	To 10

3.10 Making electrocompetent *Lactobacillus plantarum* WCFS1

Competent cells have the ability to take up free extracellular DNA. When cells take up DNA, they are said to be transformed. Electrocompetent cells take up DNA through electroporation. In electroporation, an electrical pulse is applied to the cells, making the cell wall permeable.

Electrocompetent *L. plantarum* cells were grown in media containing glycine. During growth, the glycine will replace L-alanine in the cell wall, making it more permeable for DNA uptake. The procedure was executed according to the protocol described in (Aukrust et al., 1995).

Materials

MRS

MRS + 1 % glycine

20 % glycine

30 % PEG_{1450}

MRSSM (MRS + 0.5 sucrose + 0.1 M $MgCl_2$)

Procedure

1. *L. plantarum* from glycerol stock was cultured overnight in 10 mL MRS at 37 °C.
2. 1 mL of the overnight culture was used to make a serial dilution (10^{-1} - 10^{-10}) in MRS + 1 % glycine. The cultures were incubated overnight at 37 °C.
3. 1 mL of the culture with an OD_{600} of 2.5 ± 0.5 was further diluted in 20 mL MRS + 1 % glycine. The culture was then grown until it reached the logarithmic phase (OD_{600} of 0.7 ± 0.07) and placed on ice for 10 minutes.
4. The culture was centrifuged for 5000 x g for 5-10 minutes at 4 °C, and the supernatant was discarded.
5. The pellet was resuspended in 5 mL ice-cold fresh 30 % PEG_{1450}. An additional 20 mL of 30 % PEG_{1450} was added, the tube was inverted gently and placed on ice for 10 minutes.
6. The cells were collected by centrifugation for 5000 x g for 5-10 minutes at 4 °C.
7. The pellet was resuspended in 400 µL 30 % $PEG_{1450,}$ and portions of 40 µL were pipetted into eppendorf tubes pre-frozen at -80 °C. The work was performed while the eppendorf tubes were kept on dry ice. The tubes were frozen and stored at -80 °C.

3.11 Transformation

3.11.1 Transformation of Chemically Competent *E. coli*

Materials

BHI agar plates with antibiotics

Falcon 2059 Polypropylene Round Bottom tube, 14 mL

Ligation mix

One Shot™ TOP10 chemically competent *E. coli*

S.O.C. media

Procedure

1. One vial of One Shot™ TOP10 chemically competent *E. coli* was thawed on ice for each transformation.
2. In a chilled Falcon Round Bottom tube, the chemically competent *E. coli* cells and 1 to 5 µL of DNA (10 pg to 100 ng) were added and mixed gently.
3. The tubes were incubated on ice for 30 minutes.
4. The cells were heat-shocked at 42 °C for 30 seconds without shaking and placed on ice for 2 minutes.
5. 250 µL room tempered S.O.C. medium was aseptically added to each tube.
6. The tube was placed horizontally in a shaking incubator at 37 °C for 1 hour at 225 rpm.
7. 100 µL transformation-mix was spread on BHI agar plates with 200 µg/mL erythromycin. The plates were inverted and incubated overnight at 37 °C.
8. The remaining transformation-mix was kept overnight at room temperature in case more cells needed to be plated.
9. Colonies were selected and analyzed by PCR.

3.11.2 Transformation of Electrocompetent *L. plantarum*

Materials

Bio-Rad GenePulser® II

Bio-Rad Pulse controller plus

Electrocompetent *L. plantarum* WCFS1

Electroporation cuvette, Gene Pulser®, 0.2 cm

MRSSM-media

MRS agar plates with antibiotics

Plasmid

Procedure

1. Electrocompetent *L. plantarum* WCFS1 was thawed on ice.
2. 5 µL plasmid was added to the cells.
3. The solution was transferred to a chilled electroporation cuvette without creating air bubbles.
4. An electroporator was set to these parameters:

   Voltage: 1.5 kV

   Capacitance: 25 µF

   Resistance: 400 Ω
5. The cuvette was placed in the electroporator and exposed to an electrical pulse.
6. Immediately after, 450 µL MRSSM was added to the cuvette, and the transformation-mix was transferred to an eppendorf tube.
7. The transformed cells were incubated at 37 °C for 2-4 hours without shaking.
10. 100 µL of the transformation-mix was spread on MRS agar plates with 10 µg/mL erythromycin. The plates were inverted and incubated overnight at 37 °C.
11. The remaining transformation-mix was kept overnight at room temperature in case more cells needed to be plated.

3.12 Sequencing of isolated plasmids

Plasmids were sent for Sanger sequencing to confirm the sequences of the plasmids. In an eppendorf tube, purified plasmid (400-500 ng) was combined with 2.5 µL primer (10 µM) and dH_2O for a total volume of 11 µL. The eppendorf tubes were labeled with a unique barcode before sending them to Eurofins Genomics. The results were analyzed with CLC DNA Main Workbench 7.

3.13 Preparation for analysis of gene products in *L. plantarum*

3.13.1 Cultivation and harvesting

Materials

SppIP (inducer pheromone)

PBS

MRS

Antibiotics

Procedure

1. *L. plantarum* was cultivated in MRS-media with 10 µg/ml erythromycin at 37 °C overnight.
2. The overnight cultures were diluted in 50 ml MRS-media (preheated to 37 °C) with 10 µg/ml erythromycin to an OD_{600} of 0.10-0.15.
3. The dilutions were incubated at 37 °C to an OD_{600} of 0.28-0.33.
4. The cultures were then induced with 25 ng/ml SppIP.
5. The cultures were incubated for three hours at 37 °C, then placed on ice.
6. The bacteria were harvested by centrifuging the cultures at 5000 x g and 4 °C for 5 minutes.
7. The supernatant was poured off before the pellet was washed 1-3 times with 10 ml chilled PBS. The suspension was centrifuged at 5000 x g and 4 °C for 5 minutes.
8. The pellet was resuspended in 1 ml PBS or stored at -20 °C.

3.13.2 Preparation of cell lysate

Materials

PBS

FastPrep® tube

Glass beads

FastPrep® - 24 Tissues and Cell homogenizer

Procedure

1. Harvested bacteria were resuspended in 1 ml PBS, and the suspension was transferred to a FastPrep® tube containing 0.5 g glass beads.
2. The FastPrep® tube was placed in a FastPrep® - 24 Tissues and Cell homogenizer and was run at 6.5 m/s for 45 seconds. The tube was placed on ice for 5 minutes after the run. This was repeated 1-3 times.
3. The tube was centrifuged at 16.100 x g and 4 °C for 1 minute.
4. The supernatant was transferred to an eppendorf tube and centrifuged at 16.100 x g and 4 °C for 1 minute.
5. The protein extract was transferred to a new eppendorf tube and stored at -20 °C.

3.14 Growth curve

Materials

Microwell plate, 96 wells

Multiscan FC

Sealing Film for Microplates

SkanIt Software 2.5.1

Procedure

1. Cultures of 10 ml MRS with 10 µg/ml erythromycin and *L. plantarum* were incubated at 37 °C overnight.
2. The next day, the cultures were diluted in 10 ml prewarmed MRS with 10 µg/ml erythromycin to an OD_{600} of 0.10-0.15. The cultures were incubated at 37 °C until OD_{600} reached 0.27-0.33.

3. 200 µL of the culture was transferred to a sterile 96 well Microwell plate and induced with 25 ng/µL SppIP.
4. Also, 200 µL of the culture was transferred to the sterile 96 well Microwell plate as a control and not induced.
5. The plate was sealed with film before placing it in the Multiscan FC.
6. The growth curve was created with the program SkanIt Software 2.5.1.

3.15 Western blot

Western blotting is a method used to detect specific proteins in a sample using antibody-hybridization. The proteins are first separated by SDS-PAGE gel electrophoresis, then transferred to a membrane by electroblotting. Before the membrane is exposed to antibodies, a blocking solution containing BSA is applied to the membrane. BSA prevents non-specific binding between proteins and the antibody. After blocking, the membrane is exposed to a primary antibody that binds specifically to the target protein. A secondary antibody is then applied to the membrane, which will bind to the primary antibody. The secondary antibody is conjugated with horseradish peroxidase (HRP), an enzyme that produces a detectable light-signal by cleaving a chemiluminescent substrate like luminol. If the protein of interest is present, the protein is visualized.

3.15.1 Gel electrophoresis of proteins

Sodium Dodecyl Sulfate-Polyacrylamide Gel Electrophoresis (SDS-PAGE) is a method used to separate proteins based on their molecular weight when unfolded (denatured). The proteins are denatured by the addition of lithium dodecyl sulphate (LDS), an SDS analog, and dithiothreitol (DTT), and boiling. LDS unfolds proteins by breaking non-covalent bindings, then binds to the proteins to prevent re-folding. Also, LDS is a surfactant, meaning LDS reduces the proteins' intrinsic charge. DTT also helps to denature proteins by breaking the proteins disulfide bridges. Because LDS is a surfactant and negatively charged, LDS-bound proteins will have a net negative charge. When a current is applied, the LDS-bound proteins will migrate towards a positively charged anode. Proteins with lower molecular weights will migrate longer than those with higher weight because of the pore structure of the polyacrylamide gel. A protein standard with known molecular weights is used to determine the weight of the proteins.

Materials

Novex® NuPAGE® SDS-PAGE Gel system

TGS-buffer

Magic Mark XP Western Protein Standard

Procedure

1. 7.5 µL LDS sample buffer (4 x) and 3 µL reducing agent (10 x) were mixed. 10 µL of this mix was added to 20 µL protein extract (prepared as described in section 3.13).
2. The samples were incubated in a boiling water bath for 10 minutes.
3. A NuPAGE® Novex Bis-Tris gel was placed in an electrophoresis chamber, and TGS-buffer was added to the chamber.
4. The boiled samples and Protein Standard was loaded onto the gel.
5. The gel was run for 30 minutes at 200 V.

3.15.2 Blotting with eBlot™ Fast Transfer System

The eBlot™ L1 Fast Wet Transfer System contained a PVDF membrane and was used when blotting TB antigens. For the SARS-CoV-2-antigens, a nitrocellulose membrane was used instead of the PVDF membrane. An advantage of the nitrocellulose membrane compared to the PVDF is lower background noise.

Materials

eBlot™ L1 Fast Wet Transfer System

10 % ethanol

100 % ethanol

Distilled water

Membrane (Nitrocellulose or PVDF)

Procedure

1. The protein gel (from section 3.15.1) was equilibrated with 10 % ethanol for 5-10 minutes, then placed in distilled water.
2. The PVDF membrane was activated in 100 % ethanol, then soaked in approximately 10 ml membrane equilibration buffer. The nitrocellulose membrane was only treated with equilibration buffer before placed in the transfer cassette.
3. The sponges, membrane and protein gel, was placed in a transfer cassette on the side marked "+" as shown in Figure 3.1. A roller was used to remove air bubbles between the gel and membrane.

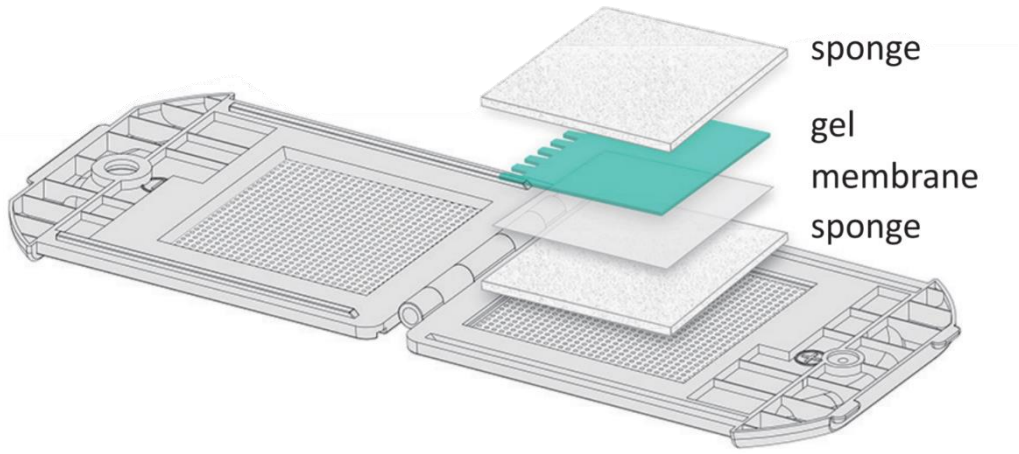

Figure 3.1. eBlot^{TM} L1 Fast Wet Transfer System.

4. The transfer cassette was closed and placed back in the instrument of the eBlotTM L1 Fast Wet Transfer System, and the program was run.
5. When the blotting was finished, the membrane was ready for hybridization.

3.15.3 SNAP i.d.® immunodetection for TB

SNAP i.d.® immunodetection system is used for hybridization of antibodies to the proteins on the membrane. The advantage of the system is using a vacuum to run the blocking solution, washing solution (TTBS) and antibodies through the membrane. Using the vacuum system reduces the time used for hybridization compared to more traditional hybridization methods.

Materials

SNAP i.d.® Protein Detection System

TTBS (TBS + 0.1 % w/v Tween-20)

Blocking solution (TTBS + 3 % BSA)

ESAT6 Mouse mcAb (ab26246) (1:1000)

HRP-Rabbit Anti-Mouse IgG (A9917) (1:20000)

Procedure

1. The blot holder was opened and wetted with distilled water before the blotted membrane (from section 3.15.2) was placed in the blot holder with the protein side downwards. The blot roller was used to remove any air bubbles.
2. The blot holder was placed with the protein side upwards in the SNAP i.d.® Protein detection system device.
3. 30 ml of the blocking solution was poured into the container (10 ml at a time), and the vacuum was turned on until all the blocking solution had gone through.
4. The primary antibody was diluted 1:1000 in 3 ml blocking solution. The solution was gently mixed before it was poured into the container and incubated for 10 minutes. The vacuum was turned on until the solution had gone through.
5. The membrane was washed three times with TTBS, 10 ml each time. The vacuum was turned on until all the liquid had gone through.
6. The secondary antibody was diluted 1:20000 in 3 ml blocking solution. The solution was gently mixed before it was poured into the container and incubated for 10 minutes. The vacuum was turned on until the solution had gone through.
7. Step 5 was repeated.
8. The membrane was removed from the blot holder, ready to detect the target proteins (section 3.15.5).

3.15.4 Hybridization of antibodies for SARS-CoV-2

This hybridization method is more traditional than the SNAP i.d.® immunodetection hybridization method. It uses a shaking device instead of a vacuum and therefore uses longer time, but the background noise is reduced compared with the SNAP i.d.® immunodetection.

Materials

TBS

TTBS (TBS + 0.05 % w/v tween-20)

Blocking buffer (5 % BSA in TBS)

SARS-CoV/SARS-CoV-2 Spike RBD Polyclonal Antibody (MBS2563840) (1 mg/ml)

HRP-Goat Anti-Rabbit IgG (65-6120) (1 mg/ml)

Procedure

1. The blotted nitrocellulose membrane (from section 3.15.2) was transferred with the protein side upwards to 25 ml TBS. The membrane was washed for 10 minutes with shaking before TBS was removed.
2. Another 25 ml TBS was poured over the membrane and washed the same way as in step 1.
3. The membrane was incubated in 25 ml blocking buffer for 1 hour with shaking.
4. The membrane was washed in 25 ml TTBS for 10 minutes with shaking. This step was repeated one time.
5. The membrane was washed in 25 ml TBS for 10 minutes with shaking.
6. The membrane was incubated in 15 ml blocking buffer with 4.5 µL of the primary antibody for 15 minutes with shaking at room temperature. The membrane (still in blocking buffer with primary antibody) was incubated overnight at 4 °C with shaking. Finally, the membrane (still in blocking buffer with primary antibody) was incubated at room temperature for 30 minutes with shaking.
7. The membrane was washed in 25 ml TTBS for 10 minutes with shaking. This step was repeated one time.
8. The membrane was washed in 25 ml TBS for 10 minutes with shaking.
9. The membrane was incubated in 15 ml blocking buffer with 2.25 µL of the secondary antibody for 1 hour with shaking at room temperature.
10. The membrane was washed in 25 ml TTBS for 10 minutes with shaking. This step was repeated 3 times.
11. The membrane was ready for the detection of the target proteins.

3.15.5 Detection of proteins using chemiluminescence

Materials

SuperSignal® West Pico Chemiluminescent Substrate

Luminol/Enhancer

Stable Peroxide Buffer

Procedure

1. 5 ml of Luminol/Enhancer and 5 ml of Stable Peroxide Buffer was mixed to a substrate solution.
2. The membrane (from section 3.15.3 or 3.15.4) was incubated in the substrate solution for 5 minutes without light exposure.
3. Azure c400 was used for visualization and imaging of the membrane.

3.16 Detection of antigens localized on the surface of *L. plantarum*

For detecting proteins localized on the surface of bacteria, a method involving antibodies conjugated with different fluorochromes can be used. A fluorochrome is a fluorescent compound that absorbs light of certain wavelengths and then emits the light at longer wavelengths. First, a primary antibody will bind to the target protein, then a secondary antibody with attached fluorochrome binds to the primary antibody. In this study, the fluorochrome used is Fluorescein Isothiocyanate (FITC). Surface localized proteins can be visualized by analyzing the FITC-stained cells with flow cytometry or confocal laser scanning microscopy.

3.16.1 Flow cytometry analysis

In flow cytometry, one cell at a time flows through a laser beam. Cells that have proteins on their surface with FITC attached to them will be detected. FITC absorbs light from the laser beam, emits the light, and a fluorescent signal is registered.

Materials

PBS

BSA

Primary antibodies: ESAT6 Mouse mcAb (ab26246) (1.02 mg/ml) or SARS-CoV/SARS-CoV-2 Spike RBD Polyclonal Antibody (MBS2563840) (1 mg/ml)

Secondary antibodies: Anti-Mouse IgG-FITC (F0257) or Anti-Rabbit IgG-FITC (F9887)

MacsQuant® Analyser and MacsQuantify™ software

Procedure

1. *L. plantarum* cells were prepared the same way as described in step 1-5 in section 3.14.1.
2. OD_{600} of the cultures were measured. Based on OD_{600}, estimated volumes of the cultures were harvested; 500 µl of cultures with OD_{600} of 1, 250 µl of cultures with OD_{600} of 1.
3. The cells were harvested by centrifuging the cultures at 5000 x g for 3 minutes, and the supernatant was discarded.
4. The cells were washed with 500 µL PBS and centrifuged at 5000 x g for 3 minutes, and the supernatant was discarded.
5. 50 µL PBS + 2 % BSA and 0.2 µL primary antibody was added to each sample, and the pellet resuspended. For SARS-CoV-2-antigens, primary antibody SARS-CoV/SARS-CoV-2 Spike RBD Polyclonal Antibody (A9917) was added, and for TB antigens, primary antibody ESAT6 Mouse mcAb (ab26246) was added. The cells were incubated with the primary antibody for 30 minutes at room temperature.
6. The samples were centrifuged at 5000 x g for 1 minute, and the supernatant pipetted off.
7. The cells were washed three times with 600 µL PBS + 2 % BSA and centrifuged at 5000 x g for 2 minutes.
8. 50 µL PBS + 2 % BSA and 0.3 µL secondary antibody was added to each sample, and the pellet resuspended. For SARS-CoV-2-antigens, secondary antibody Anti-Rabbit IgG-FITC (F9887) was added, and for TB antigens, secondary antibody Anti-Mouse IgG-FITC (F0257) was added. The cells were incubated with the secondary antibody for 30 minutes at room temperature without light exposure. After the addition of the secondary antibody, the samples were kept from light.

9. The samples were centrifuged at 5000 x g for 1 minute, and the supernatant pipetted off.
10. The cells were washed four times with 600 µL PBS + 2 % BSA and centrifuged at 5000 x g for 2 minutes.
11. The cells were resuspended in 1 ml PBS.
12. 100 µL of the sample was diluted in 900 µL PBS and mixed by pipetting. The samples were now analyzed by MacsQuant® Analyser and MacsQuantify™ software.

3.16.2 Confocal laser scanning microscopy

Confocal laser scanning microscopy follows the same principle as flow cytometry for detecting proteins on the cell surface. The same steps described in section 3.16.1 was executed for confocal laser scanning microscopy. The samples were analyzed with Zeiss LSM 700 Confocal Microscope and Zen software.

4 Results

In the following chapter, the results of this study are introduced. A total of seven vectors were constructed, three vectors containing *M. tuberculosis* antigens and four vectors containing SARS-CoV-2 antigens. The pSIP system (described in section 1.4) was used to construct all seven vectors. The vectors were constructed in *E. coli*, then transformed into *L. plantarum*. Growth curve analysis, western blot analysis and flow cytometry analysis were conducted on the recombinant *L. plantarum* containing all the different constructed vectors. The growth curve analysis was used to analyse the growth of the recombinant bacteria after they had been induced with the inducer peptide SppIP. The western blot analysis was used to analyse production of the antigens in *L. plantarum*. To detect surface displayed antigens, flow cytometry analysis was used. In addition, fluorescence microscopy was also used to detect surface displayed antigens on the recombinant bacteria. All the recombinant bacteria analysed with western blot, flow cytometry and fluorescence microscopy where also induced with SppIP. The results for the TB-constructs and SARS-CoV-2-constructs were divided into two main sections.

4.1 Tuberculosis constructs

In the present study, the TB antigens Ag85B, ESAT6 and Rv2660c (named H56) was selected for development of a recombinant vaccine delivery bacterium. The H56 fusion protein was selected because it has shown to elicit a robust immune response in animal studies (Aagaard et al., 2011). Three different vectors containing the H56 fusion protein was constructed, each with a different anchor. The anchors cloned into these vectors were a lipoprotein anchor, a LPXTG peptidoglycan anchor (LPXTG anchor) and a LysM anchor.

Previously, the antigens Ag85B and ESAT6 (named H1) has been anchored to the cell surface of *L. plantarum* showing promising immune responses (Kuczkowska et al., 2016). But the studies of Aagaard et al. (2011) showed that the H56 fusion antigen provided better immune responses than the H1 fusion antigen. The H56 fusion protein has not previously been expressed and displayed at the surface of *L. plantarum*.

4.1.1 Construction of TB antigen vectors

All the TB-vectors containing the H56 antigen were constructed based on the plasmid pJET1.2_ESAT6-Rv266v (described in Table 2.2). A dendritic cell (DC) binding sequence was included in all the constructs.

For construction of the lipoprotein anchored H56 vector, the plasmid pJET1.2_ESAT6-Rv266v was digested with the restriction enzymes KpnI and HindIII (Figure 4.1). The resulting 564 bp ESAT6_Rv2660c_DC fragment was ligated into the KpnI/HindIII digested pLp1261_H1, yielding pLp1261_H56 (Figure 4.1).

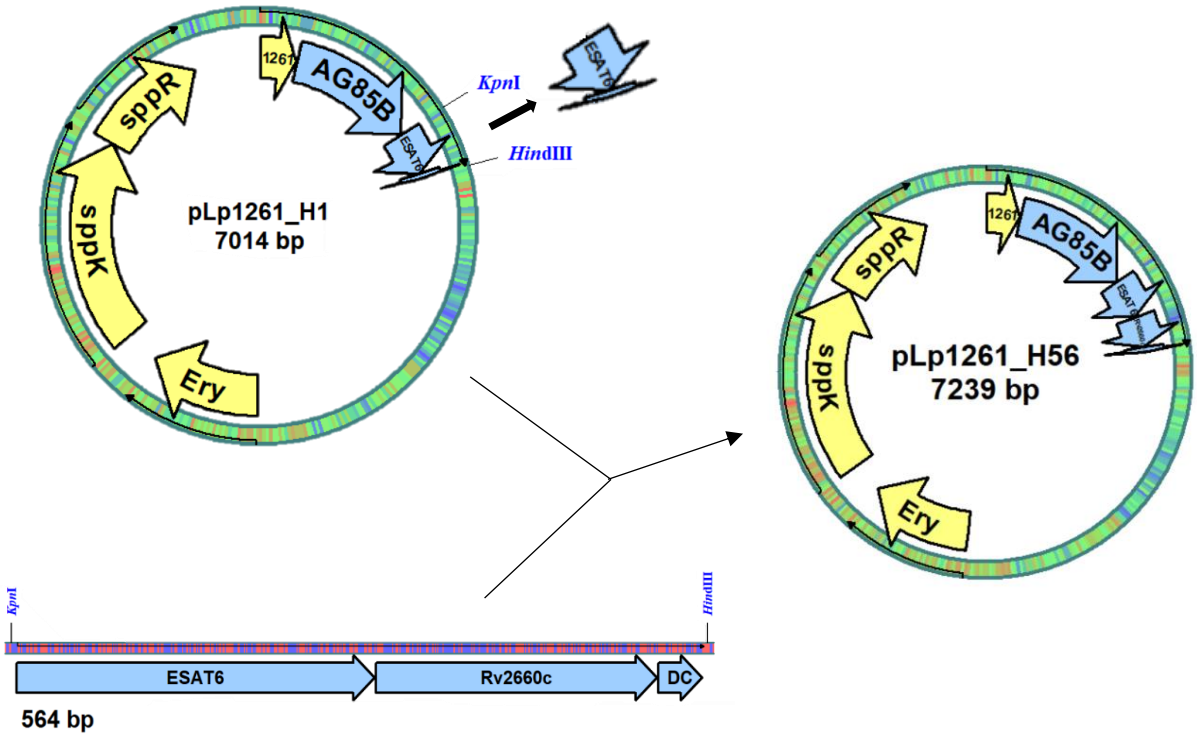

Figure 4.1. Strategy for constructing the pLp1261_H56 vector.

The LysM anchored plasmid pLp3014_H56 was constructed by digesting the 7239 bp pLp1261_H56 fragment and the 7415 bp pLp3014_H1 fragment with SalI and HindIII (Figure 4.2). With these enzymes, H56 and H1 were cut out of their respective plasmids. H56 and pLp3014 were then ligated, yielding pLp3014_H56 (Figure 4.2).

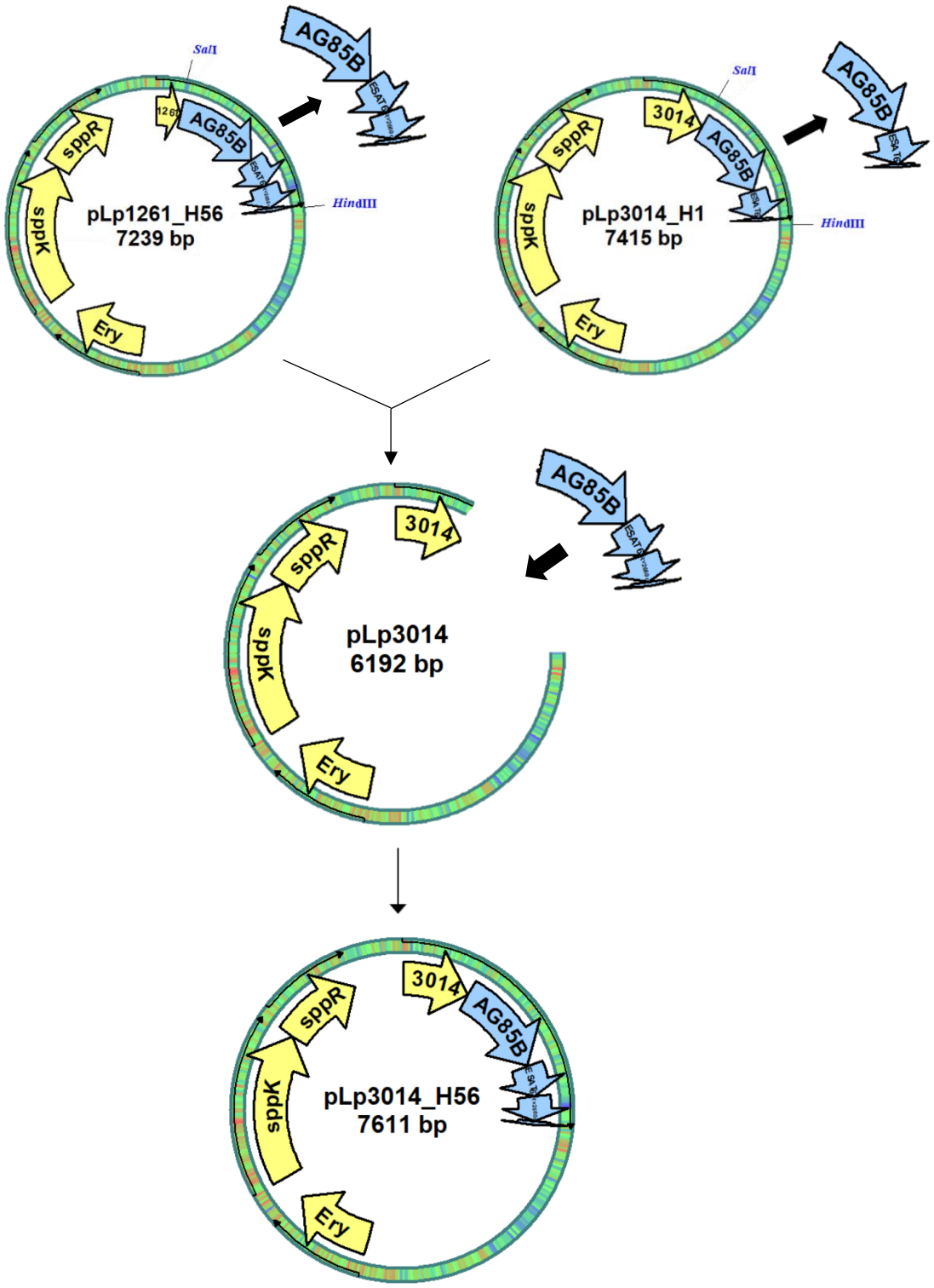

Figure 4.2. Strategy for constructing the pLp3014_H56 vector.

The LPXTG anchored plasmid pLp3001_H56 was constructed with the In-Fusion primers 1643_H56_F and 1643_H56_R (described in Table 2.3). The primers 1643_H56_F and 1643_H56_R were used to amplify the 548 bp ESAT6_RV2660c fragment with the 7239 bp pLp1261_H56 fragment as template (Figure 4.3). The 7590 bp pLp3001_H1 fragment was digested by KpnI and MluI, thereby removing the antigen ESAT6 (Figure 4.3). In the plasmid pLp3001_H1, ESAT6 was replaced with the 548 bp PCR product ESAT6_RV2660c by ligation, yielding pLp3001_H56 (Figure 4.3).

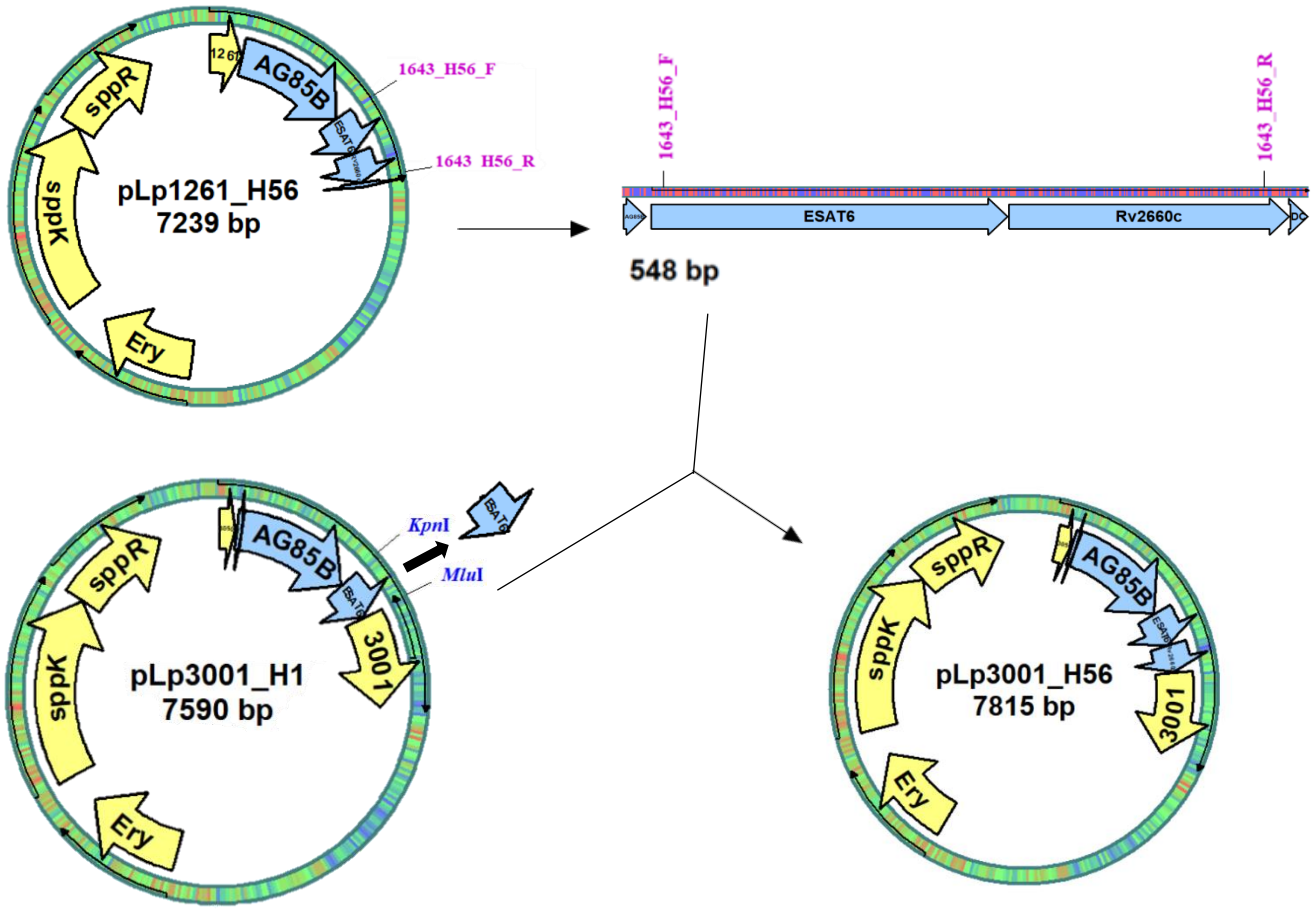

Figure 4.3. Strategy for constructing the pLp3001_H56 vector.

After ligation, all of the plasmids (described in detail in Table 2.2) were transformed into One Shot™ TOP10 chemically competent *E. coli*. All the plasmids were sequenced to confirm correct sequence. After verification of successful sequencing, the plasmids were transformed into electrocompetent *L. plantarum* WCFS1.

4.1.2 Growth curve analysis of *L. plantarum* harbouring TB plasmids

To investigate the influence of expression of the H56 antigen on the growth of *L. plantarum*, a growth curve analysis was used.

The growth curves of *L. plantarum* harbouring the different TB-constructs are shown in Figure 4.4. 200 µL of both induced bacteria and non-induced cultures (see section 3.14) were transferred to a 96 well Microwell plate and the growth was followed for 24 hours while OD_{620} was measured every 5 minutes. All the samples were grown as triplicates, and the mean of these represents the growth curves in Figure 4.4. The growth curve analysis was executed two times with similar results.

Figure 4.4 shows both uninduced (the dotted curves) and induced (the continuous colored curves) *L. plantarum* harbouring the various TB-constructs. *L. plantarum* harbouring pEV is included in the growth curve analysis as a negative control (the black curve). There are great differences between the uninduced and induced curves, the growth of the induced curves are significantly lower than the uninduced. Within the induced curves, there are also clear differences between the different anchors; the lipoprotein anchor pLp1261 shows a higher growth rate than the two anchors cell wall anchors, pLp3001 and pLp3014 (LysM anchor). All the uninduced curves and the pEV curve have similar growth curves, which is expected since no antigens are expressed.

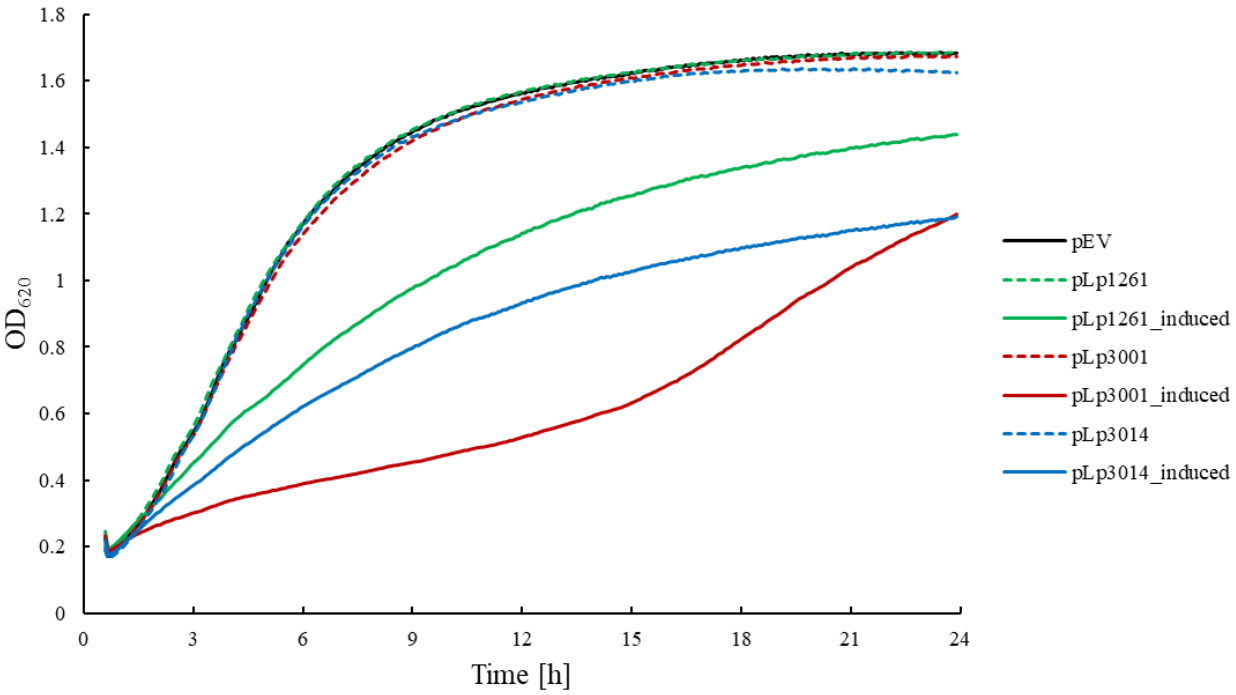

Figure 4.4. Growth curves of *L. plantarum* harbouring the different TB-constructs. All the plasmids contain the H56 fusion protein.

4.1.3 Detection of TB antigens using western blot analysis

Western blot was used to analyse the antigen production in *L. plantarum*. *L. plantarum* harbouring the different TB-constructs were harvested three hours after induction with 25 ng/µL SppIP for western blot analysis (section 3.13.1). Further, the cells were lysed to gain access to the proteins (section 3.13.2) and the crude protein extract were run on an SDS-PAGE (section 3.15.1) before blotting the proteins onto a membrane (section 3.15.2). The antigens were hybridized with specific antibodies (section 3.15.3) using the SNAP i.d. immunodetection system and proteins were visualized with chemiluminescence (section 3.15.5).

Figure 4.5 shows clear bands for all the three anchors (pLp1261, pLp3001 and pLp3014) fused with H56. The theoretical molecular weights of the target proteins are 58 kDa (pLp1261_H56), 73 kDa (pLp3001_H56) and 72 kDa (pLp3014_H56), which fit with the observed weights of the fusion antigen, although the weight of the LPXTG anchor pLp3001_H56 was slightly higher than expected. pEV was included as a negative control and gave only very faint bands (Figure 4.5).

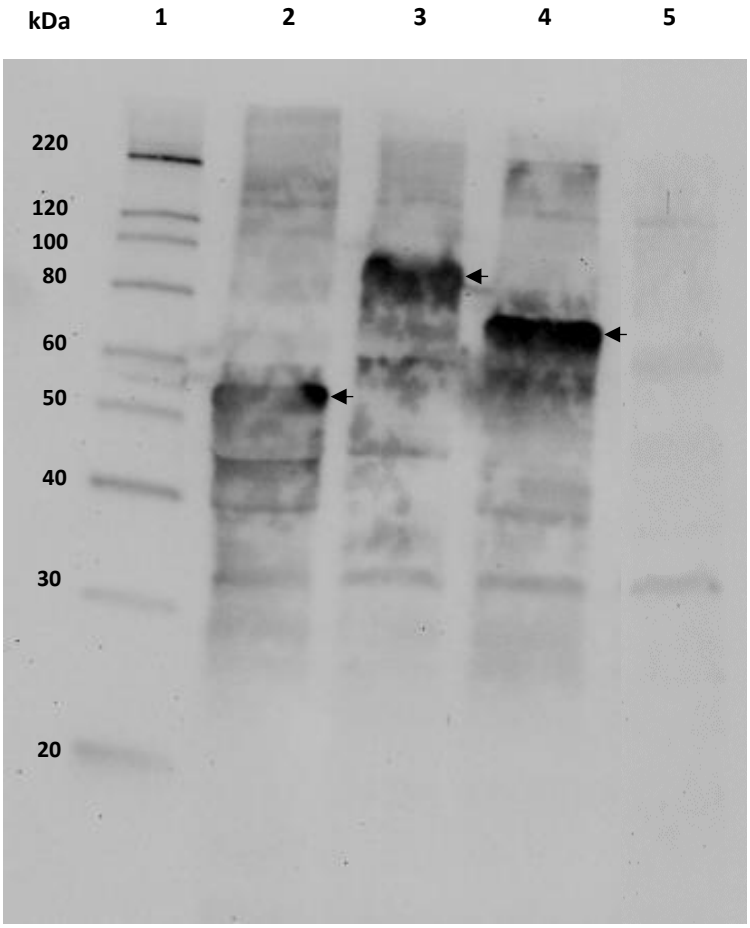

Figure 4.5. Western blot of the TB antigen (H56) fused with different anchors.
Well 1: Magic Mark XP Western Protein Standard; Well 2: pLp1261_H56; Well 3: pLp3001_H56; Well 4: pLp3014_H56; Well 5; pEV.

4.1.4 Detection of TB antigens localized on the surface of *L. plantarum* using flow cytometry

Flow cytometry was used to analyse antigen display on the surface of *L. plantarum*. Antigens on the surface of the bacteria are detected because of antibody-hybridization; secondary antibodies carrying a FITC molecule is attached to the primary antibody, which again is attached to the antigen. The shift along the x-axis in the figures showing the flow cytometry results represents the strength of the fluorescent signal which depends on the number of FITC molecules present. The number of FITC molecules again represent displayed antigens on the surface of the bacteria. For flow cytometry analysis, *L. plantarum* containing the different TB constructs were harvested three hours after induction with 25 ng/ml SppIP before treated with antibodies (see section 3.16.1). In all flow cytometry analysis, a negative control, *L. plantarum* harbouring pEV, was included.

Figure 4.6 shows flow cytometry analysis performed on *L. plantarum* harbouring the TB-constructs, pLp1261_H56 (the lipoprotein anchor), pLp3001_H56 (the LPXTG anchor), pLp3014_H56 (the LysM anchor) and pEV. The LysM anchored H56 showed the strongest signal, determined by its position on the x-axis. The weakest signal was shown for the lipoprotein anchored H56. However, all of the recombinant bacteria with surface anchored H56 clearly have a stronger signal compared to the negative control, pEV.

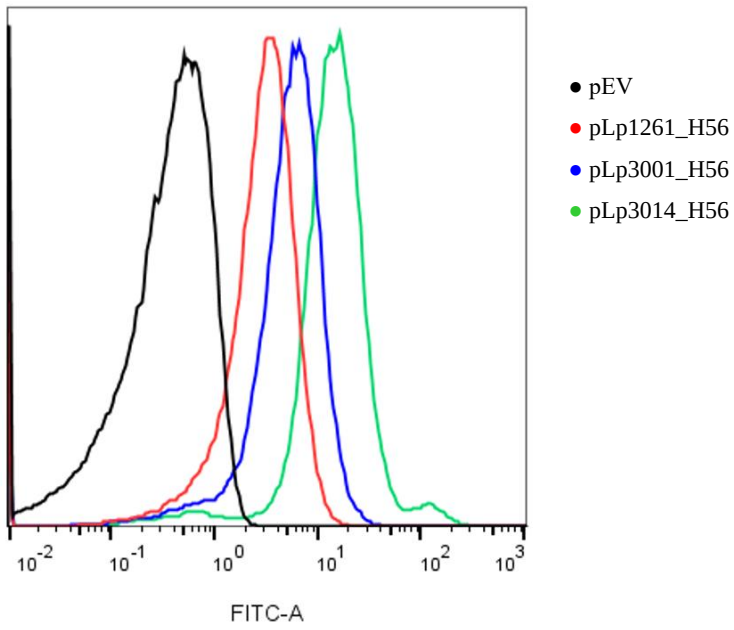

Figure 4.6. Flow cytometry analysis of *L. plantarum* harbouring the TB constructs. *L. plantarum* harbouring pEV was included as a negative control. The fluorescence intensity is shown along the x-axis.

To test the effect of the primary antibody ESAT6 Mouse mcAb (ab26246) on the fluorescent signal in the flow cytometry analysis, *L. plantarum* harbouring the lipoprotein anchored H56 (pLp1261_H56) was hybridized with different primary antibody concentrations. It is desired to use as the lowest amount of antibodies as possible due to the high costs. Previously, an antibody concentration of 4.08 ng/µL has been used as a standard for flow cytometry analysis of *L. plantarum* harbouring TB antigens. The aim of this experiment was to find the lowest possible antibody concentration that gives a strong fluorescent signal when analysing *L. plantarum* harbouring TB antigen constructs. In initial analysis, only *L. plantarum* harbouring the lipoprotein anchored H56 was analysed.

In Figure 4.7, different primary antibody concentrations were applied to *L. plantarum* harbouring the plasmid containing lipoprotein anchored H56 for the flow cytometry analysis described in section 3.16.1. The different concentrations of the primary antibody (ESAT6 Mouse mcAb (ab26246)) applied to *L. plantarum* harbouring the lipoprotein anchored H56 plasmid in Figure 4.7 were 0.51, 1.02, 2.04 and 4.08 ng/µL. The primary antibody concentration applied to the negative control, *L. plantarum* harbouring pEV, was 4.08 ng/µL. The fluorescent signal correlated to the amount of primary antibody the lipoprotein anchored H56 protein were treated with; the more primary antibody the proteins were treated with, the stronger the signal was (Figure 4.7).

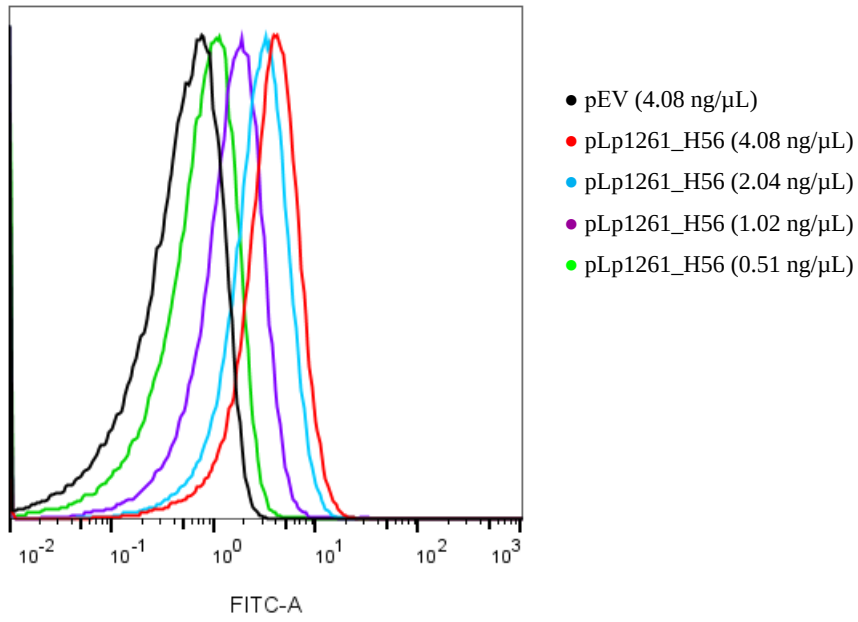

Figure 4.7. Flow cytometry analysis of *L.plantarum* harbouring pLp1261_H56. The bacteria were treated with different primary antibody concentrations in the analysis. *L. plantarum* harbouring pEV was included as a negative control. The fluorescence intensity is shown along the x-axis.

In Figure 4.8, the correlation between Median Fluorescence Intensity (MFI) and primary antibody (PA) concentration for the lipoprotein anchored H56 protein is shown. The four points in the figure represent the primary antibody concentration the lipoprotein anchored H56 protein was hybridized with, and its corresponding MFI value. The MFI values corresponds to the histograms shown in Figure 4.7. The trendline between the points was linear at first, from approximately 0.5-2 ng/µL PA, but from approximately 2-4 ng/µL, the line began to flatten out (Figure 4.8).

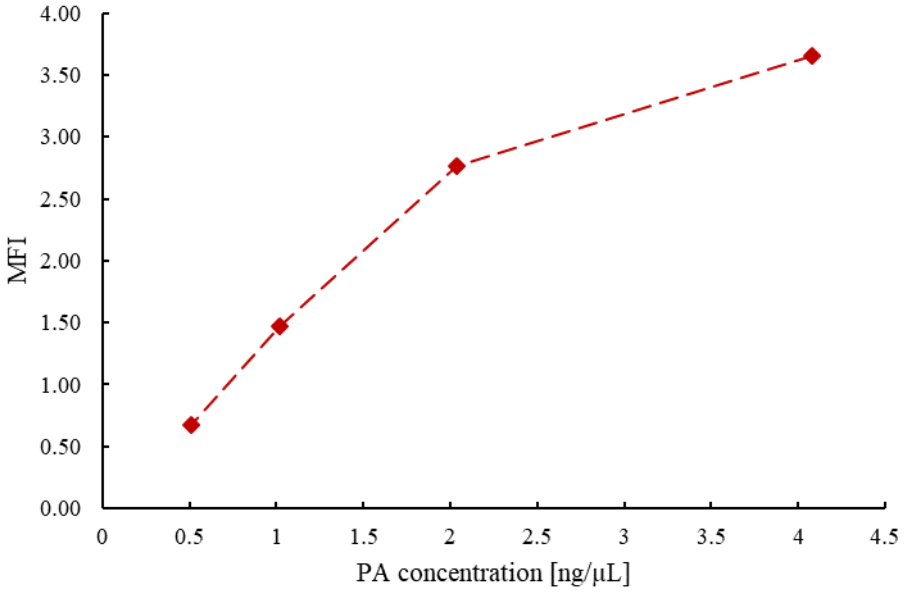

Figure 4.8. Median Fluorescence Intensity (MFI) plotted against PA concentration for the lipoprotein anchored H56 antigen (pLp1261_H56).

4.1.5 Detection of TB antigens localized on the surface of *L. plantarum* using fluorescence microscopy

In addition to flow cytometry analysis, fluorescence microscopy was also used to visualise antigen display on the surface of *L. plantarum*. *L. plantarum* harbouring the TB-constructs were harvested three hours after induction with 25 ng/ml SppIP and further treated as described in see section 3.16.2. The samples analysed with flow cytometry (Figure 4.6) were also analysed and imaged under the fluorescence microscope (Figure 4.9).

Figure 4.9 indicates that all recombinant bacteria have the antigen (H56) successfully exposed at the surface. Still, the LPXTG anchor (pLp3001_H56) and the LysM anchor (pLp3014_H56) (Figure 4.9 C and D, respectively) gave a stronger signal than the lipoprotein anchor (pLp1261_H56) (Figure 4.9 B). *L. plantarum* harbouring pEV were the only bacteria that gave no signal, as expected.

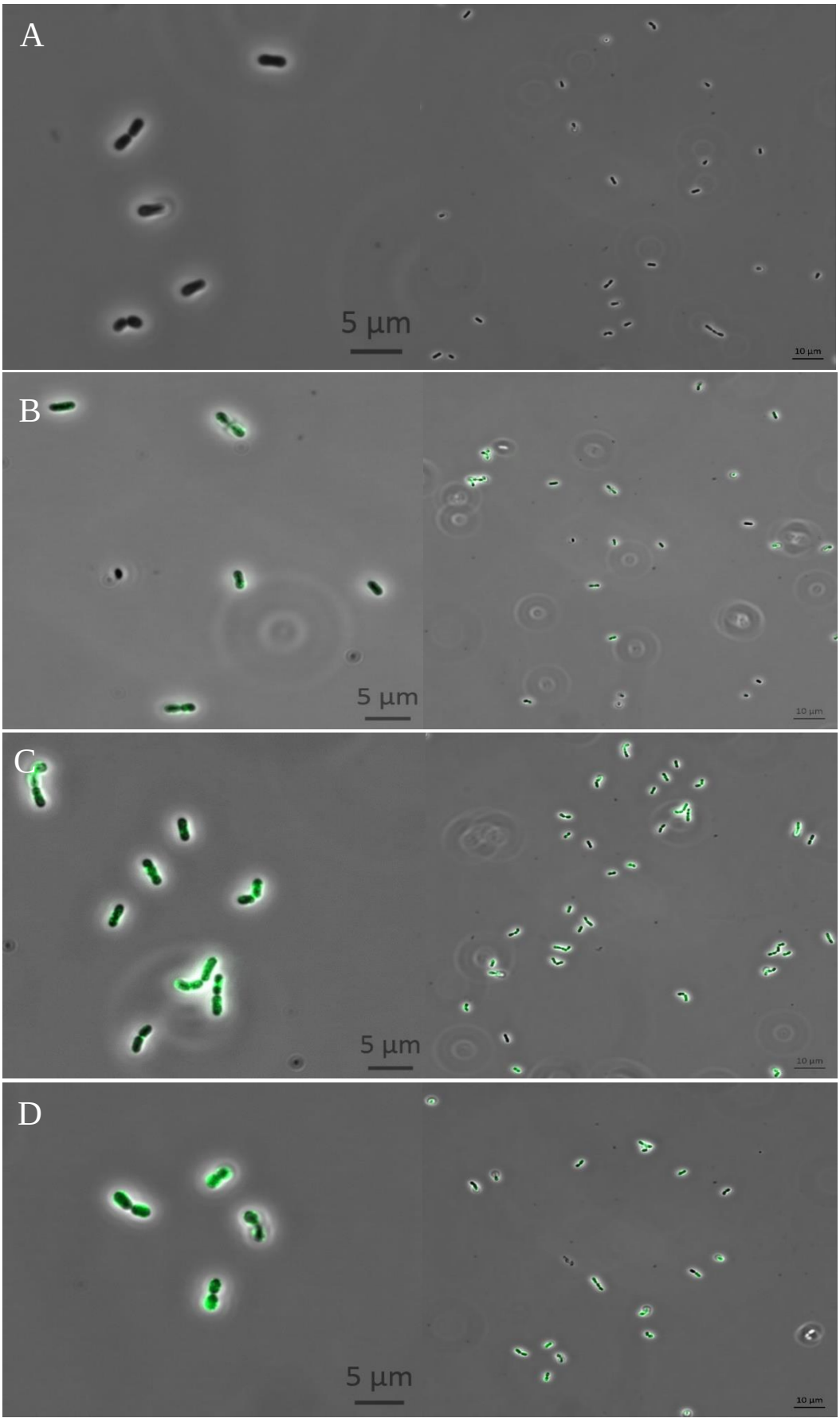

Figure 4.9. Microscopy of fluorescent recombinant *L. plantarum*. A: pEV; B: pLp1261_H56; C: pLp3001_H56; D: pLp3014_H56. The scale bar is 5 and 10 µm in the right and left image, respectively. The green colour indicates the bacteria stained with FITC-A.

4.2 SARS-CoV-2 constructs

In addition to constructing TB-vectors containing the H56 antigen, SARS-CoV-2 plasmids were constructed. The SARS-CoV-2 plasmids contained two subunits of the spike protein derived from SARS-CoV-2. The two subunits were the receptor-binding domain (RBD) and the N-terminal domain (NTD), and the SARS-CoV-2 plasmids contained either RBD or both NTD and RBD. SARS-CoV-2 is a novel virus, and antigens from the virus have not previously been expressed and displayed at the surface of *L. plantarum*.

The spike protein is the part of SARS-CoV-2 used to gain access to the host cells and thus replicate. RBD and NTD play essential parts in binding to the host cells and are vital for the virus, hence why these antigens were chosen to be expressed by *L. plantarum*. The amino acid sequence of the two subunits (NTD and RBD) was codon-optimized for *L. plantarum* (Figure 4.10).

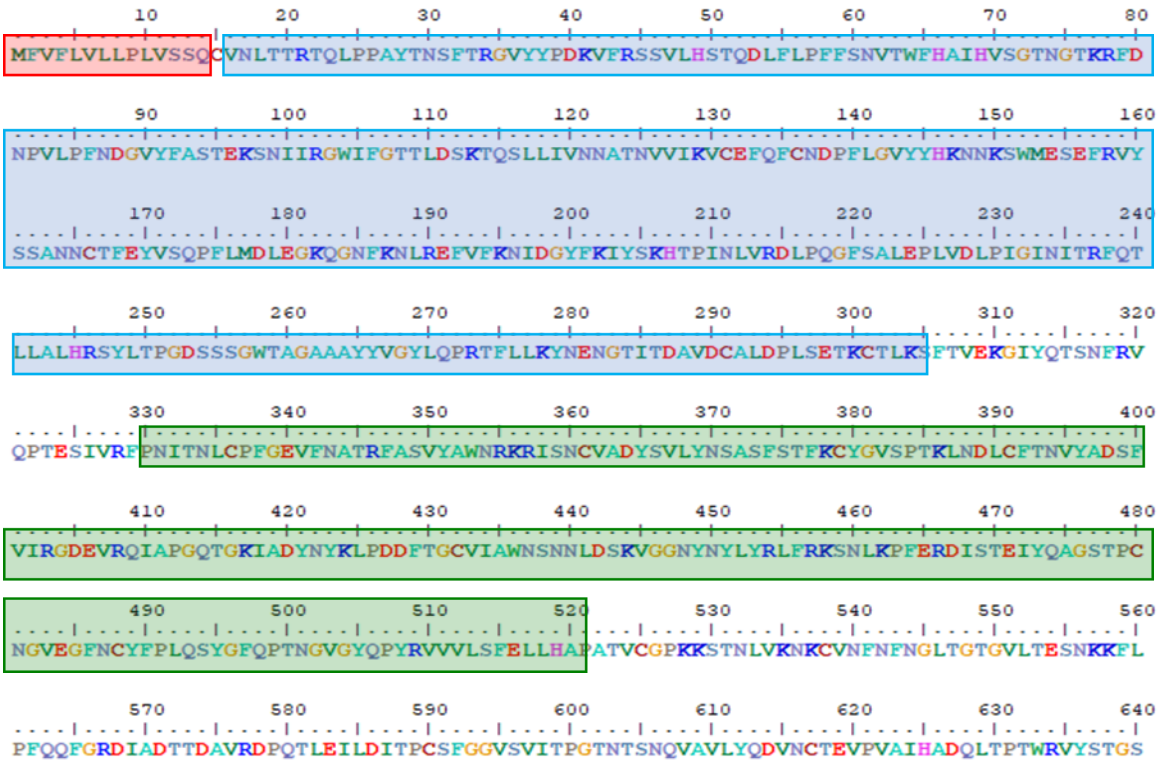

Figure 4.10. Predicted structure of the NTD and RBD domains of the spike protein. Red: signal sequence; Blue: NTD (N-terminal domain) (33 kDa); Green: RBD (receptor-binding domain), ACE2 receptor (21 kda). NTD_RBD antigen size: 57 kDa. The area between the RBD and NTD domain was called the linker region (aa 306-329). The figure was based on (Wrapp et al., 2020).

Anchoring of the SARS-CoV-2 antigens was achieved using the lipoprotein anchor and the LPXTG anchor, the same anchors used for anchoring of TB antigens. Two SARS-CoV-2 plasmids containing the lipoprotein anchor and two SARS-CoV-2 vectors containing the LPXTG anchor were constructed, where one of each vector expressed only RBD, and the two others expressed NTD_RBD.

4.2.1 Construction of SARS-CoV-2-antigen vectors

The pUC57_DC_NTD_RBD plasmid, containing codon-optimized sequence for *L. plantarum* of the NTD and RBD subunits (described in Table 2.2), was the basis for the construction of all the SARS-CoV-2-vectors. For all the constructs, a DC binding sequence was included, similar to the TB-constructs previously described.

The LPXTG anchored NTD_RBD plasmid (pLp3001_NTD_RBD) was constructed by digesting the 7590 bp pLp3001_H1 fragment and pUC57_DC_NTD_RBD with SalI/MluI (Figure 4.11). The H1 antigen was removed from the LPXTG anchored plasmid and replaced with the 1587 bp NTD_RBD fragment through ligation, yielding pLp3001_NTD_RBD (Figure 4.11).

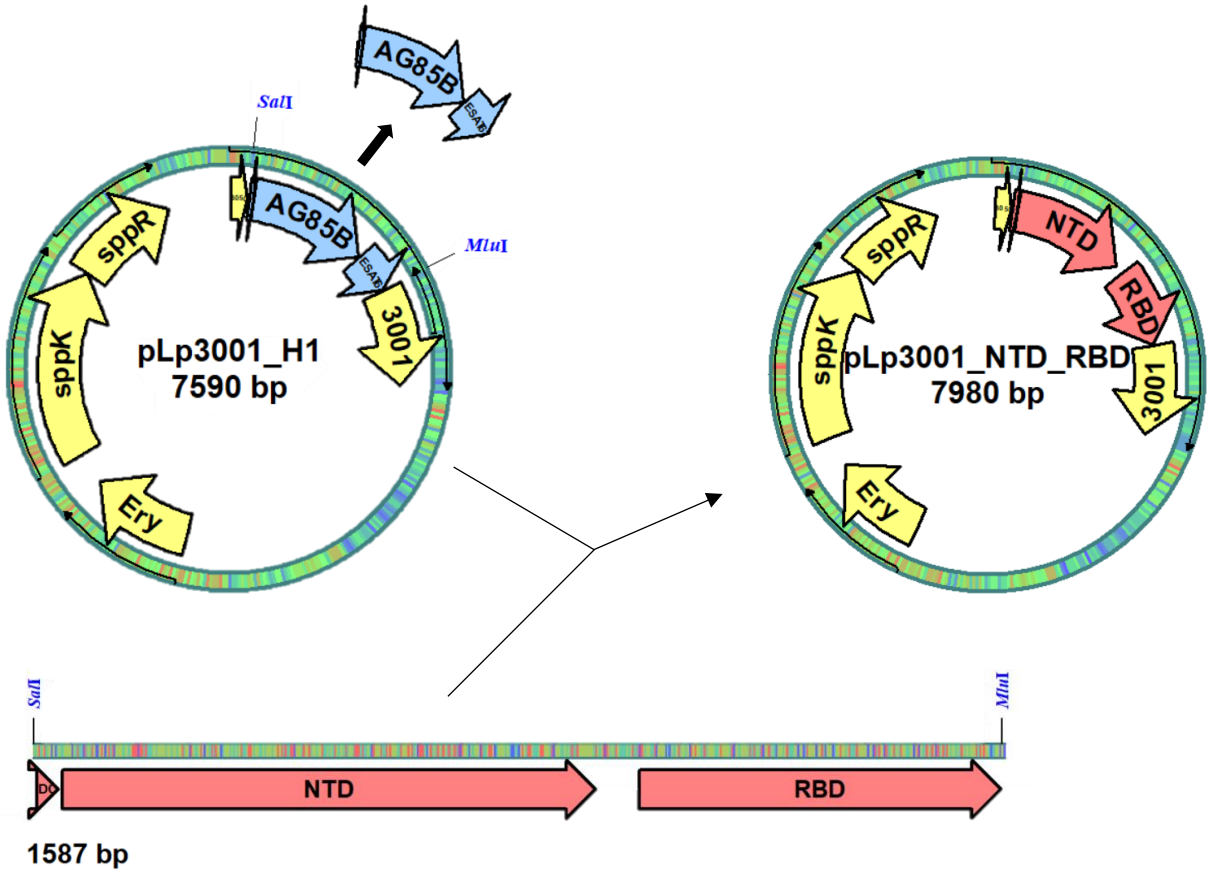

Figure 4.11. Strategy for constructing the pLp3001_NTD_RBD vector.

The LPXTG anchored RBD plasmid (pLp3001_RBD) and the lipoprotein anchored RBD and NTD_RBD plasmids (pLp1261_RBD and pLp1261_NTD_RBD) were constructed using In-Fusion cloning. For pLp3001_RBD, the primers 3001_RBD_F and 3001_RBD_R (described in Table 2.3) were used to amplify the RBD subunit of the spike protein using pUC57_DC_NTD_RBD as a template. The 7590 bp pLp3001_H1 fragment was digested with SalI and MluI, and the amplified 665 bp PCR fragment was ligated to the digested pLp3001_H1 fragment, yielding pLp3001_RBD (Figure 4.12).

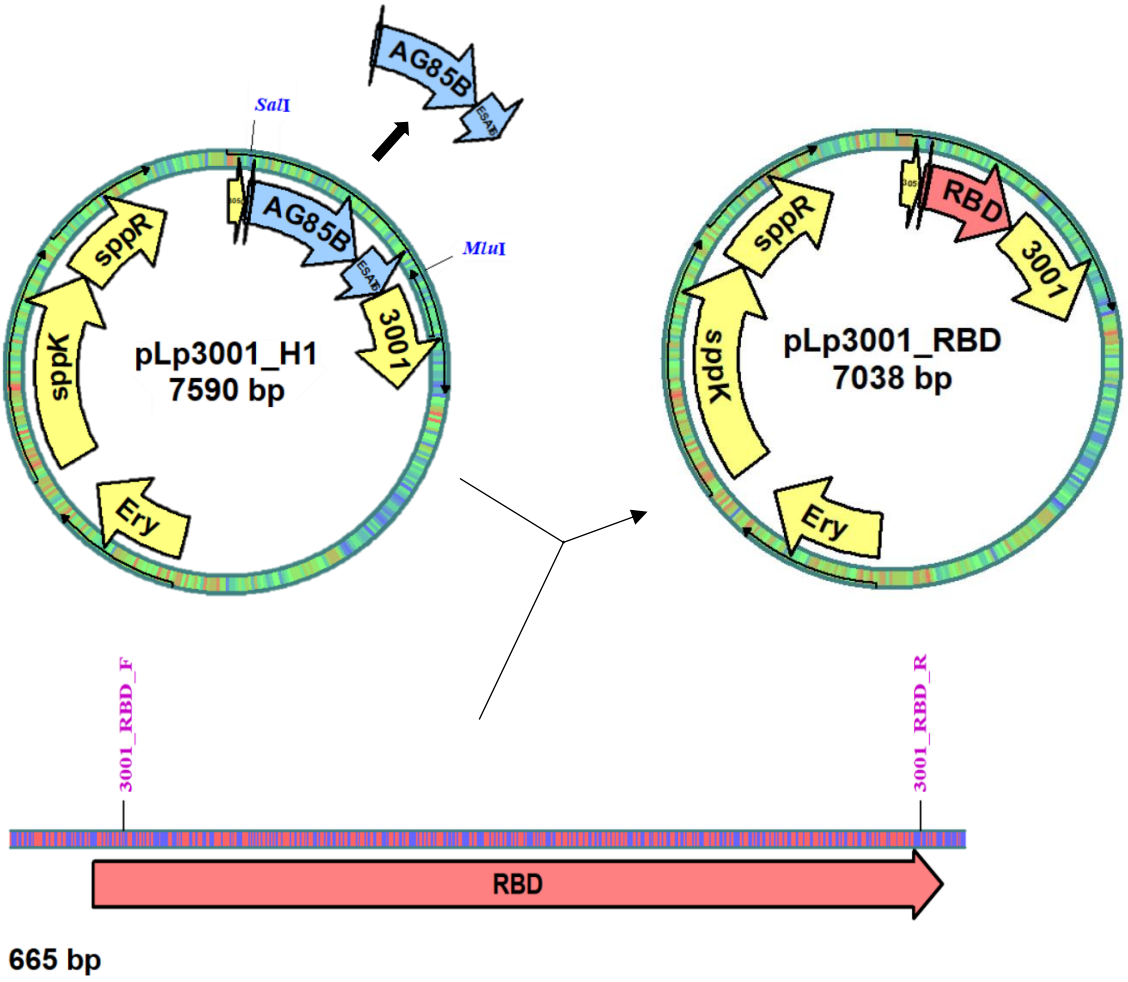

Figure 4.12. Strategy for constructing the pLp3001 _RBD vector.

The plasmids pLp1261_RBD and pLp1261_NTD_RBD were constructed the same way as pLp3001_RBD, but different primers and template were used. For pLp1261_RBD, the primers 1261_RBD_F and 1261_RBD_R were used, and for pLp1261_NTD_RBD, the primers 1261_NTD_F and 1261_RBD_R were used (described in Table 2.3). The restriction

enzymes HindIII and SalI were used to digest pLp1261_H1, and the fragment was further ligated with RBD or NTD_RBD.

After ligation, the plasmids were transformed into One Shot^{TM} TOP10 chemically competent *E. coli*. The plasmid pLp1261_RBD was, however, not transformed into competent *E. coli*, but into Stellar Competent Cells. The reason for this was several unsuccessful attempts of transforming pLp1261_R into competent *E. coli*, and when using Stellar Competent Cells, one transformation was successful. All the plasmids were sequenced to confirm correct sequence. After verification of successful sequencing, the plasmids were transformed into electrocompetent *L. plantarum* WCFS1.

4.2.2 Growth curve analysis of *L. plantarum* harbouring SARS-CoV-2-plasmids

The growth curves of *L. plantarum* harbouring the different SARS-CoV-2 plasmids containing either RBD or both NTD and RBD are shown in Figure 4.13. The protocol followed for the growth curve analysis was described in section 3.14. After the 96 well plate containing induced bacterial cultures were transferred to the Multiscan FC, the OD_{620} was measured every 5 minutes for 24 hours. As a control, *L. plantarum* harbouring a plasmid without any antigens, pEV, was included in the growth curve analysis. All the samples were grown in triplicates and the mean of these represents the growth curves in Figure 4.13. The growth curve analysis was executed two times with similar results. The growth curves of uninduced *L. plantarum* (the dotted curves) in Figure 4.13 had similar growth curves as *L. plantarum* harbouring pEV (the black curve). The figure also showed a clear difference in growth between the dotted curves and the curves belonging to induced *L. plantarum*. There was a clear difference between the growth curves of *L. plantarum* harbouring the lipoprotein anchor plasmids (pLp1261) and the LPXTG plasmids (pLp3001), regardless of which antigens (RBD or NTD_RBD) they harboured. The growth curves of *L. plantarum* harbouring the lipoprotein anchored plasmids had a higher growth rate during the whole analysis compared to *L. plantarum* harbouring the LPXTG anchored plasmids. *L. plantarum* harbouring the lipoprotein anchored plasmids had increasing growth until approximately 12 hours, before the bacteria reached the stationary phase. *L. plantarum* harbouring the LPXTG anchored plasmids grew slowly for approximately 15 hours, then the growth suddenly increased.

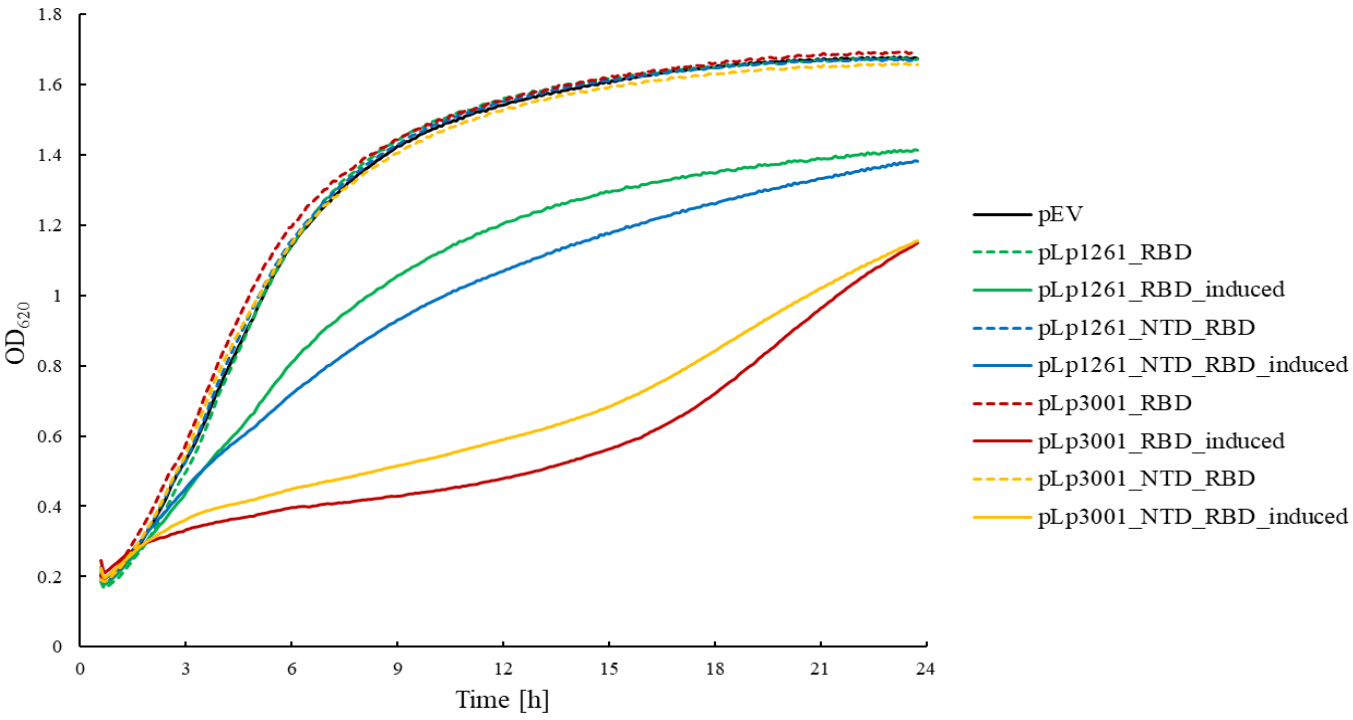

Figure 4.13. Growth curves of *L. plantarum* harbouring the different SARS-CoV-2 constructs.

4.2.3 Detection of SARS-CoV-2-antigens using western blot analysis

Figure 4.14 shows the results of the western blot analysis of *L. plantarum* harbouring the SARS-CoV-2 constructs. *L. plantarum* harbouring the different constructs were harvested three hours after induction with 25 ng/µL SppIP (section 3.13.1). Further, the cells were lysed to gain access to the proteins (section 3.13.2) and the crude protein extract were run on a SDS-PAGE (section 3.15.1) before blotting the proteins onto a membrane (section 3.15.2). The antigens were hybridized with specific antibodies (section 3.15.4) using a shaking device instead of the SNAP i.d. immunodetection system which was used for the TB-constructs. The shaking device was used because it provided less background noise compared to using the SNAP system, which was a problem when analysing *L. plantarum* harbouring the SARS-CoV-2 constructs. The proteins were at last visualized with chemiluminescence (section 3.15.5).

Figure 4.14 shows strong bands for all the protein variants, the lipoprotein anchored RBD and NTD_RBD (pLp1261_RBD and pLp1261_NTD_RBD) and the LPXTG anchored RBD and NTD_RBD (pLp3001_RBD and pLp3001_NTD_RBD). The theoretical molecular weights of the proteins, which are 33 kDa (pLp1261_RBD), 68 kDa (1261_NTD_RBD), 47 kDa (pLp3001_RBD) and 83 kDa (pLp3001_NTD_RBD) fit with the measured weights (Figure 4.14). Though, the LPXTG anchored RBDs (pLp3001_RBD) observed molecular weight was slightly higher than the theoretical weight, which also was observed for the LPXTG anchored H56 protein (pLp1261_H56, a TB-construct). pEV was included as a negative control and gave only very faint bands (Figure 4.14).

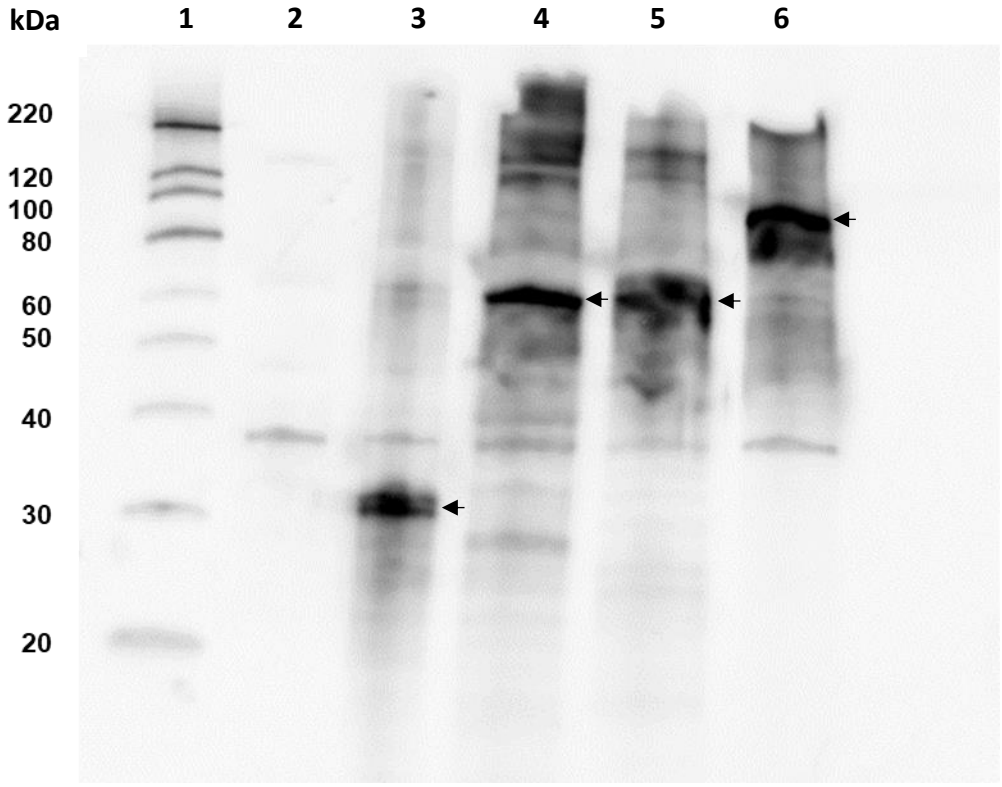

Figure 4.14. Western blot of the SARS-CoV-2-antigens (RBD or RBD-NTD) fused with different anchors. Well 1: Magic Mark XP Western Protein Standard; Well 2: pEV; Well 3: pLp1261_RBD; Well 4: pLp1261_NTD_RBD; Well 5; pLp3001_RBD; Well 6; pLp3001_NTD_RBD.

4.2.4 Detection of SARS-CoV-2-antigens localized on the surface of *L. plantarum* using flow cytometry

For flow cytometry analysis, *L. plantarum* harbouring the different SARS-CoV-2 constructs were harvested three hours after induction with 25 ng/ml SppIP before treated with antibodies (see section 3.16.1). In all flow cytometry analysis, a negative control, *L. plantarum* harbouring pEV, was included.

Flow cytometry analysis of *L. plantarum* harbouring all the SARS-CoV-2-constructs is shown in Figure 4.15. The flow cytometry analysis was executed two times with similar results. The LPXTG anchored NTD_RBD protein (pLp3001_NTD_RBD) gave the strongest signal, followed by the LPXTG anchored RBD protein (pLp3001_RBD), the lipoprotein anchored NTD_RBD protein (pLp1261_NTD_RBD) and the lipoprotein anchored RBD protein (pLp1261_RBD), respectively. All of the various anchored antigens gave stronger signals than pEV, indicating that all spike-antigens were exposed and anchored at the bacterial surface.

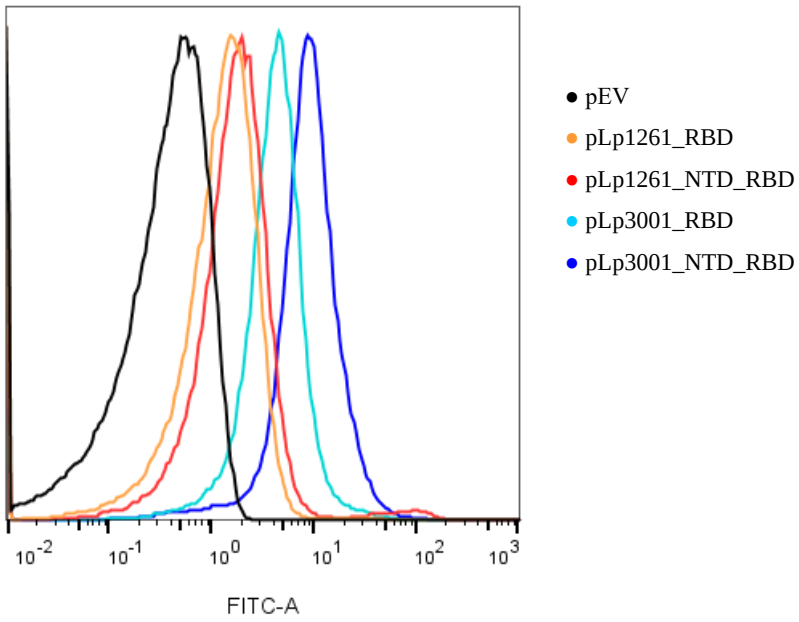

Figure 4.15. Flow cytometry analysis of *L. plantarum* harbouring the SARS-CoV-2 constructs. *L. plantarum* harbouring pEV was included as a negative control. The fluorescence intensity is shown along the x-axis.

Previously, *L. plantarum* constructs containing TB antigens have been harvested 3 hours after induction with SppIP for flow cytometry analysis. In Figure 4.16 and Figure 4.17, the bacteria in the flow cytometry analysis were harvested at six different points after induction (after 2, 3, 4, 5, 6 and 24 hours) (section 3.16.1). The bacteria were harvested at different times to investigate when the surface-displayed antigens showed the strongest fluorescent signal in the flow cytometry analysis. For TB, it is known that harvesting *L. plantarum* three hours after induction gives the strongest fluorescent signal, but for SARS-Cov-2 this has never been tested. In the initial analysis, only the lipoprotein anchored NTD_RBD (pLp1261_NTD_RBD) (Figure 4.16) and the LPXTG anchored NTD_RBD (pLp3001_NTD_RBD) (Figure 4.17) were analysed.

The signal from *L. plantarum* harbouring the lipoprotein anchored NTD_RBD (pLp1261_NTD_RBD) harvested after 4, 5, 6 and 24 hours was more or less the same (Figure 4.16). Bacteria harvested after 2 and 3 hours (red and orange histograms in Figure 4.16, respectively), showed a slightly weaker signal than the bacteria harvested at the other time points.

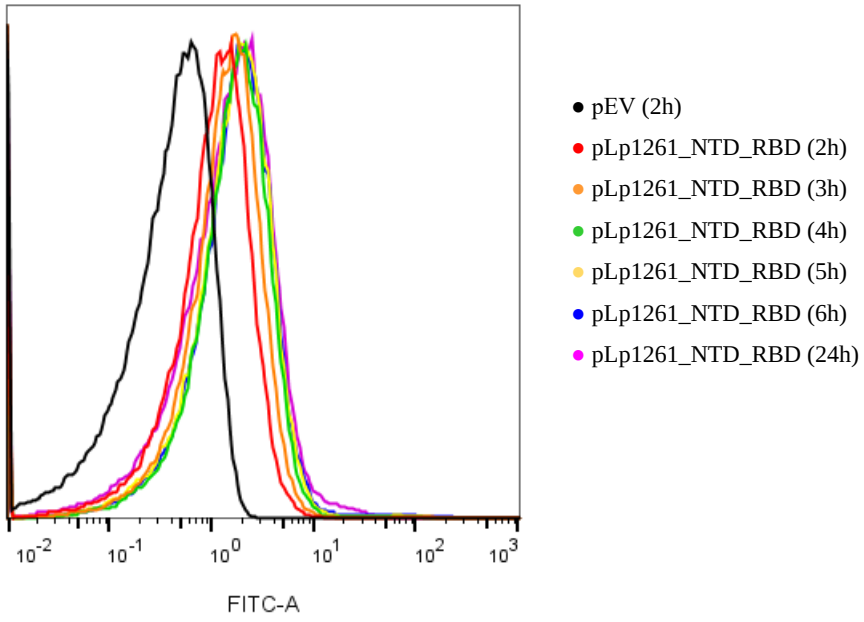

Figure 4.16. Flow cytometry analysis of *L. plantarum* harbouring pLp1261_NTD_RBD. The bacteria were harvested at different times before flow cytometry analysis, represented by the different histograms. *L. plantarum* harbouring pEV was included as a negative control. The fluorescence intensity is shown along the x-axis.

L. plantarum harbouring the LPXTG anchored NTD_RBD (pLp3001_NTD_RBD) harvested after 2, 3, 4, 5 and 6 hours gave more or less the same signal. Interestingly, the recombinant bacteria harvested after 24 hours showed no signal (similar to pEV) (Figure 4.17).

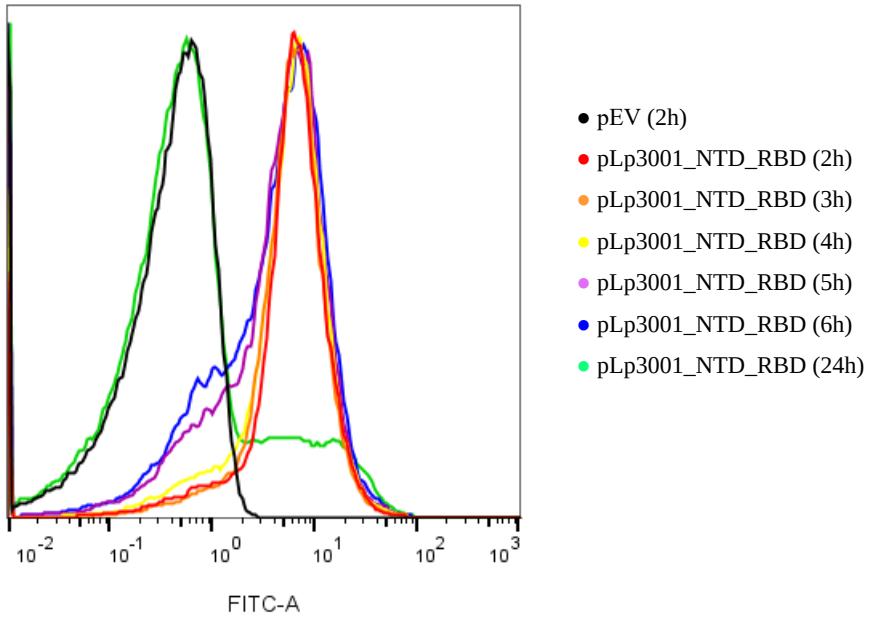

Figure 4.17. Flow cytometry analysis of *L. plantarum* harbouring pLp3001_NTD_RBD. The bacteria were harvested at different times before flow cytometry analysis, represented by the different histograms. *L. plantarum* harbouring pEV was included as a negative control. The fluorescence intensity is shown along the x-axis.

To test the effect of the primary antibody on the fluorescent signal in the flow cytometry analysis, *L. plantarum* harbouring the lipoprotein anchored NTD_RBD (pLp1261_NTD_RBD) was hybridized with different primary antibody concentrations. Antibodies are expensive reagents and the amount used should be limited as much as possible. The primary antibody SARS-CoV/SARS-CoV-2 Spike RBD Polyclonal Antibody is a new antibody that was not already optimized for flow cytometric analysis of *L. plantarum* harbouring SARS-CoV-2 antigens. Therefore, the optimization was based on the concentrations used for flow cytometry analysis of *L. plantarum* harbouring TB antigens previously mentioned. The aim of this experiment was to find the lowest possible antibody concentration that gives a strong fluorescent signal when analysing *L. plantarum* harbouring SARS-CoV-2 constructs with flow cytometry analysis. In the initial analysis, only *L. plantarum* harbouring the lipoprotein anchored NTD_RBD (pLp1261_NTD_RBD) was analysed.

L. plantarum harbouring the lipoprotein anchored NTD_RBD (pLp1261_NTD_RBD) were hybridized with the primary antibody concentrations 0.50, 1.0, 2.0 and 4.0 ng/µL (Figure 4.18). The negative control (pEV) was hybridized with a primary antibody concentration of 4.0 ng/µL. All the histograms of the lipoprotein anchored NTD_RBD were clustered together, separated only by small shifts (Figure 4.18). The lipoprotein anchored NTD_RBD hybridized with the highest primary antibody concentration (4.0 ng/µL) gave the strongest signal, but still, the signal was close to the negative control. The signal correlated with the primary antibody concentration; the stronger the signal was, the higher the primary antibody concentration the recombinant bacteria were hybridized with.

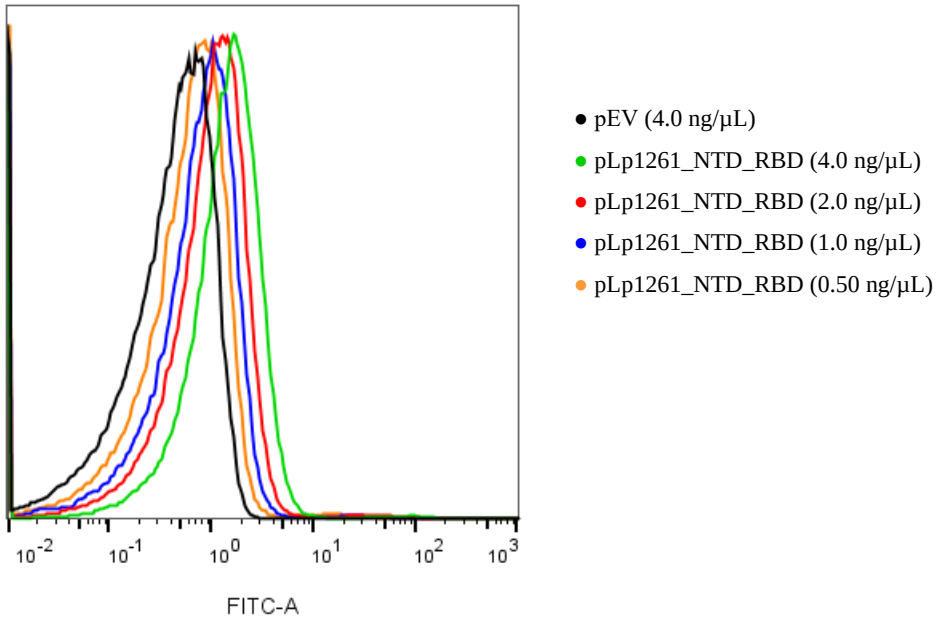

Figure 4.18. Flow cytometry analysis of *L. plantarum* harbouring pLp1261_NTD_RBD. The recombinant bacteria were added different primary antibody concentrations in the flow cytometry analysis. *L. plantarum* harbouring pEV was included as a negative control. The fluorescence intensity is shown along the x-axis.

The correlation between the median fluorescence intensity (MFI) and primary antibody (PA) concentration is shown for the lipoprotein anchored NTD_RBD (Figure 4.19). The four points in the figure represented the primary antibody concentration the lipoprotein anchored NTD_RBD protein was hybridized with and its corresponding MFI value. The MFI values correspond to the histograms shown in Figure 4.18. The trendline between the points was linear through all the points, which indicates that the fluorescent signal increase as the concentration of the primary antibody increases.

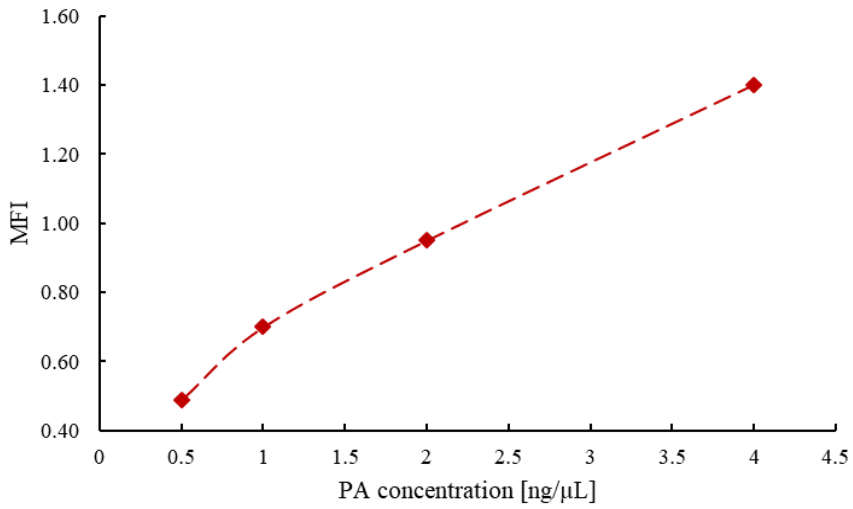

Figure 4.19. Median Fluorescence Intensity (MFI) plotted against primary antibody (PA) concentration for the lipoprotein anchored NTD_RBD antigen (pLp1261_NTD_RBD).

4.2.5 Detection of SARS-CoV-2-antigens localized on the surface of *L. plantarum* using fluorescence microscopy

L. plantarum harbouring the SARS-CoV-2-constructs were harvested three hours after induction with 25 ng/ml SppIP and further treated as described in section 3.16.2. The samples analysed with flow cytometry (Figure 4.15) was also analysed and imaged under the fluorescence microscope (Figure 4.20). Figure 4.20 indicates that all recombinant bacteria have the antigen (RBD or NTD_RBD) successfully exposed at the surface, but the LPXTG anchors (pLp3001_RBD and pLp3001_NTD_RBD) (shown in images D and E in Figure 4.20, respectively) gave a stronger signal than the lipoprotein anchors (pLp1261_RBD and pLp1261_NTD_RBD) (shown in images B and C in Figure 4.20, respectively). *L. plantarum* harbouring pEV were the only bacteria that gave no signal, as expected.

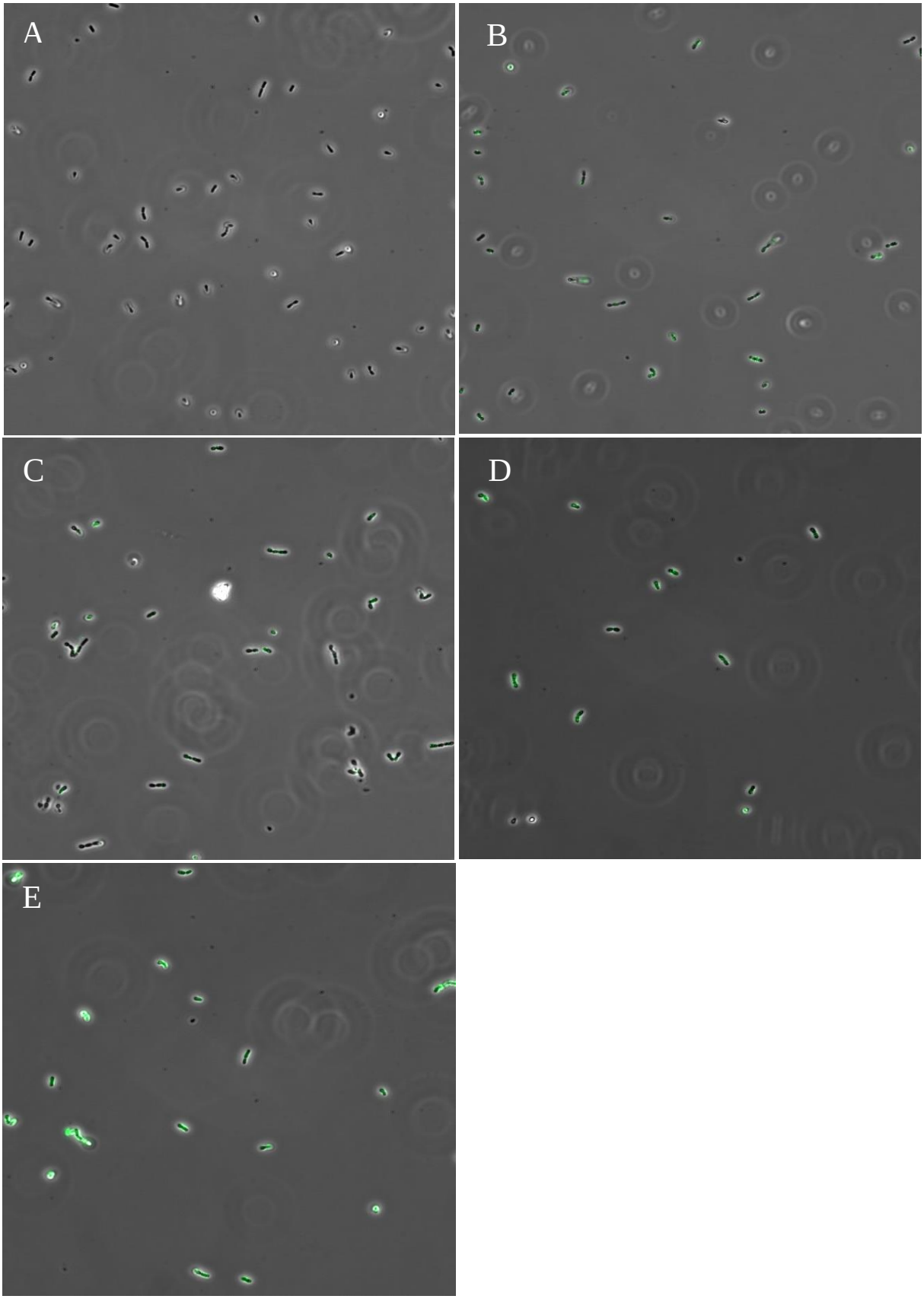

Figure 4.20. Microscopy of recombinant *L. plantarum*. A: pEV; B: pLp1261_RBD; C: pLp1261_NTD_RBD; D: pLp3001_RBD; E: pLp3001_NTD_RBD. Only bacteria with surface localized antigens appear green.

5 Discussion

5.1 Construction of plasmids

In this study, the *M. tuberculosis* antigens Ag85B, ESAT6 and Rv2660c (named H56) were cloned into the pSIP-vector expression system to produce and display the fused antigens on the surface of *L. plantarum*. Previously, only the *M. tuberculosis* antigens Ag85B and ESAT6 (named H1) have been expressed using the pSIP-system in *L. plantarum* (Kuczkowska et al., 2016; Kuczkowska et al., 2019). H56 was expressed in *L. plantarum* in this study because a study by Aagaard et al. (2011) has shown stronger immune responses against tuberculosis in mice using the H56 fusion antigen compared to the H1 fusion antigen. Due to the ongoing pandemic of COVID-19, antigens from SARS-CoV-2 (the virus causing COVID-19), RBD and NTD, were also cloned into the pSIP-system in *L. plantarum* to investigate whether the system could produce and display SARS-CoV-2 antigens on the surface of *L. plantarum*.

Thus, both TB antigens and SARS-CoV-2-antigens were successfully cloned into the pSIP-system. Three different anchors were utilized for anchoring of the antigens; a lipoprotein anchor (pLp1261), a LysM anchor (pLp3014) and a LPXTG peptidoglycan anchor (LPXTG anchor) (pLp3001). The three anchors attach the antigen to the cell surface in different places; the lipoprotein anchor to the cell membrane, while the LysM and LPXTG anchors to the cell wall via different mechanisms (Michon et al., 2016). Because of their different positions on the surface of the bacteria, these three anchors were chosen. The antigens' position on the surface of the bacteria may affect the growth of the induced recombinant bacteria and the accessibility of antigens displayed at the bacteria's surface. Previously it has been shown that bacteria harbouring the lipoprotein anchor grows better than bacteria harbouring the LPXTG anchor (Berggreen, 2020; Øverland, 2013), which also is believed to be the case in this study. The hypothesis for flow cytometry analysis was that the cell wall anchored antigens would show a stronger fluorescent signal than the cell membrane-anchored antigens. This is because the cell wall is located outside the cell membrane, thus closer and more available to the surroundings. Different locations of the antigen on the surface of the bacteria may also induce different immune responses as a vaccine. Antigens anchored to the cell membrane will be more embedded in the cell wall and protected from degradation than if anchored to the cell

wall (Michon et al., 2016). However, antigens anchored to the cell wall might induce a higher immune response if not degraded because they will be more accessible to immune cells.

The H56 fusion antigen was cloned into vectors containing all the different anchors, while the SARS-CoV-2 antigens were only cloned into the vectors containing the lipoprotein anchor and LPXTG anchor. These two anchors were chosen for the SARS-CoV-2 vectors because one anchor is positioned at the cell membrane, and the other is positioned at the cell wall. Two different versions of the SARS-CoV-2-antigens were also cloned into the pSIP-systems, one where only the RBD domain was inserted and the other where both NTD and RBD domains were inserted (Figure 1.5). Different versions of the SARS-CoV-2 antigens were constructed because the antigen's length might affect the growth of the recombinant bacteria or availability of displayed antigens on the surface of the bacteria. Two versions containing the lipoprotein anchor and the LPxTG anchor were constructed to investigate whether the length of the antigens or the type of anchor would affect the growth and antigen surface-display the most. The length of the antigen could impact growth and surface-display because it can be more stressful for the bacteria to produce, secrete, and display a larger protein. Or it might be the opposite; the longer the antigens are, the more available to the environment they might be, simply because they reach longer out of the bacteria. When it comes to using these recombinant bacteria as vaccines, the hypothesis is that these domains, NTD and RBD, can induce an immune response against SARS-CoV-2 and produce neutralizing antibodies which will block the binding of the virus to the host cells. The RBD domain might not induce a strong enough immune response alone, which is why two different versions of the SARS-CoV-2 antigens were constructed.

In total, seven plasmids were successfully constructed. The seven plasmids are: the lipoprotein anchored H56 (pLp1261_H56), the LysM anchored H56 (pLp301_H56), the LPXTG anchored H56 (pLp3001_H56), the lipoprotein anchored RBD (pLp1261_RBD), the lipoprotein anchored NTD_RBD (pLp1261_NTD_RBD), the LPXTG anchored RBD (pLp3001_RBD) and the LPXTG anchored NTD_RBD (pLp3001_NTD_RBD).

5.2 Growth of recombinant *L. plantarum*

Adding the inducer SppIP to the growth culture with recombinant bacteria harbouring the different pSIP-vectors results in the expression of the antigens. The growth of induced cultures of *L. plantarum* harbouring all the constructed vectors were clearly impaired

compared to the cultures not induced, and *L. plantarum* harbouring pEV (Figure 4.4; Figure 4.13). These results are expected as previous studies have shown that bacterial growth might be reduced when expressing heterologous proteins (Fredriksen et al., 2010; Kuczkowska et al., 2015; Lulko et al., 2007). Bacterial growth might be reduced when expressing heterologous proteins because overproducing the target proteins can cause stress for the bacteria. In stressful situations, most likely, the bacteria mainly execute activities to survive, which leads to a reduced focus on replicating itself; thus, the bacterial growth will be reduced. The cultures not induced and *L. plantarum* harbouring pEV showed similar growth (Figure 4.4; Figure 4.13), which is expected. The similar growths most likely confirm that the cultures not induced are not producing the heterologous proteins since *L. plantarum* harbouring pEV does not harbour heterologous proteins, and thus is not producing them. In addition, the fact that the cultures not induced and *L. plantarum* harbouring pEV have similar growths and are clearly distinguished from the induced cultures supports the hypothesis that it is stressful for the bacteria to produce the heterologous proteins. The western blot analysis confirms that all the induced recombinant bacteria do produce the heterologous proteins (Figure 4.5; Figure 4.14), and the flow cytometry analysis confirms that the induced cultures are displayed at the surface of the bacteria (Figure 4.6; Figure 4.15).

The growth of *L. plantarum* harbouring the lipoprotein anchor was, regardless of which antigens it was fused to, higher than the growth of *L. plantarum* harbouring either the LysM anchor or the LPXTG anchor (Figure 4.4; Figure 4.13). Interestingly, this indicates that bacteria with antigens anchored to the membrane might be more favorable than bacteria with antigens anchored to the cell wall regarding the growth. The reason might be that it is less stressful for the bacteria to secrete the antigens to the membrane than to the cell wall (which might include more steps). As mentioned in section 1.5.3, the LPXTG anchor depends on the enzyme sortase to cleave the LPXTG motif after secretion in order to be anchored to the cell wall (Michon et al., 2016). However, the growth difference of *L. plantarum* harbouring the lipoprotein anchored H56 and LysM anchored H56, which is also a cell wall anchor, is not as high as the difference between *L. plantarum* harbouring the lipoprotein anchored H56, and LPXTG cell wall anchored H56 (Figure 4.4). The reason why bacteria harbouring the LysM anchor grew better than the LPXTG anchor might be because after the LysM fused antigen is secreted, the anchor binds non-covalently to the cell wall and is not dependent on an enzyme in order to bind to the cell wall like the LPXTG anchor does (Michon et al., 2016). In a study by Berggreen (2020), which also compared the same LPXTG anchor (pLp3001) and the same

lipoprotein anchor (pLp1261), the growth patterns for bacteria harbouring the two anchors was similar as the growth patterns observed in this study.

Another interesting observation is the variation in growth patterns for *L. plantarum* harbouring the different anchors. The growth of *L. plantarum* harbouring the LysM anchor and the lipoprotein anchor fused with H56 showed similar patterns; the growth was exponential at first but flattened out at the end (Figure 4.4). For *L. plantarum* harbouring the LPXTG anchor, the growth pattern was quite different (Figure 4.4; Figure 4.13); the growth is quite low compared to the bacteria harbouring the other anchors up until approximately 15 hours, at this point the growth of the bacteria suddenly increases (Figure 4.4; Figure 4.13). This growth pattern was the same for *L. plantarum* harbouring the LPXTG anchor, regardless of which antigens the bacteria harboured. The most likely explanation for the sudden increase in the growth after approximately 15 hours is that the system has stopped producing the heterologous proteins. Due to a stop in production of the heterologous proteins, the bacteria are most likely less stressed and can be more focused on replication, thus this sudden increase in growth. A possible explanation as to why the bacteria has stopped producing the heterologous proteins is that the inducer peptide SppIP is consumed or degraded. The increased growth after approximately 15 hours was also observed by Berggreen (2020).

Both the TB-vectors and SARS-CoV-2-vectors included the lipoprotein anchor and the LPXTG anchor. The growth curves of the respective anchors showed similar patterns regardless of which antigens were fused to them (Figure 4.4; Figure 4.13). This indicates that the choice of the anchor is of greater significance than the type of antigen fused to the anchor regarding the growth rate, both in general and especially after three hours. Growth after three hours is especially important because it is the timepoint the bacteria normally are harvested for the different analysis used in this study (western blot, flow cytometry and fluorescence microscopy) and the timepoint the bacteria normally are harvested for vaccine experiments in animal studies (Kuczkowska et al., 2016; Kuczkowska et al., 2019). The growth rate after three hours for *L. plantarum* harbouring the lipoprotein anchor is higher than both cell wall anchors, but the growth rate of *L. plantarum* harbouring the LysM anchor is again higher than bacteria harbouring the LPXTG anchor. This means that a larger volume must be harvested for vaccines to get the same number of bacteria harbouring the cell wall anchors as bacteria harbouring the cell membrane anchor, which is a disadvantage and makes the vaccine more demanding to produce.

As mentioned earlier, two versions of the SARS-CoV-2 vectors were constructed for each anchor: one containing only the RBD antigen and the other containing both antigens NTD and RBD. The growth curves of *L. plantarum* harbouring the lipoprotein anchor showed similar patterns regardless of which version of the antigens they were fused to, which also was the case for the growth curves of *L. plantarum* harbouring the LPXTG anchor (Figure 4.13). The hypothesis was that the RBD antigen would impair the bacteria's growth less than the NTD_RBD antigen because the RBD antigen is approximately half the size of the NTD_RBD antigen. The size may affect the growth because the longer the antigen is, the longer proteins the bacteria have to produce, secrete and surface display, which might cause the bacteria more stress. And as mentioned earlier, the more stress the bacteria are exposed to, the less likely it is that the bacteria use energy on replicating itself rather than concentrating on the most important tasks for keeping the bacteria alive. Interestingly, only the bacteria harbouring the lipoprotein anchor showed a higher growth when fused to RBD instead of NTD_RBD, not the bacteria harbouring the cell wall anchor (Figure 4.13). Seemingly, the choice of anchor has a larger effect on the growth of the bacteria than the size of the antigens. Interestingly, the OD_{620} after three hours was higher for bacteria harbouring the cell wall anchor fused with NTD_RBD compared to when only fused with RBD, while no difference was observed at this time point between the two versions of the lipoprotein anchor (Figure 4.13). The observations indicate that it does not matter which of the two lipoprotein-anchored vectors is used as a vaccine regarding growth, but the NTD_RBD vector of the two cell wall anchored vectors is somewhat more favorable as a vaccine because less volume needs to be harvested.

5.3 Characterization of antigen production

Western blot was used to confirm the production of antigens by *L. plantarum* harbouring the different plasmids constructed in this study. All constructed strains successfully produced the antigens, both the strains harbouring the H56 antigen (Figure 4.5) and the SARS-CoV-2 antigens (Figure 4.14). However, the weight of the H56 antigen and the RBD antigen fused with the LPXTG anchor was slightly higher than their theoretical weight. Other studies have also observed that the LPXTG anchor fused with antigens has a higher measured weight than their theoretical weight would indicate (Kuczkowska et al., 2016). An explanation for this might be that the anchor protein contains parts of the cell wall, which leads to a higher measured weight.

All the anchors fused with H56, showed strong and thick bands (Figure 4.5). This is also the case for the anchors fused with SARS-CoV-2 antigens; however, the band belonging to the lipoprotein anchored RBD may seem slightly weaker than bands belonging to the rest of the SARS-CoV-2 anchored proteins (Figure 4.14). The results show that both H56 and SARS-CoV-2 antigens are being produced in sufficient quantities, indicating that the induction system works as it should.

The western blot analysis of *L. plantarum* harbouring the TB-constructs was successful at the first attempt. However, when analysing *L. plantarum* harbouring the SARS-CoV-2-constructs, this was not the case. The analysing of the SARS-antigens required some adjustments including a new primary antibody and reducing the amount of protein loaded onto the SDS-PAGE from 10 µL to 2 µL of the lipoprotein anchored RBD, and 5 µL of the rest of the SARS-CoV-2 anchored proteins before the produced antigens were visible in the western blot. Also, a different hybridization method (see section 3.15.4) compared to the method used for the TB-constructs, were used to reduce the background noise in the western blot.

5.4 Characterization of surface-displayed antigens

While the western blot analysis was used to confirm the production of the antigens, flow cytometry analysis was used to investigate whether the antigens were successfully anchored and exposed at the surface of *L. plantarum*.

First, standard flow cytometry analysis was conducted for *L. plantarum* harbouring the TB-constructs and for *L. plantarum* harbouring the SARS-CoV-2 constructs (Figure 4.6; Figure 4.15). Previously, it had been developed a standard flow cytometry protocol when working with TB antigens, which was followed (see section 3.16.1). In the protocol, the bacteria are harvested three hours after induction. Due to the novelty of the SRAS-CoV-2 antigens, a standard flow cytometry protocol had not yet been established for these antigens. Therefore, the same protocol as for the TB antigens was followed in the initial analysis.

The initial flow cytometry analysis showed a stronger signal for the antigens anchored to the cell wall, with either the LysM anchor (pLp3014) or the LPXTG anchor (pLp3001), than the antigens anchored to the cell membrane with the lipoprotein anchor (pLp1261) (Figure 4.6; Figure 4.15). This variation in signal-strength is most likely caused by the anchor's location on the bacteria. Antigens anchored to the cell wall will be more exposed than the antigens

anchored to the cell membrane which most likely explains why the cell wall anchored antigens gave a stronger signal in the flow cytometry analysis. The cell wall anchored antigens are more exposed because of the structure of the cell; the cell wall is on the outside of the cell membrane and thus in more contact with the surroundings. Therefore, a disadvantage of anchoring the proteins to the membrane might be that it can offer reduced interactions with the surroundings, regarding flow cytometry analysis, availability for secondary antibodies to attach to the proteins. More accessibility of secondary antibodies might give a stronger fluorescent signal because more FITC molecules would be attached to the target protein-primary antibody complex. On the contrary, target proteins anchored to the cell wall will most likely be more open to the interactions with the secondary antibodies. Still, they might also be more exposed to protein degradation, which proteins anchored to the cell membrane will be more protected against. This hypothesis is also supported by the location of the two cell wall anchors; the LysM anchor is located further out on the cell wall than the LPXTG anchor (Figure 1.2) and might reflect the results which showed a stronger signal for the LysM anchor than the LPXTG anchor (Figure 4.6). Another possible explanation why the cell wall anchors gave a stronger signal might be that the bacteria harbouring these anchors simply produce more protein than the bacteria harbouring the cell membrane anchors. But this does not seem likely when looking at the western blot analysis, which showed similar production of the antigens, regardless of the type of anchor being fused to the antigens (Figure 4.5; Figure 4.14). Interestingly, there was great variations between the signals of the LPXTG anchors fused with the SARS-CoV-2 antigens compared to the lipoprotein anchors, which showed almost the same signal for both versions (Figure 4.15). This might indicate that when the antigens are anchored to the cell wall and thus more exposed to the surroundings, the size of the antigen has a more significant impact on the fluorescent signal than if the antigen is anchored to the membrane where the antigens might be in less contact with the surroundings because they are more embedded. Figure 4.9 and Figure 4.20 shows that all the bacteria gave a fluorescent signal after fluorescence microscopy, and that the lipoprotein anchored antigens show a weaker fluorescence signal than the cell wall anchored antigens do, thereby confirms the flow cytometry results.

As mentioned earlier, a vaccine candidate involving *L. plantarum* and SARS-CoV-2 had not been worked on previously. To achieve the best possible results for these vaccine candidates, further flow cytometry analysis was conducted to try optimizing the protocol for *L. plantarum* harbouring SARS-CoV-2 antigens.

In the further flow cytometry analysis, the bacteria used for the analysis were harvested at different times after induction of the expression. The aim was to find the time point where the antigens would give the strongest flow cytometric signals, possibly relating to the highest amount of antigen anchored to the bacteria. Bacteria harbouring the long versions of the SARS-CoV-2 antigens (NTD_RBD) were harvested 2, 3, 4, 5, 6 and 24 hours after induction. Figure 4.16 and Figure 4.17 show that the time of harvesting did not affect the fluorescent signal to a large degree. However, *L. plantarum* harbouring the lipoprotein anchored NTD_RBD harvested 2 and 3 hours after induction showed a slightly weaker signal than the bacteria harvested at later time points (Figure 4.16). This indicates that bacteria should perhaps be harvested at later time points than 2 and 3 hours, for both later flow cytometry analysis and later animal experiments.

Interestingly, the bacteria harvested 4, 5, 6 and 24 hours after induction had similar signal strength (Figure 4.16). This means that there can be more flexibility in the experiment regarding when the bacteria should be harvested. Another factor to consider when the signal strength is similar, is the amount of bacteria culture that needs to be harvested. When harvesting bacteria after 6 hours compared to 4 hours, the OD value most likely will be higher, and thus less culture needs to be harvested. This might be especially important when harvesting for vaccine experiments on animals. Even though the bacteria harvested after 24 hours has similar signal strength as the bacteria harvested at the other time points, the OD value is most likely very high and the cultures might be more difficult to work with because the solutions is thicker compared to when bacteria is harvested at earlier timepoints. For *L. plantarum* harbouring the LPXTG anchored NTD_RBD, the fluorescence signal from all the time points (except 24 hours) are similar (Figure 4.17). The same dilemma as for the bacteria harbouring the lipoprotein anchored NTD_RBD arises here; when to harvest the bacteria compared to how much bacteria that needs to be harvested. Something that should be investigated further is why the bacteria harbouring the lipoprotein anchored NTD_RBD harvested after 4, 5, 6, and 24 hours gave similar fluorescent signals (Figure 4.16). This was also observed for the bacteria harbouring the LPXTG anchored NTD_RBD harvested after 2, 3, 4, 5 and 6 hours (Figure 4.17). The observations of bacteria harbouring the LPXTG anchor might be explained by the growth pattern of the bacteria, where the growth is relatively low between 2-6 hours (Figure 4.13). When the growth is low, few new bacteria are produced. If this is the case than few new bacteria with surface-displayed proteins will get secondary antibodies attached to them; therefore, the signal will remain the same because approximately

the same number of bacteria will have the secondary antibodies attached to their surface proteins. However, bacteria harbouring the lipoprotein anchored NTD_RBD had a relatively rapidly increasing growth between 4-6 hours after induction, while the fluorescent signal remained similar (Figure 4.13). Perhaps there are antigens on the surface of the bacteria not detected because too low concentrations of antibodies are added. This might be supported by the results of the flow cytometry analysis conducted on bacteria harbouring the lipoprotein anchored NTD_RBD, which was hybridized with different concentrations of the primary antibody (Figure 4.18; Figure 4.19). The results indicates that the antibody concentration used might be too low. Or perhaps, the number of new bacteria without surface-displayed antigens is not enough to dilute the bacteria with surface anchored antigens, so the signal will not be weaker or disappear as it did for the bacteria harbouring the LPXTG anchored NTD_RBD.

An interesting observation was that *L. plantarum* harbouring the LPXTG anchored NTD_RBD harvested 24 hours after induction showed no fluorescent signal (Figure 4.17). The lack of fluorescent signal indicates that the antigens are no longer located on the surface of the bacteria. Most likely, this means that the antigens are no longer being produced by the bacteria, which might be because the inducer (SppIP) is consumed or degraded. This hypothesis is supported by the growth of the *L. plantarum* harbouring the LPXTG anchored NTD_RBD (Figure 4.13). As mentioned previously, the growth of *L. plantarum* harbouring the LPXTG anchored antigens grew slowly until approximately 15 hours after induction. At approximately 15 hours, the growth rate increased considerably. The fact that the growth suddenly increased indicates that the conditions for the bacteria were improved, and the most likely explanation is that the bacteria no longer produced the antigens. The bacteria harbouring the lipoprotein anchored NTD_RBD probably also stopped producing the antigens, but it does not show in the growth curve because the bacteria had already reached the stationary phase. Most likely the growth had already began flattening out naturally due to less availability of nutrients from the media when the production of the antigens stopped working. It is important to notice that *L. plantarum* harbouring the lipoprotein anchored NTD_RBD harvested 24 hours after induction had, as opposed to *L. plantarum* harbouring the LPXTG anchored NTD_RBD, a strong fluorescent signal (Figure 4.16). It is interesting that bacteria with the cell wall anchored antigens do not show any fluorescent signal after 24 hours, but bacteria with the cell membrane-anchored antigens do. Also, in this case, looking at the growth pattern of the bacteria might offer an explanation to the different fluorescent signals observed after 24 hours. *L. plantarum* harbouring the lipoprotein anchored antigens

has an exponential growth at first and flattens out at the end, while the growth of *L. plantarum* harbouring the cell wall anchored antigens is low at first, but have a sudden increase in growth after approximately 15 hours and is still slightly increasing after 24 hours (Figure 4.13). It is assumed that the production of the heterologous proteins are stopped after 15 hours, based on the growth observations of bacteria harbouring the LPXTG anchor (Figure 4.13). The fact that the growth of the bacteria between 15-24 hours is quite low, indicates that almost the same number of bacteria with surface displayed antigen is still in the solution, thus the signal strength is still strong. However, the growth of bacteria harbouring the LPXTG anchor have increased drastically between 15-24 hours, which means that there are a much higher number of bacteria in the solution after 24 hours than 15 hours, which was never induced and thereby does not have surface displayed antigen. This most likely explains why the bacteria harbouring the LPXTG anchored antigens no longer show fluorescent signal after 24 hours (Figure 4.17).

Antibodies are expensive additives, and as little as possible of the antibodies should be used to reduce the costs of the experiments. Therefore, another flow cytometry analysis was conducted to test the correlation between antibody concentration and the fluorescent signal. These analyses were executed for *L. plantarum* harbouring the lipoprotein anchored H56 antigen (TB antigens) (Figure 4.7) and for *L. plantarum* harbouring the lipoprotein anchored NTD_RBD antigen (SARS-CoV-2 antigens) (Figure 4.18). Thus, the bacteria harboured the same anchor but different antigens. The bacteria were hybridized with different concentrations of the primary antibody without changing any other parameters. The concentration of the secondary antibody remained the same for all the samples. The results of the flow cytometry analysis of *L. plantarum* harbouring H56 showed more separated signals (Figure 4.7) compared to *L. plantarum* harbouring NTD_RBD (Figure 4.18). *L. plantarum* harbouring H56 hybridized with the highest concentration (4.08 ng/µL) of primary antibody and the second highest concentration (2.04 ng/µL) gave close to the same signal, meaning that the concentration used of the primary antibody used for flow cytometric analyzation of the TB antigens, can be reduced by half. Figure 4.8 support this conclusion, where it was observed that the median fluorescence intensity (MFI) values seem to flatten out for the last two concentrations of the primary antibody. However, two points are not enough to give a clear indication, which is why further tests should be conducted with at least one more point of antibody concentration to make sure the MFI values for certain flattens out. If it is correct that the MFI values flatten out, this indicates that the bacteria have been saturated by the primary

antibody, and a further increase of the primary antibody concentration will not result in a stronger fluorescent signal. For *L. plantarum* harbouring the NTD_RBD, the fluorescent signals of the samples hybridized with different concentrations of the primary antibody were not very separated (Figure 4.18). Also, the correlation between the MFI signal and primary antibody concentration was linear, meaning that an increase of the primary antibody concentration would most likely result in an increase of the fluorescent signal (Figure 4.19). Both of these observations imply that the concentration of the primary antibody used for the SARS-CoV-2-antigens in the flow cytometry analysis was too low, and a higher concentration of the primary antibody might have given stronger fluorescent signals. This was not investigated in this study because of lack of time, but later, it should be tested.

5.5 Conclusions and future prospects

L. plantarum both produced and surface-displayed both TB antigens (H56) and SARS-CoV-2 antigens (NTD_RBD and RBD) successfully in this study. H56 were anchored to the surface of the bacteria with a lipoprotein anchor, a LPXTG anchor and a LysM anchor, while the SARS-CoV-2 antigens were anchored with a lipoprotein anchor and a LPXTG anchor. The results indicate that the type of anchor affects the growth of the recombinant bacteria more than the type of antigen being fused to the anchor, and the growth of bacteria harbouring the cell membrane anchor shows better growth compared to the bacteria harbouring the cell wall anchors. The growth of the recombinant bacteria harbouring the lipoprotein anchors showed similar patterns independently on whether they were fused to H56 or the SARS-CoV-2 antigens. The same was observed for the recombinant bacteria harbouring the LPXTG anchors. The production of the H56 antigens and the SARS-CoV-2 antigens was very similar, independently of which anchors they were fused to. The fluorescent signal was stronger for the cell wall anchors than the cell membrane anchors, both represented by flow cytometry results and fluorescent microscopy. This is most likely caused by the location of the anchors and that the antigens fused to the cell wall anchors are more exposed and available to the surroundings, thus for the secondary antibodies to attach to the proteins.

Further analysis that would be interesting to conduct based on this study, is to run western blot analysis on the bacteria harbouring the LPXTG anchors to investigate if and possibly when the bacteria stops producing the antigens, and if this is correlated to the sudden increase observed after approximately 15 hours in the growth of these bacteria. It would also be

interesting to include bacteria harbouring both the lipoprotein anchor and LysM anchor in this western blot analysis and compare them with the LPXTG anchor.

Also, further flow cytometry analysis with *L. plantarum* harbouring lipoprotein anchored NTD_RBD should be conducted, which includes hybridizing the antigens with a primary antibody concentration higher than 4.0 ng/µL, which was the highest concentration used in this study. This is to test if a higher concentration of primary antibody gives a stronger fluorescent signal, which the results in Figure 4.18 and Figure 4.19 indicate. It should also be considered to conduct a flow cytometry analysis of *L. plantarum* harbouring the LPXTG anchored NTD_RBD, to investigate if hybridizing the bacteria with a higher concentration of the primary antibody confirms the flattening trend of the MFI signal observed in this study.

It could also be interesting to exchange the inducible promotors in this study with constitutive promotors and compare the production and surface display of the antigens in *L. plantarum* when using inducible and constitutive promoters. Using constitutive promotors would mean a continuous production of the heterologous proteins and not being dependent on adding external stimuli to start producing the proteins. This would be an advantage when using the recombinant bacteria as a vaccine, because it would simplify the production of the vaccine.

An issue with the pSIP system (Figure 1.1) (described in section 1.3) used in this study, is that the antibiotic-resistant gene *ery* is included in the system as a selection marker. Antibiotic resistance is a rising problem today, and a vaccine can not contain an antibiotic-resistant gene to add to the problem. Another promising selection marker for use in *L. plantarum* is the alanine racemase gene (*alr*) gene, which converts L-alanine to D-alanine, an essential component for the growth of prokaryotic cells (Hols et al., 1997; Nguyen et al., 2011). The *alr* gene has already been cloned into the pSIP system for the purpose of producing ingredients and additives in the food industry (Nguyen et al., 2011). It would be interesting to exchange *alr* with *ery* in the pSIP system used in this study, in the pursuit of making a usable vaccine candidate.

The vaccine candidates constructed in this study, *L. plantarum* harbouring H56 antigens in three different versions and *L. plantarum* harbouring SARS-CoV-2 antigens in four different versions, should be included in further animal studies for testing of immune response against their respective diseases. In the animal studies, *L. plantarum* harbouring H1 antigens should also be included, and immune responses between the recombinant bacteria harbouring H1 antigens and H56 antigens should be compared.

Based on the work with the H56 fusion antigen, bacteria harbouring the lipoprotein anchor and the LysM anchor, showed the most promise as vaccine candidates against tuberculosis. Although the growth of the bacteria harbouring the lipoprotein anchor was highest, both bacteria harbouring the lipoprotein anchor and LysM anchor showed significantly higher growth compared to bacteria harbouring the LPXTG anchor. Also, after three hours, which is normally when bacteria are harvested for western blot, flow cytometry and fluorescence microscopy, and when bacteria have been harvested in animal studies to test immune response, the growth of bacteria harbouring the lipoprotein anchor and LysM anchor is higher than bacteria harbouring the LPXTG anchor. All the recombinant bacteria showed clear fluorescence signals, but bacteria harbouring the LysM anchor gave the strongest signal, and the lipoprotein anchor gave the weakest signal. The weaker signal from bacteria harbouring the lipoprotein anchor might not be a disadvantage, as it can mean that the antigens are more protected from degradation when the recombinant bacteria are delivered as a vaccine.

Based on the work with the SARS-CoV-2 antigens, bacteria harbouring the LPXTG anchored NTD_RBD showed more promise as a vaccine candidate than the LPXTG anchored RBD due to higher growth and stronger fluorescence signal. However, the difference between the two versions of the bacteria harbouring the lipoprotein anchor was small regarding both growth (especially at three hours) and fluorescence signal. It is difficult to assess whether the plasmids containing the lipoprotein anchored or the LPXTG anchored SARS-CoV-2 antigens are the most promising vaccine candidates. Bacteria harbouring the lipoprotein anchored antigens clearly showed higher growth, while bacteria harbouring the LPXTG anchored antigens showed stronger fluorescence signal. But due to the growth results of bacteria harbouring the lipoprotein anchored SARS-CoV-2 antigens, these are considered to be more promising as vaccine candidates. However, if the LPXTG anchor could be improved, resulting in higher growth, *L. plantarum* harbouring the LPXTG NTD_RBD would be the best vaccine candidate against COVID-19. All vaccine candidates containing the SARS-CoV-2 antigen has been sent to a collaboration partner for further testing in animal studies, but so far, the experiments have not led to any promising results.

6 References

Aagaard, C., Hoang, T., Dietrich, J., Cardona, P. J., Izzo, A., Dolganov, G., Schoolnik, G. K., Cassidy, J. P., Billeskov, R. & Andersen, P. (2011). A multistage tuberculosis vaccine that confers efficient protection before and after exposure. *Nature Medicine*, 17 (2): 189-94. doi: 10.1038/nm.2285.

Aguirre, M. & Collins, M. (1993). Lactic acid bacteria and human clinical infection. *Journal of Applied Bacteriology*, 75 (2): 95-107.

Andersen, P. & Doherty, T. M. (2005). The success and failure of BCG — implications for a novel tuberculosis vaccine. *Nature Reviews Microbiology*, 3 (8): 656-662. doi: 10.1038/nrmicro1211.

Aukrust, T. W., Brurberg, M. B. & Nes, I. F. (1995). Transformation of Lactobacillus by electroporation. *Methods in Molecular Biology*, 47: 201-8. doi: 10.1385/0-89603-310-4:201.

Berggreen, H. (2020). *Celleveggankring av Mycobacterium tuberculosis-antigener på overflaten til Lactobacillus plantarum*. Ås: Norwegian University of Life Sciences.

Bermúdez-Humarán, L. G., Kharrat, P., Chatel, J.-M. & Langella, P. (2011). Lactococci and lactobacilli as mucosal delivery vectors for therapeutic proteins and DNA vaccines. *Microbial cell factories*, 10 Suppl 1 (Suppl 1): S4-S4. doi: 10.1186/1475-2859-10-S1-S4.

Buist, G., Steen, A., Kok, J. & Kuipers, O. P. (2008). LysM, a widely distributed protein motif for binding to (peptido)glycans. *Molecular Microbiology*, 68 (4): 838-47. doi: 10.1111/j.1365-2958.2008.06211.x.

Chen, Y., Liu, Q. & Guo, D. (2020). Emerging coronaviruses: Genome structure, replication, and pathogenesis. *Journal of Medical Virology*, 92 (4): 418-423. doi: 10.1002/jmv.25681.

Chi, X., Yan, R., Zhang, J., Zhang, G., Zhang, Y., Hao, M., Zhang, Z., Fan, P., Dong, Y., Yang, Y., et al. (2020). A neutralizing human antibody binds to the N-terminal domain of the Spike protein of SARS-CoV-2. *Science*, 369 (6504): 650-655. doi: 10.1126/science.abc6952.

Comstock, G. W., Woolpert, S. F. & Livesay, V. T. (1976). Tuberculosis studies in Muscogee County, Georgia. Twenty-year evaluation of a community trial of BCG vaccination. *Public health reports (Washington, D.C. : 1974)*, 91 (3): 276-280.

de Ruyter, P. G., Kuipers, O. P., Beerthuyzen, M. M., van Alen-Boerrigter, I. & de Vos, W. M. (1996). Functional analysis of promoters in the nisin gene cluster of Lactococcus lactis. *Journal of bacteriology*, 178 (12): 3434-3439. doi: 10.1128/jb.178.12.3434-3439.1996.

Diep, D. B., Mathiesen, G., Eijsink, V. G. & Nes, I. F. (2009). Use of lactobacilli and their pheromone-based regulatory mechanism in gene expression and drug delivery. *Current Pharmaceutical Biotechnology*, 10 (1): 62-73. doi: 10.2174/138920109787048571.

Dietrich, J., Billeskov, R., Doherty, T. M. & Andersen, P. (2007). Synergistic effect of bacillus calmette guerin and a tuberculosis subunit vaccine in cationic liposomes: increased immunogenicity and protection. *Journal of Immunology*, 178 (6): 3721-30. doi: 10.4049/jimmunol.178.6.3721.

Estrada, E. (2020). COVID-19 and SARS-CoV-2. Modeling the present, looking at the future. *Physics Reports*, 869: 1-51. doi: https://doi.org/10.1016/j.physrep.2020.07.005.

European Medicines Agency. (2021). *Treatments and vaccines for COVID-19: authorised medicines*. Available at: https://www.ema.europa.eu/en/human-

regulatory/overview/public-health-threats/coronavirus-disease-covid-19/treatments-vaccines/treatments-vaccines-covid-19-authorised-medicines (accessed: 02.02.2021).
Fogel, N. (2015). Tuberculosis: A disease without boundaries. *Tuberculosis*, 95 (5): 527-531. doi: https://doi.org/10.1016/j.tube.2015.05.017.
Fredriksen, L., Mathiesen, G., Sioud, M. & Eijsink, V. G. H. (2010). Cell Wall Anchoring of the 37-Kilodalton Oncofetal Antigen by Lactobacillus plantarum for Mucosal Cancer Vaccine Delivery. *Applied and Environmental Microbiology*, 76 (21): 7359-7362. doi: 10.1128/aem.01031-10.
Fredriksen, L., Kleiveland, C. R., Hult, L. T. O., Lea, T., Nygaard, C. S., Eijsink, V. G. H. & Mathiesen, G. (2012). Surface display of N-terminally anchored invasin by Lactobacillus plantarum activates NF-κB in monocytes. *Applied and environmental microbiology*, 78 (16): 5864-5871. doi: 10.1128/AEM.01227-12.
Hart, P. D. & Sutherland, I. (1977). BCG and vole bacillus vaccines in the prevention of tuberculosis in adolescence and early adult life. *British medical journal*, 2 (6082): 293-295. doi: 10.1136/bmj.2.6082.293.
He, H., Yang, H. & Deng, Y. (2015). Mycobacterium tuberculosis dormancy-associated antigen of Rv2660c induces stronger immune response in latent Mycobacterium tuberculosis infection than that in active tuberculosis in a Chinese population. *European Journal of Clinical Microbiology & Infectious Diseases*, 34 (6): 1103-1109. doi: 10.1007/s10096-015-2335-8.
Hikmet, F., Méar, L., Edvinsson, Å., Micke, P., Uhlén, M. & Lindskog, C. (2020). The protein expression profile of ACE2 in human tissues. *Molecular Systems Biology*, 16 (7): e9610. doi: https://doi.org/10.15252/msb.20209610.
Hols, P., Defrenne, C., Ferain, T., Derzelle, S., Delplace, B. & Delcour, J. (1997). The alanine racemase gene is essential for growth of Lactobacillus plantarum. *Journal of bacteriology*, 179 (11): 3804-3807. doi: 10.1128/jb.179.11.3804-3807.1997.
Holzapfel, W. H., Haberer, P., Snel, J., Schillinger, U. & Huis in't Veld, J. H. (1998). Overview of gut flora and probiotics. *International Journal of Food Microbiology*, 41 (2): 85-101. doi: 10.1016/s0168-1605(98)00044-0.
Khailany, R. A., Safdar, M. & Ozaslan, M. (2020). Genomic characterization of a novel SARS-CoV-2. *Gene Reports*, 19: 100682. doi: https://doi.org/10.1016/j.genrep.2020.100682.
Kleerebezem, M., Boekhorst, J., van Kranenburg, R., Molenaar, D., Kuipers, O. P., Leer, R., Tarchini, R., Peters, S. A., Sandbrink, H. M., Fiers, M. W. E. J., et al. (2003). Complete genome sequence of Lactobacillus plantarum WCFS1. *Proceedings of the National Academy of Sciences*, 100 (4): 1990-1995. doi: 10.1073/pnas.0337704100.
Kleerebezem, M., Hols, P., Bernard, E., Rolain, T., Zhou, M., Siezen, R. J. & Bron, P. A. (2010). The extracellular biology of the lactobacilli. *FEMS Microbiology Reviews*, 34 (2): 199-230. doi: 10.1111/j.1574-6976.2009.00208.x.
Kuczkowska, K., Mathiesen, G., Eijsink, V. G. H. & Øynebråten, I. (2015). Lactobacillus plantarum displaying CCL3 chemokine in fusion with HIV-1 Gag derived antigen causes increased recruitment of T cells. *Microbial Cell Factories*, 14 (1): 169. doi: 10.1186/s12934-015-0360-z.
Kuczkowska, K., Kleiveland, C. R., Minic, R., Moen, L. F., Øverland, L., Tjåland, R., Carlsen, H., Lea, T., Mathiesen, G. & Eijsink, V. G. H. (2016). Immunogenic Properties of Lactobacillus plantarum Producing Surface-Displayed Mycobacterium tuberculosis Antigens. *Applied and environmental microbiology*, 83 (2): e02782-16. doi: 10.1128/AEM.02782-16.
Kuczkowska, K., Myrbråten, I., Øverland, L., Eijsink, V. G. H., Follmann, F., Mathiesen, G. & Dietrich, J. (2017). Lactobacillus plantarum producing a Chlamydia trachomatis

antigen induces a specific IgA response after mucosal booster immunization. *PLOS ONE*, 12 (5): e0176401. doi: 10.1371/journal.pone.0176401.
Kuczkowska, K., Øverland, L., Rocha, S. D. C., Eijsink, V. G. H. & Mathiesen, G. (2019). Comparison of eight Lactobacillus species for delivery of surface-displayed mycobacterial antigen. *Vaccine*, 37 (43): 6371-6379. doi: https://doi.org/10.1016/j.vaccine.2019.09.012.
Kuipers, O. P., de Ruyter, P. G., Kleerebezem, M. & de Vos, W. M. (1997). Controlled overproduction of proteins by lactic acid bacteria. *Trends in Biotechnology*, 15 (4): 135-40. doi: 10.1016/s0167-7799(97)01029-9.
Lam, T. T.-Y., Jia, N., Zhang, Y.-W., Shum, M. H.-H., Jiang, J.-F., Zhu, H.-C., Tong, Y.-G., Shi, Y.-X., Ni, X.-B., Liao, Y.-S., et al. (2020). Identifying SARS-CoV-2-related coronaviruses in Malayan pangolins. *Nature*, 583 (7815): 282-285. doi: 10.1038/s41586-020-2169-0.
Langermans, J. A., Doherty, T. M., Vervenne, R. A., van der Laan, T., Lyashchenko, K., Greenwald, R., Agger, E. M., Aagaard, C., Weiler, H., van Soolingen, D., et al. (2005). Protection of macaques against Mycobacterium tuberculosis infection by a subunit vaccine based on a fusion protein of antigen 85B and ESAT-6. *Vaccine*, 23 (21): 2740-50. doi: 10.1016/j.vaccine.2004.11.051.
Lu, R., Zhao, X., Li, J., Niu, P., Yang, B., Wu, H., Wang, W., Song, H., Huang, B., Zhu, N., et al. (2020). Genomic characterisation and epidemiology of 2019 novel coronavirus: implications for virus origins and receptor binding. *The Lancet*, 395 (10224): 565-574. doi: https://doi.org/10.1016/S0140-6736(20)30251-8.
Luca, S. & Mihaescu, T. (2013). History of BCG Vaccine. *Maedica*, 8 (1): 53-58.
Lulko, A. T., Veening, J. W., Buist, G., Smits, W. K., Blom, E. J., Beekman, A. C., Bron, S. & Kuipers, O. P. (2007). Production and secretion stress caused by overexpression of heterologous alpha-amylase leads to inhibition of sporulation and a prolonged motile phase in Bacillus subtilis. *Applied and Environmental Microbiology*, 73 (16): 5354-62. doi: 10.1128/aem.00472-07.
Marteau, P. & Rambaud, J. C. (1993). Potential of using lactic acid bacteria for therapy and immunomodulation in man. *FEMS Microbiology Reviews*, 12 (1-3): 207-20. doi: 10.1111/j.1574-6976.1993.tb00019.x.
Mathiesen, G., Sveen, A., Piard, J.-C., Axelsson, L. & Eijsink, V. G. H. (2008). Heterologous protein secretion by Lactobacillus plantarum using homologous signal peptides. *Journal of Applied Microbiology*, 105 (1): 215-226. doi: 10.1111/j.1365-2672.2008.03734.x.
Michon, C., Langella, P., Eijsink, V. G. H., Mathiesen, G. & Chatel, J. M. (2016). Display of recombinant proteins at the surface of lactic acid bacteria: strategies and applications. *Microbial Cell Factories*, 15 (1): 70. doi: 10.1186/s12934-016-0468-9.
Målbakken, N. (2014). *Development of a non-GMO tuberculosis vaccine, using Lactobacillus as a delivery vehicle.* Ås: Norwegian University of life Sciences.
Naqvi, A. A. T., Fatima, K., Mohammad, T., Fatima, U., Singh, I. K., Singh, A., Atif, S. M., Hariprasad, G., Hasan, G. M. & Hassan, M. I. (2020). Insights into SARS-CoV-2 genome, structure, evolution, pathogenesis and therapies: Structural genomics approach. *Biochimica et Biophysica Acta (BBA) - Molecular Basis of Disease*, 1866 (10): 165878. doi: https://doi.org/10.1016/j.bbadis.2020.165878.
Neutra, M. R. & Kozlowski, P. A. (2006). Mucosal vaccines: the promise and the challenge. *Nature Reviews Immunology*, 6 (2): 148-158. doi: 10.1038/nri1777.
Nguyen, T. T., Mathiesen, G., Fredriksen, L., Kittl, R., Nguyen, T. H., Eijsink, V. G., Haltrich, D. & Peterbauer, C. K. (2011). A food-grade system for inducible gene expression in Lactobacillus plantarum using an alanine racemase-encoding selection

marker. *Journal of Agricultural and Food Chemistry*, 59 (10): 5617-24. doi: 10.1021/jf104755r.
Pavan, S., Hols, P., Delcour, J., Geoffroy, M. C., Grangette, C., Kleerebezem, M. & Mercenier, A. (2000). Adaptation of the nisin-controlled expression system in Lactobacillus plantarum: a tool to study in vivo biological effects. *Applied and Environmental Microbiology*, 66 (10): 4427-32. doi: 10.1128/aem.66.10.4427-4432.2000.
Petrosillo, N., Viceconte, G., Ergonul, O., Ippolito, G. & Petersen, E. (2020). COVID-19, SARS and MERS: are they closely related? *Clinical Microbiology and Infection*, 26 (6): 729-734. doi: https://doi.org/10.1016/j.cmi.2020.03.026.
Salvetti, E., Torriani, S. & Felis, G. E. (2012). The genus Lactobacillus: a taxonomic update. *Probiotics and antimicrobial proteins*, 4 (4): 217-226.
Sterne, J. A., Rodrigues, L. C. & Guedes, I. N. (1998). Does the efficacy of BCG decline with time since vaccination? *International Journal of Tuberculosis and Lung Disease*, 2 (3): 200-7.
Sutcliffe, I. C. & Harrington, D. J. (2002). Pattern searches for the identification of putative lipoprotein genes in Gram-positive bacterial genomes. *Microbiology (Reading)*, 148 (Pt 7): 2065-2077. doi: 10.1099/00221287-148-7-2065.
Sørvig, E., Grönqvist, S., Naterstad, K., Mathiesen, G., Eijsink, V. G. H. & Axelsson, L. (2003). Construction of vectors for inducible gene expression in Lactobacillus sakei and L. plantarum. *FEMS Microbiology Letters*, 229 (1): 119-126. doi: 10.1016/s0378-1097(03)00798-5.
Sørvig, E., Mathiesen, G., Naterstad, K., Eijsink, V. G. H. & Axelsson, L. (2005). High-level, inducible gene expression in Lactobacillus sakei and Lactobacillus plantarum using versatile expression vectors. *Microbiology*, 151 (7): 2439-2449. doi: https://doi.org/10.1099/mic.0.28084-0.
van Roosmalen, M. L., Geukens, N., Jongbloed, J. D., Tjalsma, H., Dubois, J. Y., Bron, S., van Dijl, J. M. & Anné, J. (2004). Type I signal peptidases of Gram-positive bacteria. *Biochimica et Biophysica Acta*, 1694 (1-3): 279-97. doi: 10.1016/j.bbamcr.2004.05.006.
Wang, Q., Zhang, Y., Wu, L., Niu, S., Song, C., Zhang, Z., Lu, G., Qiao, C., Hu, Y., Yuen, K.-Y., et al. (2020). Structural and Functional Basis of SARS-CoV-2 Entry by Using Human ACE2. *Cell*, 181 (4): 894-904.e9. doi: https://doi.org/10.1016/j.cell.2020.03.045.
Wiull, K. (2018). *Implementation of a two-plasmid CRISPR/Cas9 system in Lactobacillus plantarum: A new approach in the development of a novel vaccine against Mycobacterium tuberculosis*. Ås: Norwegian University of Life Sciences.
World Health Organization. (2020a). *Coronavirus disease (COVID-19)*. Available at: https://www.who.int/news-room/q-a-detail/coronavirus-disease-covid-19 (accessed: 08.11).
World Health Organization. (2020b). *Global Tuberculosis Report 2020*.
World Health Organization. (2021). Draft landscape and tracker of COVID-19 candidate vaccines. Available at: https://www.who.int/publications/m/item/draft-landscape-of-covid-19-candidate-vaccines (accessed: 02.02.2021).
Wrapp, D., Wang, N., Corbett, K. S., Goldsmith, J. A., Hsieh, C.-L., Abiona, O., Graham, B. S. & McLellan, J. S. (2020). Cryo-EM structure of the 2019-nCoV spike in the prefusion conformation. *Science*, 367 (6483): 1260-1263. doi: 10.1126/science.abb2507.
Wyszyńska, A., Kobierecka, P., Bardowski, J. & Jagusztyn-Krynicka, E. K. (2015). Lactic acid bacteria—20 years exploring their potential as live vectors for mucosal

vaccination. *Applied Microbiology and Biotechnology*, 99 (7): 2967-2977. doi: 10.1007/s00253-015-6498-0.
Ye, Z.-W., Yuan, S., Yuen, K.-S., Fung, S.-Y., Chan, C.-P. & Jin, D.-Y. (2020). Zoonotic origins of human coronaviruses. *International journal of biological sciences*, 16 (10): 1686-1697. doi: 10.7150/ijbs.45472.
Zhang, T., Wu, Q. & Zhang, Z. (2020). Probable Pangolin Origin of SARS-CoV-2 Associated with the COVID-19 Outbreak. *Current Biology*, 30 (7): 1346-1351.e2. doi: https://doi.org/10.1016/j.cub.2020.03.022.
Zhou, P., Yang, X.-L., Wang, X.-G., Hu, B., Zhang, L., Zhang, W., Si, H.-R., Zhu, Y., Li, B., Huang, C.-L., et al. (2020). A pneumonia outbreak associated with a new coronavirus of probable bat origin. *Nature*, 579 (7798): 270-273. doi: 10.1038/s41586-020-2012-7.
Øverland, L. (2013). *Secretion and anchoring of proteins in Lactobacillus plantarum: Studies of a dendritic cell-targeted Mycobacterium tuberculosis antigen.* Ås: Norwegian University of Life Sciences.

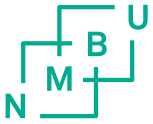

Norges miljø- og biovitenskapelige universitet
Noregs miljø- og biovitskapelege universitet
Norwegian University of Life Sciences

Postboks 5003
NO-1432 Ås
Norway